

**ASSESSING THE GROWING SEASON CARBON BUDGET OF AN ARCTIC
SEDGE FEN**

by

JONATHAN VANDEWINT

A thesis submitted to the Faculty of Graduate and Postdoctoral Affairs in partial
fulfillment of the requirements for the degree of

Master of Science

in

Geography

Carleton University
Ottawa, Ontario, Canada

© 2011

Jonathan Vandewint



Library and Archives
Canada

Published Heritage
Branch

395 Wellington Street
Ottawa ON K1A 0N4
Canada

Bibliothèque et
Archives Canada

Direction du
Patrimoine de l'édition

395, rue Wellington
Ottawa ON K1A 0N4
Canada

Your file *Votre référence*
ISBN: 978-0-494-81683-7
Our file *Notre référence*
ISBN: 978-0-494-81683-7

NOTICE:

The author has granted a non-exclusive license allowing Library and Archives Canada to reproduce, publish, archive, preserve, conserve, communicate to the public by telecommunication or on the Internet, loan, distribute and sell theses worldwide, for commercial or non-commercial purposes, in microform, paper, electronic and/or any other formats.

The author retains copyright ownership and moral rights in this thesis. Neither the thesis nor substantial extracts from it may be printed or otherwise reproduced without the author's permission.

In compliance with the Canadian Privacy Act some supporting forms may have been removed from this thesis.

While these forms may be included in the document page count, their removal does not represent any loss of content from the thesis.

AVIS:

L'auteur a accordé une licence non exclusive permettant à la Bibliothèque et Archives Canada de reproduire, publier, archiver, sauvegarder, conserver, transmettre au public par télécommunication ou par l'Internet, prêter, distribuer et vendre des thèses partout dans le monde, à des fins commerciales ou autres, sur support microforme, papier, électronique et/ou autres formats.

L'auteur conserve la propriété du droit d'auteur et des droits moraux qui protègent cette thèse. Ni la thèse ni des extraits substantiels de celle-ci ne doivent être imprimés ou autrement reproduits sans son autorisation.

Conformément à la loi canadienne sur la protection de la vie privée, quelques formulaires secondaires ont été enlevés de cette thèse.

Bien que ces formulaires aient inclus dans la pagination, il n'y aura aucun contenu manquant.


Canada

ABSTRACT

This study provides a complete growing season carbon budget of an arctic sedge fen and an examination of the controls on spatial and temporal variations in carbon dioxide (CO₂) and methane (CH₄) fluxes at the small plot and ecosystem scale during the 2009 growing season at Daring Lake, NT. Soil moisture and temperature exerted control over CH₄ exchange at the plot scale, while frictional velocity and soil temperature appeared to be equally important at the ecosystem scale. Air temperature, leaf area, and photosynthetically active radiation, were important variables controlling CO₂ flux at both the plot and ecosystem scales. Over the growing season, the fen was a sink of 66.3 g C m⁻² from CO₂ exchange, a source of 2.4 g C m⁻² from CH₄ emission, and a source of 0.9 g C m⁻² from dissolved organic carbon export, resulting in a net C uptake of 63 g C m⁻².

ACKNOWLEDGEMENTS

First and foremost, I thank Dr. Elyn Humphreys. I am grateful for the nostalgic memory of my research in the Arctic. Without her guidance, support, and trust, this thesis would not have been possible. I would also like to thank my assistant Samantha Piquette for her hard work in the field and the enjoyable memories of fishing, swimming, and Han Solo. Many thanks go to Mike Treberg for all things technical. I would like to extend my appreciation to Dr. Ed Gregorich at Agriculture and Agrifood Canada and to Dr. Tim Moore at McGill University for laboratory use and sample processing. Without the funding provided by the Department of Wildlife and Environment, Government of N.W.T., through the direction of Steve Mathews, research at the Tundra Ecological Research Station at Daring Lake would not have been as pleasurable.

Funding for this project was provided by the Northern Scientific Training Program (NSTP) governed by Indian and Northern Affairs Canada.

I would like to thank my friends and family for their support and distraction while pursuing my masters.

TABLE OF CONTENTS

ABSTRACT.....	ii
ACKNOWLEDGEMENTS	iii
TABLE OF CONTENTS	iv
LIST OF TABLES	vi
LIST OF FIGURES	viii
LIST OF SYMBOLS AND ABBREVIATIONS	xii
1.0 INTRODUCTION	1
2.0 BACKGROUND	5
2.1.1 Arctic Soil Carbon	5
2.1.2 Arctic Environment.....	6
2.1.3 Wetland Environment	7
2.2 Fluxes of CO ₂ , CH ₄ , and DOC.....	9
2.2.1 CO ₂ , CH ₄ , and DOC Cycling	11
2.2.1.1 CO ₂ Flux	11
2.2.1.2 CH ₄ Flux	12
2.2.1.3 DOC Flux.....	15
2.2.1.4 Carbon Budget Studies	16
3.0 METHODS	18
3.1 Site Description.....	18
3.2 Experimental Design.....	23
3.3 Data collection	25
3.3.1 NEE Chamber System	25
3.3.2 Opaque Chamber System.....	26
3.3.3 Environmental Variables.....	27
3.4 Ecosystem Exchange of CO ₂ and CH ₄	28
3.4.1 Eddy Covariance Measurements of CO ₂ and CH ₄	28
3.4.2 Environmental Variables.....	29
3.5 Dissolved Organic Carbon.....	30
3.6 Data Analysis	30

3.6.1	Chamber Flux Calculation	30
3.6.2	NEE of CO ₂ and CH ₄ Flux Calculation	31
3.6.3	Light-Temperature Response	32
3.6.4	DOC Flux Calculation	33
3.6.5	Flux Footprint	34
3.6.6	Gap-filling and C budget Calculations	34
3.7	Statistical Analysis	35
4.0	RESULTS	37
4.1	Site Characteristics.....	37
4.2	Carbon Exchange	41
4.2.1	Spatial Variations in CO ₂ Fluxes	41
4.2.2	Spatial Variations in CH ₄ Fluxes	46
4.3.1	Temporal Variations in CO ₂ Fluxes	51
4.3.2	Temporal Variations in CH ₄ Fluxes.....	57
4.4	General Seasonal Trends in CH ₄ and CO ₂ Exchange	60
4.5.1	Daily Variation in Ecosystem CH ₄ and CO ₂ Exchange.....	63
4.5.2	Diurnal Variation in Ecosystem CH ₄ and CO ₂ Flux.....	66
4.6	Spatial Variation in Ecosystem CH ₄ and CO ₂ Flux	73
4.7	Growing Season C Budget and GWP	77
5.0	DISCUSSION	83
5.1	CO ₂ Fluxes	83
5.2	CH ₄ Fluxes	87
5.3	Carbon Exchange Rates at the Daring Lake Fen and other Arctic Sites	95
5.4	Growing Season Carbon Budget and GWP	99
6.0	CONCLUSION.....	103
7.0	REFERENCES	106

LIST OF TABLES

<p>Table 1. Soil and vegetation characteristics of the lawn and tussock environments. Values in brackets are the standard error of the mean (± 1 SE) for the 8 tussock and 8 lawn collars. Values with different superscripts denote significant differences between communities ($p < 0.05$). * Source (Hayne, 2009).</p>	37
<p>Table 2. Environmental characteristics of the lawn and tussock communities. Values in brackets are ± 1 SE. Values with different superscripts denote significant differences between communities ($p < 0.05$).</p>	38
<p>Table 3. Average NEE and component fluxes for the two vegetation communities. NEE_{max} is the net ecosystem exchange of CO_2 for PAR greater than $1000 \mu mol m^{-2} s^{-1}$. GEP_{max} is the average gross ecosystem production for PAR greater than $1000 \mu mol m^{-2} s^{-1}$. ER is the average ecosystem respiration in the dark measured using the flow-through chambers (ER_F) and the static chambers (ER_S). Values in brackets represent ± 1 SE. Values with different superscripts denote significant differences between communities ($p < 0.05$).</p>	42
<p>Table 4. Parameters for Equation 3 describing the response of NEE to PAR and chamber air temperature for the two communities. GP_{max} is maximum gross photosynthesis, α is the initial slope of the curve, R_{10} is ecosystem respiration at a reference temperature of $10^\circ C$, n is the number of observations, Q_{10} is rate of increase in ER for a $10^\circ C$ increase in temperature, and RMSE is the root mean square error. Values in brackets represent ± 1 SE. Values with different superscripts denote significant differences between communities ($p < 0.05$).</p>	42
<p>Table 5. The range and mean CH_4 flux for the lawn and tussock communities. Values in brackets represent ± 1 SE. Values with different superscripts denote significant differences between communities ($p < 0.05$). The number of samples for lawns and tussocks is 132.</p>	47
<p>Table 6. Spearman's rho correlation coefficients showing significant relationships between environmental variables and CO_2 fluxes with p-values given in brackets. Net ecosystem exchange (NEE_{max}); gross ecosystem production (GEP_{max}); ecosystem respiration (flow-through chamber) (ER_F); ecosystem respiration (static chamber) (ER_S).</p>	54
<p>Table 7. Spearman's rho correlation coefficients showing significant relationships between environmental variables and ecosystem respiration (static chamber) (ER_S), for lawn and tussock communities with p-values given in brackets.</p>	54
<p>Table 8. Spearman's rho correlation coefficients showing significant relationships between environmental variables and CH_4 flux for lawn and tussock communities separately and combined with significant p-values given in brackets.</p>	58

Table 9. Spearman’s rho correlation coefficients showing significant relationships between CH₄ flux and environmental variables for flux values above 12 °C. P- values are given in brackets and considered significant when $p < 0.05$ 69

Table 10. Parameters for Equation 3 describing the response of NEE to PAR and average ecosystem air temperature for the study period. GP_{max} is maximum gross photosynthesis, α is the initial slope of the curve, R₁₀ is ecosystem respiration at a reference temperature of 10 °C, n is the number of observations, Q₁₀ is rate of increase in ER for a 10 °C increase in temperature*, RMSE is the root mean square error, and Temp is the average air temperature for the study period. Values in brackets indicate approximate standard error. 72

Table 11. Average daytime (10am – 6pm) NEE for footprint distances from tower of 70 m or less and for distances greater than 70 m for the three sectors during the study period. Error associated with NEE is ± 1 SE. Numbers in brackets indicate the number of observations. Different superscript letters indicate significant differences within a column ($p < 0.05$). NEE, net ecosystem exchange of CO₂. 76

Table 12. CH₄ input and model parameters for the growing season of 2009 using Equation 5. T_{ref}, average temperature for the sampling period, u*_{ref}, average frictional velocity for the sampling period, a, b, c are fit parameters, RMSE, root-mean standard error, r², correlation coefficient, n, number of samples. Errors associated with fit parameters are \pm SE. The number of daily averages used was 27. 80

Table 13. Average dissolved organic carbon (DOC), slope (dh/dz), and flow rates for three measurement periods during summer of 2009, Daring Lake. Values within brackets indicate standard error of the mean. The number of samples for each measurement is 3. 82

Table 14. Average ecosystem storage change of dissolved organic carbon, DOC, for three measurement periods during the summer of 2009, Daring Lake. Values within brackets indicate standard error of the mean. Positive values indicate loss of DOC from the ecosystem. The number of samples for each measurement is 6. 82

Table 15. GWP and modelled carbon balance for the growing season (June 1 – August 31) 2009 at Daring lake, NT. Positive numbers indicate ecosystem carbon loss and negative numbers indicate ecosystem carbon uptake and negative forcing potential to warm atmosphere. 82

LIST OF FIGURES

- Figure 1. Map of the research area at Daring Lake, NT with the location of the Tundra Ecological Research Station (TERS), fen and study site (Adapted from Nobrega and Grogan, 2008). 19
- Figure 2. Vegetation map (edited from Obst, 2008) showing the location of micrometeorological tower within the wet fen at Daring Lake, NT. Inner ring represents radius of 70 m and outer ring a radius of 100 m. Three sectors are delineated: 0° - 135° (sedge fen dominated by lawn topography to NE, rocky upland area to SE); 135° - 225° (sedge fen with tussock topography, small, open water bodies and rocky upland area); 225° - 360° (sedge fen and shrub peat mound areas). 21
- Figure 3. Top panel – NE aerial view of Darling Lake, NT including Yamba Lake in top left. Yellow circle gives approximate location of micrometeorological tower. Bottom panel – Micrometeorological setup with a view to the north. Lawn and tussock topography is shown in foreground. 22
- Figure 4. Plot locations of 16 permanent collars installed at Daring Lake, NT, 2009. Closed circles represent lawns and open circles represent tussocks. The closed black square represents micrometeorological tower, open squares represent solar panels, and closed triangle represents the generator. UTM coordinate system in Easting and Northing, Map 12N (North America). Locations are within 2 meter accuracy. 24
- Figure 5. Daily average water table depth relative to the lawn surface, total daily precipitation, and average soil volumetric water content (VWC) for the 0 – 20 cm layer of lawns (closed circles) and tussocks (open circles) at Daring Lake, NT from July 11th to August 15th, 2009. Error bars represent ± 1 standard error (± 1 SE). 39
- Figure 6. Average daily air temperature (solid line), average daily daytime air temperature ($PAR > 10 \text{ W m}^{-2}$) (dotted line), average soil temperature at 2 cm depth for lawns (closed circles) and tussocks (open circles), daily photosynthetically active radiation (PAR), and thaw layer depth at Daring Lake, NT from July 11th to August 15th, 2009. Error bars represent ± 1 SE. The number of samples for each 2 cm soil temperature symbol is 8. The number of samples for each thaw layer depth symbol is 15. 40
- Figure 7. The top and bottom panels show the relationship between net ecosystem exchange of CO_2 (NEE) and photosynthetically active radiation (PAR) for lawns and tussocks, respectively. The light response curves are shown as solid lines. Curves (solid lines) are determined using Equation 3 with parameters listed in Table 4. 43
- Figure 8. The relationship between net ecosystem exchange of CO_2 (NEE_{max}) (top panel) and gross ecosystem exchange of CO_2 (GEP_{max}) (bottom panel) to % vascular. Error bars represent ± 1 SE. The number of samples for each symbol is 13. Lines are given for

significant linear regressions ($NEE_{max} = -0.04 (\% \text{ Vascular}) + 0.55, r^2 = 0.56$; $GEP_{max} = -0.05 (\% \text{ Vascular}) - 0.92, r^2 = 0.43$). 45

Figure 9. Relationship between CH₄ Flux and volumetric water content (VWC) for lawns (dark circles) and tussocks (open circles). Error bars represent ± 1 SE. The number of samples for each symbol is 16. Lines are given for significant linear regressions ($CH_4 \text{ Flux} = 37.35(\text{VWC}) + 18.62, r^2 = 0.24$). 48

Figure 10. Relationship between 2 cm soil temperature and CH₄ flux for lawns (dark circles) and tussocks (open circles). Error bars represent ± 1 SE. The number of samples for each symbol is 16. Lines are given for significant linear regressions ($CH_4 \text{ Flux} = 11.72 (\text{Temperature}) - 128.1, r^2 = 0.66$). 49

Figure 11. The relationship between ecosystem respiration (static chamber) (ER_S) and CH₄ flux for lawns (dark circles) and tussocks (open circles). Error bars represent ± 1 SE. The number of samples for each symbol is 16. Lines are given for significant linear regressions ($ER_S = 0.02 (CH_4 \text{ Flux}) + 0.72, r^2 = 0.80$). 50

Figure 12. The average daily flux for lawns (closed circles) and tussocks (open circles) using the flow-through and opaque static chamber systems. Gross ecosystem production (GEP); net ecosystem exchange (NEE); ecosystem respiration (flow-through chamber) (ER_F); ecosystem respiration (static chamber) (ER_S). Error bars represent ± 1 SE. The number of samples for each symbol is 8. 52

Figure 13. The relationship between ecosystem respiration (flow-through chamber), ER_F, and temperature at 2 cm depth (top panel), average volumetric water content (VWC) (middle panel), and water table depth (bottom panel). Closed circles represent lawns and open circles represent tussocks. Error bars represent ±1 SE. The number of samples for each symbol is 8. Lines are given for significant linear regressions. Top panel lawns ($ER_F = 0.1 (\text{Temperature}) + 0.24, r^2 = 0.77$) and tussocks ($ER_F = 0.13 (\text{Temperature}) - 0.27, r^2 = 0.64$); middle panel ($ER_F = 2.16 (\text{Temperature}) + 1.13, r^2 = 0.25$); bottom panel ($ER_F = 0.11 (\text{Temperature}) + 2.89, r^2 = 0.25$). 55

Figure 14. The relationship between ecosystem respiration (static chamber) (ER_S) and temperature at 2 cm depth (top panel), average volumetric water content (VWC) (middle panel), and CH₄ Flux (bottom panel). Closed circles represent lawns and open circles represent tussocks. Error bars represent ± 1 SE. The number of samples for each symbol is 8. Lines are given for significant linear regressions. Top panel (L: $ER_S = 0.12 (\text{Temperature}) - 0.17, r^2 = 0.82$; T: $ER_S = 0.07 (\text{Temperature}) + 0.41, r^2 = 0.37$), middle panel (L: $ER_S = -3.04 (\text{VWC}) + 4.01, r^2 = 0.36$; T: $ER_S = 2.54 (\text{VWC}) + 0.14, r^2 = 0.27$), bottom panel (L: $ER_S = 0.01 (CH_4 \text{ Flux}) + 0.62, r^2 = 0.28$; T: $ER_S = 0.04 (CH_4 \text{ Flux}) - 0.02, r^2 = 0.36$). 56

Figure 15. The relationship between CH₄ flux and temperature at 2 cm depth (top panel), average volumetric water content (VWC) (middle panel), and water table depth (bottom panel). Error bars represent ±1 SE. The number of samples for each symbol is 8. Lines

are given for significant linear regressions. Top panel ($\text{CH}_4\text{Flux} = 1.01 (\text{Temperature}) + 20.5, r^2 = 0.15$), middle panel ($\text{CH}_4\text{Flux} = 63.16 (\text{VWC}) + 7.97, r^2 = 0.57$), bottom panel (L: $\text{CH}_4\text{Flux} = 1.39 (\text{WT}) + 70.54, r^2 = 0.17$; T: $\text{CH}_4\text{Flux} = 2.07 (\text{WT}) + 52.94, r^2 = 0.47$). 59

Figure 16. Daily daytime (10 am - 6 pm) average eddy covariance and chamber measurements of CH_4 flux and net ecosystem exchange CO_2 (NEE). Eddy covariance fluxes are shown for days when there were at least 6 half hours with good quality measurements. Chamber fluxes are means of 8 different collar measurements for each plotted day. Error bars represent ± 1 SE. Chamber fluxes are represented by closed circles for lawns, open circles for tussocks, triangles for shrub peat mounds, and open squares represent tower fluxes. 62

Figure 17. The relationship between daily daytime (10am – 6pm) CH_4 flux and 5 cm soil temperature (top panel) and friction velocity (u_*) (bottom panel). Error bars represent ± 1 SE. The number of 30 min fluxes for each symbol ranges from 6 to 16. 64

Figure 18. The relationship between daily daytime (10am – 6pm) net ecosystem exchange of CO_2 (NEE) and photosynthetically active radiation (PAR). The top panel illustrates the relationship for air temperature below 12°C and the bottom panel is for air temperature above 12°C . Lines are given for significant linear regressions. Top Panel: ($\text{NEE} = -0.0006 (\text{PAR}) - 2.52, r^2 = 0.05$) and bottom panel: ($\text{NEE} = -0.003 - 0.81, r^2 = 0.25$). Error bars represent ± 1 SE. The number of 30 min fluxes for each symbol ranges from 6 to 16..... 65

Figure 19. Diurnal variation of CH_4 flux, friction velocity (u_*), and 5 cm soil temperature for days with different turbulence conditions. Column 1 represents whole days (14 < half-hour measurements < 49) when mean u_* was above 0.24 m s^{-1} and the standard deviation (SD) was below 0.07 m s^{-1} , column 2 represents u_* below 0.24 m s^{-1} and the SD was below 0.07 m s^{-1} , and column 3 represents mixed u_* (all other days) with a SD above 0.07 m s^{-1} . Half-hour measurements with u_* below 0.1 m s^{-1} were not included. Error bars represent ± 1 SE. The number of 30 min measurements for each symbol ranges from 10 to 21..... 67

Figure 20. The relationship between 30 min CH_4 flux and frictional velocity, u_* . Data are binned by u_* (0.03 m s^{-1} wide) and separated by temperature above (open circles) and below (closed circles) 12°C . Error bars represent ± 1 SE. The number of 30 min fluxes for each symbol ranges from 6 to 53..... 68

Figure 21. The relationship between 30 min CH_4 flux and 5 cm soil temperature. Data is binned by temperature (0.5°C) and separated by u_* . Open circles represent data below 0.24 m s^{-1} and closed circles represent data above 0.24 m s^{-1} . Error bars represent ± 1 SE. The number of 30 min fluxes for each symbol ranges from 5 to 58..... 68

Figure 22. The relationship between 30 min CH_4 flux and all variables above 12°C separated by CH_4 flux above and below $30 \text{ nmol m}^{-2} \text{ s}^{-1}$. Closed circles represent CH_4 flux below $30 \text{ nmol m}^{-2} \text{ s}^{-1}$ and open circles represent CH_4 flux above $30 \text{ nmol m}^{-2} \text{ s}^{-1}$... 70

Figure 23. The relationship between nighttime (PAR less than $20 \mu\text{mol m}^{-2} \text{s}^{-1}$) net ecosystem exchange of CO_2 , NEE CO_2 , and frictional velocity, u^* . Data are binned by u^* (0.05 m s^{-1} wide) and separated by temperature above (open circles) and below (closed circles) $8.5 \text{ }^\circ\text{C}$. Positive values indicate net ecosystem carbon loss. Error bars represent $\pm 1 \text{ SE}$. The number of samples for each symbol ranges from 18 to 70. 71

Figure 24. The relationship between net ecosystem exchange of CO_2 , NEE, and photosynthetically active radiation, PAR for the study period. Symbols correspond to 30 minute averages of NEE which were above the frictional velocity threshold of 0.1 m s^{-1} at night (PAR < $20 \mu\text{mol m}^{-2} \text{s}^{-1}$). The curved line corresponds to Equation 3 with parameters listed in Table 10. Negative values represent ecosystem uptake of carbon. . 72

Figure 25. The relationship between 30 minute averages of CH_4 flux, friction velocity, u^* , and footprint distance for three spatially different areas within the fetch of the eddy covariance tower. Closed circles represent sector 1 ($0^\circ - 135^\circ$), open circles represent sector 2 ($135^\circ - 225^\circ$), and closed triangles represent sector 3 ($225^\circ - 360^\circ$). Data are binned by footprint (10 m wide) and u^* (0.05 m s^{-1} wide). Error bars represent $\pm 1 \text{ SE}$. The number of samples for each symbol ranges from 6 to 36. 75

Figure 26. The relationship between net ecosystem exchange of CO_2 , NEE, and footprint distance for three spatially different areas within the fetch of the eddy covariance tower. Closed circles represent sector 1 ($0^\circ - 135^\circ$), open circles represent sector 2 ($135^\circ - 225^\circ$), and closed triangles represent sector 3 ($225^\circ - 360^\circ$). Error bars represent $\pm 1 \text{ SE}$. The number of samples for each symbol ranges from 9 to 50. 76

Figure 27. Half-hour measured net ecosystem exchange (NEE) (top), gap-filled daily NEE (middle) and cumulative NEE (bottom) for 1 June to 31 August 2009. Positive values represent a net C loss to the atmosphere while negative values represent a net C accumulation by the ecosystem. 79

Figure 28. Daily integrated mean values of eddy covariance CH_4 emission versus modelled emission rates from Equation 5 and modelled parameters from Table 12. CH_4 , methane. 80

Figure 29. Daily CH_4 flux (middle) and cumulative CH_4 flux (bottom), modelled, for 1 June to 31 August 2009. Positive values result in net C loss to atmosphere. CH_4 , methane. 81

LIST OF SYMBOLS AND ABBREVIATIONS

Symbol	Units	Definition
α	mol CO ₂ mol ⁻¹ photons	Effective quantum yield
A	m ²	area
C		carbon
CH ₃ COH		methanol
CH ₃ COOH		acetate substrate
CO ₂		carbon dioxide
CH ₄		methane
cm		centimeters
DIC		dissolved inorganic carbon
DOC		dissolved organic carbon
dh/dz	m m ⁻¹	slope
dx/dt	ppm s ⁻¹	gas species mixing ratio
°C		degrees Celsius
EC		eddy covariance
ER	μmol CO ₂ m ⁻² s ⁻¹	ecosystem respiration of CO ₂
ER _a	μmol CO ₂ m ⁻² s ⁻¹	autotrophic respiration
ER _h	μmol CO ₂ m ⁻² s ⁻¹	heterotrophic respiration
ER _F	μmol CO ₂ m ⁻² s ⁻¹	ecosystem respiration of CO ₂ flow-through chamber
ER _S	μmol CO ₂ m ⁻² s ⁻¹	ecosystem respiration of CO ₂ static chamber
F		flux
FID		flame-ionization detector
FMGA		closed-path fast methane gas analyzer
GEP	μmol CO ₂ m ⁻² s ⁻¹	gross ecosystem photosynthesis
GEP _{max}	μmol CO ₂ m ⁻² s ⁻¹	gross ecosystem photosynthesis at maximum PAR (field)
GP _{max}	μmol CO ₂ m ⁻² s ⁻¹	gross ecosystem photosynthesis at maximum PAR (model)
GWP		global warming potential
H		hydrogen
H ₂		hydrogen gas
H ₂ O		water
ha		hectares
IPCC		international panel on climate change
IRGA		infrared gas analyzer
κ		permeability constant 10 ⁻⁴
km		kilometers
l		liter
LAI		leaf area index
m		meters
mg		milligrams

min		minutes
ml		milliliters
mm		millimeters
N		north
NEE	$\mu\text{mol CO}_2 \text{ m}^{-2} \text{ s}^{-1}$	net ecosystem exchange of CO ₂ (field)
NEE _{max}	$\mu\text{mol CO}_2 \text{ m}^{-2} \text{ s}^{-1}$	net ecosystem exchange of CO ₂ (model)
NPP		plant productivity
NT		north west territories, Canada
O		oxygen atom
O ₂		oxygen molecule (air)
P	Pa	atmospheric pressure
PAR	$\mu\text{mol photons m}^{-2} \text{ s}^{-1}$	photosynthetically active radiation
Pg		petagram
ppm		parts per million
Q	$\text{m}^3 \text{ s}^{-1}$	discharge rate
Q ₁₀		rate of increase in respiration over 10 °C
R	$\text{J mol}^{-1} \text{ K}^{-1}$	ideal gas constant 8.314 J mol ⁻¹ K ⁻¹
R _{ref}	$\mu\text{mol CO}_2 \text{ m}^{-2} \text{ s}^{-1}$	respiration at reference temperature T _{ref}
R ₁₀	$\mu\text{mol CO}_2 \text{ m}^{-2} \text{ s}^{-1}$	respiration at reference temperature of 10 °C
SE		standard error of the mean
SOC		soil organic carbon
T	°C or Kelvin	temperature
TERS		tundra ecosystem research station
T _{ref}	°C	reference temperature of 10 °C
u*	m s^{-1}	frictional velocity
u* _{ref}	m s^{-1}	mean frictional velocity
V	m^3	volume
VPD	kPa	vapour pressure deficit
VWC	$\text{m}^3 \text{ m}^{-3}$	volumetric water content
WT	cm	water table depth

1.0 INTRODUCTION

Global surface temperatures have risen by 0.6 °C since the beginning of the industrial revolution (IPCC, 2007). General circulation models forecast disproportionate increases in temperature and precipitation in high latitudes when compared to temperate and tropical regions (IPCC, 2007; ACIA, 2004). In the last fifty years, parts of Siberia, Alaska, and north-western Canada have experienced 2-3 °C warming (ACIA, 2004), and by the end of the 21st century, a 4-8 °C temperature rise is expected in the Arctic (IPCC, 2007). The rate and magnitude of biogeochemical cycling may be affected in arctic ecosystems due to the potential to respond strongly and rapidly to changes in temperature and moisture conditions (Oechel and Vourlitis, 1994; Zhuang *et al.*, 2006; Zimov *et al.*, 2006). Terrestrial surface-atmosphere feedbacks to the climate system occur through exchanges of energy and water vapour and through exchanges of greenhouse gases such as carbon dioxide (CO₂) and methane (CH₄) (Chapin *et al.* 2000). A better understanding of the carbon (C) cycle of arctic terrestrial ecosystems and the biotic and abiotic factors that affect them is particularly important as these vast areas store large amounts of C in soils that remain frozen or saturated for much of the year. Moreover, with climate change in these regions, this C pool could become susceptible to decomposition and subsequently be released to the atmosphere. Should warming in northern areas promote the loss of C to the atmosphere, this could result in a positive feedback to climate change. Increasing concentrations of CO₂ and CH₄ gas in the atmosphere results in positive radiative forcing which leads to increased surface temperatures (ACIA, 2004). Understanding how arctic ecosystems respond to and influence global warming is critical in order to model and predict future climate change.

Globally, it is estimated that there is 1672 Pg of organic C in northern permafrost soils (Tarnocai *et al.*, 2009). Globally, northern circumpolar regions have approximately 496 Pg of C in the top 1 m and 1024 Pg of C in the top 3 m of soil with the remaining C in deeper yedoma and deltaic deposits (Tarnocai *et al.*, 2009). With the current atmospheric C pool estimated to be 750 Pg, the below ground northern circumpolar C pool represents over twice the amount presently stored in the atmosphere (Kuhry *et al.*, 2010).

The C fluxes that determine the C budget of terrestrial wetland ecosystems include CO₂ and CH₄ fluxes as well as the flow of dissolved organic C (DOC) and inorganic C (DIC) primarily through groundwater flow. The majority of studies examining ecosystem-scale terrestrial C cycling in arctic terrain have been carried out in Alaska (Vourlitis and Oechel, 1999; Vourlitis *et al.*, 2000; Kwon *et al.*, 2006), Siberia (Corradi *et al.*, 2005; Grondahl *et al.*, 2008; Sachs *et al.*, 2008; Wille *et al.*, 2008; Merbold *et al.*, 2009; Gazovic *et al.*, 2010), and Europe and Scandinavia (Soegaard and Nordstrom, 1999; Friberg *et al.*, 2000; Aurela *et al.*, 2007; Riutta *et al.*, 2007; Fox *et al.*, 2008; Nilsson *et al.*, 2008). In Canada, small plot-scale studies have been carried out in the High Arctic (Welker *et al.*, 2004; Oberbauer *et al.*, 2007) and in the Southern Arctic to examine spatial variations in CO₂ exchanges for a variety of upland and wetland tundra types (Griffis *et al.*, 2000; Nobrega and Grogan, 2008; Hayne, 2009; Wilson and Humphreys, 2010), but very few studies have investigated whole ecosystem-scale fluxes of the terrestrial CO₂ cycle in Canada's Arctic in either wetland (Griffis *et al.*, 2000; Lafleur *et al.*, 2001) or upland tundra (Lafleur and Humphreys, 2008). Elsewhere, only a limited number of studies have examined both CO₂ and CH₄ exchanges in arctic wetland

tundra using small plot-scale measurements using chambers (Christensen *et al.*, 2000; Nykanen *et al.*, 2003; Grondahl *et al.*, 2008; Hayne, 2009) and ecosystem-scale measurements using micrometeorological techniques (Friborg *et al.*, 2003; Grondahl *et al.*, 2008). While many studies have been conducted in arctic environments, there is limited knowledge of C dynamics in Canadian arctic wetland environments. As Canada contains approximately 33% of the total arctic landmass (Lafleur and Humphreys, 2008), and a vast quantity of C is found within the top 1 m of soil, particularly in arctic peatlands, the current magnitude and direction of the C budget of Canadian arctic peatlands has global implications.

In 1994, a long-term ecosystem monitoring station, the Tundra Ecosystem Research Station (TERS) at Daring Lake, Northwest Territories, Canada (64°52 N latitude, 111°34 W longitude) was established by the Government of Northwest Territories Department of Renewable Resources. In 2004, the Canadian Tundra Ecosystem Carbon Study was established at TERS to monitor exchanges of CO₂, CH₄, energy and water vapour between the atmosphere and the tundra. Flux monitoring and manipulation experiments occur annually in order to improve our understanding of the C cycle of the ecosystems found in this region.

This thesis examines the fluxes of CO₂, CH₄, and DOC for a sedge fen, also known as a wet sedge meadow, at Daring Lake during the growing season of 2009. A combination of small plot-scale measurements using chamber systems and ecosystem-scale measurements using an eddy covariance system were made to assess the C budget of the sedge fen and improve our understanding of the biotic and abiotic factors controlling the exchanges of C for this ecosystem.

This research will address the following three objectives:

- 1) To quantify the temporal variation of ecosystem-scale CO₂ and CH₄ exchanges of a sedge fen at 30 min and day-to-day time scales.
- 2) To examine the mechanisms controlling both the spatial and temporal exchanges of CO₂ and CH₄ of this ecosystem.
- 3) To determine the full growing season C budget of this ecosystem, including the exchange of CO₂ and CH₄ with the atmosphere and loss of DOC.

More specifically, the following hypotheses will be tested:

- 1) During the study period, the sedge fen is a C sink with more C taken up as CO₂ than lost as CH₄ and DOC.
- 2) Temporal and spatial variability in CO₂ flux is influenced most by factors that influence photosynthesis such as leaf area, light, and temperature.
- 3) Temporal and spatial variability in CH₄ flux is influenced most by factors that affect anaerobic decomposition such as soil moisture conditions and soil temperatures.

2.0 BACKGROUND

2.1.1 Arctic Soil Carbon

In total, northern permafrost regions contain about 1672 Pg of C, which accounts for approximately 50% of the global below ground organic carbon pool and is more than three times larger than the total global forest C biomass (Kuhry *et al.*, 2010). 88% of the northern circumpolar soil organic C stock, or 1466 Pg, is found in perennially frozen soils (deeper than the active layer) and deposits (Kuhry *et al.*, 2010). Of the organic C found in the top 1 m of soil in permafrost regions (496 Pg C), northern circumpolar peatlands contain approximately 30% of the total soil organic carbon (SOC) while covering approximately 19% of the total area (Tarnocai *et al.*, 2009).

With continued climate warming, this C pool could become susceptible to decomposition (Post *et al.*, 1982; Bartlett and Harris, 1993; Tarnocai *et al.*, 2009). The C pool has been accumulating over several millennia as the photosynthetic uptake of CO₂ exceeds losses of CO₂, CH₄, and DOC through decomposition processes. Factors inhibiting decomposition include low temperatures, low quality substrate, and anoxia due to saturated conditions (Davidson and Janssens, 2006). Permafrost thaw could result in the release of large amounts of greenhouse gases (CO₂ and CH₄), due to the remobilization of previously frozen SOC (Schuur *et al.*, 2008). However, as soils warm, concurrent changes in soil moisture, nutrient regimes, and changes in the rate and duration of photosynthetic uptake of CO₂ by current and new plant communities will influence to what extent the C budget of terrestrial arctic ecosystems will change (Schuur *et al.*, 2008).

The fate of northern C pools represents one of the most potentially significant carbon-climate feedback effects due to the size of the C pools and the intensity of high latitude climate warming, and yet, it is one of the least understood of the feedback processes (Schuur *et al.*, 2008).

2.1.2 Arctic Environment

Callaghan *et al.* (2005) define the Arctic tundra as a region above the northern limit of the boreal forest with extreme climate, strong seasonal temperature gradients and a high degree of natural variability. The landscape is snow-covered for most of the year with a short growing season. There are three main types of ecosystems: dry tundra, mesic tundra, and wet tundra which are governed by latitude, climatic, and hydrologic gradients (Welker *et al.*, 2004). Tundra ecosystems are characterized by weakly developed soils, exposed bedrock outcrops, large number of lakes, and a variety of vegetation (grasses, sedges, small flowering herbs, low shrubs, lichens, and mosses) adapted to extreme environments (Bartlett and Harris, 1993). Arctic tundra has been divided between two (Bliss, 1997) and as many as seven (Alexandrova, 1980) subdivisions in the past. For the purpose of this paper, two functional subdivisions, high Arctic tundra and low Arctic tundra (Bliss, 1997) will be defined. According to Walker (2005), the high Arctic tundra consists of mineral soils with very low-stature vegetation (very close to the soil surface), while the low Arctic tundra is composed of peat-rich soils with closed vegetation (shrub and dwarf trees).

Within the arctic landscape, permafrost, defined as subsurface materials that remain at or below 0° C for two or more years (Burn and Nelson, 2006), is widespread (Zhang *et al.*, 1999). Permafrost impedes drainage and promotes the formation of

wetlands (Bartlett and Harris, 1993). Due to the extensive presence of permafrost in the Arctic, peat forming wetlands (peatlands) are widespread and, as defined, must contain a minimum of 40 cm of peat (Warner and Rubec, 1997). Peatlands store large quantities of C due to anaerobic (lack of oxygen) conditions which slow the breakdown of organic matter (Davidson and Janssens, 2006).

The active layer, defined as the seasonal maximum extent of thaw layer depth (Burn and Nelson, 2006), is primarily controlled by temperature and topography. In the low Arctic, annual active layer depth ranges from 40 – 80 cm (ACIA, 2004). Spring snowmelt causes much of the permafrost land surface to be saturated due to the impedance of drainage by permafrost, shallow drainage gradients, and relatively low evapotranspiration rates (Bockheim *et al.*, 1999). Upland areas surrounding low lying areas drain relatively quickly and supply low lying areas with water during the growing season. Water levels in low lying areas may be above, at, or just below the surface. Saturation in these areas causes microtopography differences which may be brought about by frost heave, vegetation differences, decomposition rates, and water movement (Nungesser, 2003)

2.1.3 Wetland Environment

There are two main types of peatlands: bogs and fens. Bogs typically have a fluctuating water table at or slightly below the peat surface, nutrients supplied only through precipitation, an acidic pH of around 3 or 4, and *Sphagnum* moss as the dominant flora with the presence of shrubs and sedges (Warner and Rubec, 1997). Fens, in contrast, receive their nutrients from groundwater flow into the wetland, have a fluctuating water table (depending on precipitation, evapotranspiration, and topography),

and may be characterized by a large variety of vegetation including sedges and grasses and when acidic and nutrient poor, may also have *Sphagnum* moss (Warner and Rubec, 1997).

Wetland surfaces are not commonly uniform. Many wetlands have relatively dry, elevated mounds (tussocks or hummocks) rising from low-lying, generally saturated areas (lawns or hollows) (Nungesser, 2003; Lai, 2009). Tussocks can range in height from several centimeters up to a meter and are generally oval but can be circular; while, low-lying saturated areas can either be in the form of open, flat small spaces between tussocks or large flat lawn areas or saturated pools (Nungesser, 2003). Microtopography within wetland environments has been found to remain relatively unchanged over centuries to millennia and general agreement indicates that tussocks and lawns maintain themselves indefinitely (Barber, 1981); however, the mechanisms which control formation and control over time are not well understood (Nungesser, 2003). Johnson and Damman (1991) infer that morphological differences between tussocks and lawns are caused by varying decomposition rates. Some studies suggest that *Sphagnum* species within tussocks decay at a slower rate and retain their physical structure longer than those within hollows, indicating that peat accumulates at a higher rate within tussocks (Johnson and Damman, 1991; Ohlson and Dahlberg, 1991). However, Nungesser (2003) argues that there is no single factor that can determine the growth and resilience of tussock and lawn microtopography; rather, it is likely that a covariance between moisture, *Sphagnum* growth and decay, and peat accumulation that dictates the overall morphology of a wetland through time.

2.2 Fluxes of CO₂, CH₄, and DOC

Fluxes of C in arctic wetland ecosystems are dominated by atmospheric exchanges of CO₂ and CH₄ and the loss of DOC. As global warming continues, CO₂ and CH₄ production associated with accelerated decomposition processes (with warmer soil temperatures) represent the dominant pathways through which this stored C may be released to the atmosphere (Christensen, 1995). Warming could also increase active layer depth in permafrost soils and facilitate the export of previously frozen DOC to other ecosystems and eventually to water bodies where it is used as a food source for bacteria, resulting in greater CO₂ emissions to the atmosphere (Bushaw *et al.*, 1996). Warming could result in negative effects on freshwater ecosystems, altering the timing and concentration of DOC flux (Bushaw *et al.*, 1996; Shindler and Curtis, 1997; Gergel *et al.*, 1999) which controls aquatic microbial diversity, productivity, biogeochemical cycles, and attenuation of ultra violet and visible radiation, impacting overall water quality (Pastor *et al.*, 2003; Waldron *et al.*, 2008).

For relatively dry soils, CO₂ is the dominant greenhouse gas exchanged between terrestrial ecosystems and the atmosphere. In moist, anaerobic soils, such as wetlands and peatlands, CH₄ exchange may be significant. In view of atmospheric warming, CH₄ has a 72-fold (over 20 years) greater warming effect on the atmosphere per gram than that of CO₂. Therefore, it is important to quantify both gas fluxes in order to determine the greenhouse warming potential (GWP) of an ecosystem (Friborg *et al.*, 2003). GWP is defined as the time-integrated radiative forcing of a gas over a given period relative to the same amount of CO₂ over that period (IPCC, 2007). However, it is important that the appropriate 'period' be used to assess the GWP of an ecosystem. While CO₂ is relatively

stable in the atmosphere, CH₄ denatures comparatively quickly. Consequently, the greenhouse gas inventory for an ecosystem should be evaluated over an ecosystem's lifetime, which for wetlands, may be several thousand years (Frolking *et al.*, 2006).

While there have been studies that have investigated CO₂ and CH₄ fluxes in arctic ecosystems (Vourlitis and Oechel, 1999; Christensen *et al.*, 2000; Lafleur and Humphreys, 2008; Willie *et al.*, 2008), these studies either employed the use of chambers (< 1 m²) to assess the C budget or only measured CO₂ or CH₄ exchange at an ecosystem scale (up to ~1 km²) using micrometeorological techniques. At present, there have been very few studies that have facilitated direct comparison of the combined greenhouse forcing effects of these two gases from natural ecosystems (Friborg *et al.*, 2003). While chamber techniques have been used to assess CO₂ and CH₄ fluxes within arctic ecosystems, the accuracy of upscaling these measurements to the ecosystem scale is uncertain due to the spatial and temporal variability of biotic and abiotic factors (Riutta *et al.*, 2007; Willie *et al.*, 2008). Therefore, there exists a need for ecosystem-scale measurements of both CO₂ and CH₄ flux within arctic environments in order to accurately determine the flux of C to the atmosphere. In addition, there also exists a need to assess the DOC budget of many of these ecosystems. DOC can play a pivotal role in assessing the C sink/source status of an ecosystem (Strack *et al.*, 2008)

Eddy covariance and chamber techniques are two well established methods to determine trace gas flux at the ecosystem and small plot scales, respectively. The primary advantage of the chamber technique is the ability to enclose small areas of an ecosystem in order to investigate the influence of small scale variations in ecosystem characteristics (e.g. plant composition, soil characteristics, microtopography, etc) on

fluxes. However, for non-automated versions, the measurements must be made manually such that only a small sample size in time and space is obtained, the equipment can be heavy and cumbersome to carry in remote areas, and the operator and the chamber itself disturbs the ecosystem by isolating it from the surrounding atmosphere such that light, gas concentrations, temperature and humidity do not remain at ambient conditions during a measurement. The primary benefits of the eddy covariance technique include instantaneous measurements of fluxes continuously for a measurement period at the ecosystem scale. However, for the eddy covariance technique to provide meaningful measures of biotic fluxes, relatively level and homogeneous terrain is required.

2.2.1 CO₂, CH₄, and DOC Cycling

2.2.1.1 CO₂ Flux

Net ecosystem exchange of CO₂ (NEE) is the difference between photosynthetic uptake of CO₂ and the emission of CO₂ through respiration within an ecosystem. Gross ecosystem production (GEP) is the rate of photosynthetic uptake of CO₂ by plants. Ecosystem respiration (ER) is defined here as the production of CO₂ through several biochemical processes. Aerobic respiration, oxidation of CH₄, and anaerobic fermentation of glucose to organic acids all result in the formation of CO₂ (Luo and Zhou, 2006). ER can be divided into two main components, autotrophic respiration (plant respiration) (ER_a) and heterotrophic respiration (microorganism respiration) (ER_h), such that ER is equal to the sum of both ER_a and ER_h for a given period. The metabolic process of plant functioning controls ER_a; as such, it is strongly related to plant productivity. Plant growth is influenced by such abiotic factors as temperature, nutrient and moisture availability, and photosynthetically active radiation (PAR). ER_h is

controlled by substrate availability and quality, temperature, and moisture characteristics of the soil (Elberling, 2007). Anoxic conditions, low temperatures, small microbial populations, and high refractory content of litter causes low decomposition rates in northern peatlands (Moore and Basiliko, 2006) resulting in CO₂ accumulation rates of 76 Tg C y⁻¹ globally (Gorham 1991).

2.2.1.2 CH₄ Flux

The cycling of CH₄ in peatlands involves numerous biogeochemical processes which are controlled by various chemical, physical, and biological factors (Kutzbach *et al.*, 2004; Lai, 2009). Production of CH₄ in northern peatlands results in approximately 46 Tg CH₄-C y⁻¹ released to the atmosphere (Gorham, 1991), which is equivalent to 12.2% of global input (Wuebbles and Hayhoe, 2002). Net contribution of wetland CH₄ to the atmosphere is the difference between production and oxidization of CH₄ in the anoxic and oxic regions.

Whalen (2005) describes the two main ways in which CH₄ is generated as a metabolite by methanogens (CH₄ producing microbes) during energy production in anaerobic conditions. Acetate substrate (CH₃COOH) is used by acetotrophic methanogens to produce CH₄ and CO₂ and is known as acetoclastic methanogenesis. Hydrogen gas (H₂) and CO₂ are used by hydrogenotrophic methanogens during the reduction process to produce CH₄ and water. Generally, acetoclastic methanogenesis occurs in upper peat layers where decomposition of fresh root litter and root exudates are the predominate source of energy for microorganisms. In lower peat layers, where organic material is recalcitrant (resists bioactivity), H₂ and CO₂ methanogenesis predominates (Hornibrook *et al.*, 1997).

Oxidation of CH_4 by methanotrophs in the aerobic zones may occur after CH_4 production through methanogenesis in underlying anaerobic peat layers. Methanotrophic activity occurs as high affinity oxidation, primarily at CH_4 concentrations close to atmospheric values, and as low affinity oxidation, dominant in northern peatlands where CH_4 concentrations are very high (Segers, 1998). Methanotrophs at low affinity break the oxygen molecule (O_2) into oxygen atoms (O) and form water (H_2O) and methanol (CH_3OH). Methanotrophy generally reaches peak rates at the interface between anaerobic and aerobic zones where the ratio of oxygen to substrate CH_4 is favorable (Dedysh, 2002). Water tables near or at the surface minimize the potential for CH_4 oxidation, while water tables at depth allow for greater methanotrophic activity and reduce net emissions of CH_4 . Segers (1998) found that the potential for CH_4 oxidation is approximately an order of magnitude greater than that of CH_4 production. Therefore, the consumption and release of CH_4 relates to transport to and through zones of oxidation.

There are three main pathways by which CH_4 may reach the atmosphere from production zones in peatlands: diffusion, ebullition, and plant mediated transport (Lai, 2009). A concentration gradient generally develops between the saturated anaerobic zone of CH_4 production and the unsaturated aerobic zone of CH_4 oxidation. As such, this concentration gradient drives the molecular diffusion of CH_4 to the surface. Diffusive flux is considerably slower than the other two mechanisms, yet provides the necessary contact of CH_4 with the methanotrophic community, ultimately controlling the rate of CH_4 oxidization (Whalen, 2005). Ebullition releases CH_4 to the atmosphere when supersaturation occurs at very high rates of methanogenesis deep in the pore water of anaerobic peat layers. Ebullition occurs when the partial pressure of gases in solution are

greater than the hydrostatic pressure of peat (Chanton and Whiting, 1995). The bubbles attach to pore walls by adhesive forces until they grow in size and their pressure is greater than the forces of attraction, resulting in gas bubble ejection. Ebullition is caused by atmospheric pressure drop, reduction in hydrostatic pressure, or a rise in temperature (Strack *et al.*, 2005; Tokida *et al.*, 2007). Tokida *et al.* (2007) found in a northern peatland that ebullition accounted for approximately 50 to 65% of total CH₄ flux. Plant mediated transport of CH₄ may also occur through the presence of aerenchyma tissue found in vascular plants such as *Carex* spp. (Bellisario *et al.*, 1999; Strom *et al.*, 2003, Strack *et al.*, 2004). The primary function of aerenchyma tissue is to deliver oxygen to submerged organs in anoxic peat below the water table; however, at the same time, they can serve as direct conduits for CH₄ in the root zone to flow to the atmosphere, bypassing the methane-oxidizing, aerobic peat layers (Whalen, 2005). The two primary mechanisms in plant-mediated transport of CH₄ are molecular diffusion and bulk flow. Many studies involving aerenchyma adapted vascular vegetation such as sedges have found increased rates of CH₄ emission relative to sites without sedges or with sedge removal (Whalen and Reeburgh, 1990; Canton and Whiting, 1992; Torn and Chapin, 1993; King *et al.*, 1998).

Temporal and spatial variation in CH₄ flux is attributed to variation in water table depth (WT), air and soil temperature, peat acidity, vegetation type, and plant productivity (NPP) (Lai, 2009). Segers (1998) also suggests that an important control on methanogenesis is the supply of organic substrate once anaerobic conditions are established in peat layers. In addition to organic substrate, soil temperature and WT interact strongly to influence the production and oxidation of methane (Granberg *et al.*,

1997). With a high water table near or at the surface, increases in temperature at depth in the anaerobic zone will result in increased methane production and emission; however, when the water table decreases below the surface, and the zone of oxidation increases, temperature in the oxic zone has an increasing influence to temperatures in the anoxic zone on methane production and emission (Granberg *et al.*, 1997). In addition, as the anaerobic zone decreases from the surface, temperatures within this zone will also decrease, limiting the potential for greater methane production (Granberg *et al.*, 1997). Therefore, increases in temperature at depth will influence the production of methane; however, it is strongly related to changes in water table.

2.2.1.3 DOC Flux

DOC is defined as small (less than 0.45 μm in diameter) organic material (Wangersky, 1993). Dissolved inorganic carbon (DIC) is defined as the total amount of inorganic carbon within a solution and refers to C supplied by carbonate sources (Worrall *et al.*, 2003), including CO_2 , carbonic acid, bicarbonate anion, and carbonate (Schumacher, 2002). Temperature, soil moisture, soil solution chemistry, vegetation community and site hydrology have all been found to play an integral role in influencing DOC concentrations and fluxes (Moore *et al.*, 1998; Kalbitz *et al.*, 2000; Strack *et al.*, 2008). Many studies conclude that the major factor controlling DOC flux is storm events which cause large amounts of water to flow through the soil and over land (Waddington and Roulet, 1997; Clark *et al.*, 2007; Pawson *et al.*, 2008; Strack *et al.*, 2008). However, Clark *et al.* (2007) suggests that ultimately DOC is controlled by discharge volume which is a function of the topography of the wetland and the surrounding area, precipitation in the form of rain and snow, and snow melt. Boreal peatland studies in Sweden have shown

that DOC loss via groundwater movement can account for up to 10 times the amount of C lost via CH₄ emissions to the atmosphere (Waddington and Roulet, 1996). Waddington and Roulet (1997) found that the total mass flux of DOC accounted for approximately 20% of CO₂ fixation. While, Fraser *et al.* (2001) found in a northern ombrotrophic peatland that DOC flux was equal to 12% of the C stored through NEE and between 28 to 48% of sequestered long-term C; DOC flux from northern peatlands ranges from 1 to 48 g C m⁻² y⁻¹; however, in arctic areas, where catchments are dominated by peat, relief is negligible, and precipitation is equal to evapotranspiration, DOC flux measurements tend to be smaller (i.e. less than 10 g C m⁻² y⁻¹) (Fraser *et al.*, 2001).

2.2.1.4 Carbon Budget Studies

There have been many northern studies that have investigated some aspect of ecosystem/watershed-scale CO₂, CH₄, or DOC exchange in the Arctic (Waddington and Roulet, 1997; Griffis *et al.*, 2000; Lafleur *et al.*, 2001; Friborg *et al.*, 2000; Friborg *et al.*, 2003; Lafleur and Humphreys, 2008; Fox *et al.*, 2008; Willie *et al.*, 2008); however, there has only been one study that the author is aware of that concurrently measured CO₂ and CH₄ exchange at the ecosystem scale (Friborg *et al.*, 2003), and to the author's knowledge, there have not been any studies that directly relate CO₂, CH₄, and DOC to the total C budget of an arctic ecosystem. There have been a few studies that have related all three components of the C budget within non-arctic peatland ecosystems (e.g. Worrall *et al.*, 2003, Roulet *et al.*, 2007). Results from studies in the Arctic indicate that CO₂ and CH₄ flux shows great spatial variability within plot-to-plot comparisons in the same ecosystem with regard to sink/source magnitude (Christensen *et al.*, 2000; Corradi *et al.*, 2005). Some studies have also shown that inter-annual variability in CO₂ fluxes can

result in net C release one year and a C sink the next (Oechel *et al.*, 1993, Vourlitis and Oechel, 1999; Oechel *et al.*, 2000) with the possibility that the change between sink/source status may be due to a variety of environmental conditions brought about by natural inter-annual climate variability.

Christensen *et al.* (2000) found in certain northern wetland and tundra environments that CO₂ and CH₄ fluxes are influenced by soil saturation, temperature, active layer depth, growing season length, topography, and plant species. Many studies conclude that there is no one single environmental variable that governs the flux of CO₂ and CH₄ (Whalen *et al.*, 1992; Bartlett and Harris, 1993; Torn and Chapin, 1993; Bubier and Moore, 1994). Climate change is expected to influence all of these variables, such that it is possible that some arctic ecosystems may change from an annual sink of C to a source of C (Vourlitis and Oechel, 1999; Oechel *et al.*, 2000; Friberg *et al.*, 2003; Lafleur and Humphreys, 2008) with important consequences to the global C budget.

Fluxes of CO₂, CH₄, and DOC can all play an important role in determining the overall C sink/source strength of a system. There remains uncertainty regarding the current magnitude of CO₂, CH₄, and DOC fluxes for arctic wetlands. Although much is known regarding the environmental controls which affect these C fluxes at varying spatial and temporal scales, there remains uncertainty regarding their effects on the spatial and temporal variations in the C budget of arctic peatland ecosystems. Further estimates of the current C budgets of these ecosystems and how they respond to variations in temperature and moisture will help improve our understanding of important terrestrial surface-atmosphere feedbacks to the climate system.

3.0 METHODS

3.1 Site Description

The field study site is located close to Daring Lake, central Northwest Territories, Canada (64° 52' N, 111° 34' W) at TERS, approximately 70 km above the tree line and 300 km northeast of Yellowknife within the Southern Arctic Ecozone. The research area is located in a sedge fen approximately 1 km from the TERS (Figure 1). Research was conducted in collaboration with the Canadian Tundra Ecosystem Carbon Study at Daring Lake, established in 2004 to investigate the magnitude of and controls on C fluxes within these tundra ecosystems (Lafleur and Humphreys, 2008).

The climate is characterized as having short, snow-free, growing seasons with mean monthly temperatures above 0° C from June through September. The growing season typically spans mid June to early September. The mean annual temperature is -13 °C and precipitation varies from 200-400 mm (Lafleur and Humphreys, 2008; Natural Resources Canada, 2009). The area has a shallow seasonal active layer between 0.3 – 1.2 m deep, with variation in depth depending on soil type and vegetation, and is underlain by continuous permafrost to a depth of >160 m (Dredge *et al.*, 1999). The period from May 15 to Aug 31 2009 had an average air temperature of 6.5 °C and 80.9 mm of rain, making 2009 slightly cooler and drier than the average of 8.4 °C and 103.7 mm recorded at the site over the same dates from 1997 to 2005 (Lafleur and Humphreys, 2008).

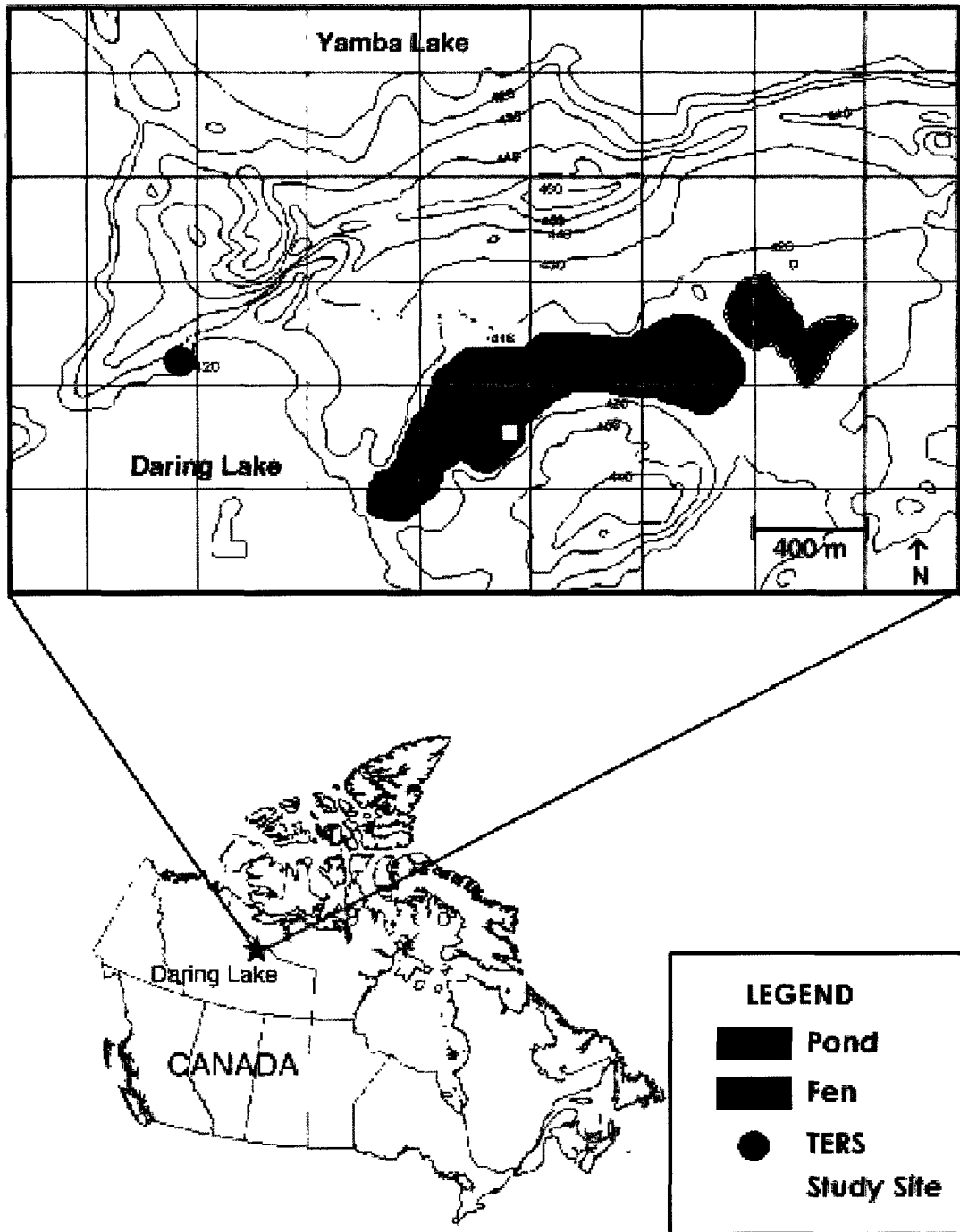


Figure 1. Map of the research area at Daring Lake, NT with the location of the Tundra Ecological Research Station (TERS), fen and study site (Adapted from Nobrega and Grogan, 2008).

The roughly 48 ha sedge fen where the study took place lies along the bottom of a shallow ~1.5 km long by 1.0 km wide valley, draining into Daring Lake. The age of the fen is approximately 1920 ± 80 yrs before present (Okolo, 2008). The fen includes a variety of vegetation communities (Figure 2) including raised peat mounds with dwarf birch (*Betula glandulosa*) but is dominated by lawns and tussocks populated by sedges (*Carex* spp., *Eriophorum* spp.), bog rosemary (*Andromeda polifolia*), and a nearly continuous ground cover of moss (*Sphagnum* spp.) (Figure 3). For the tussock and lawn communities, peak LAI of all vascular plants was $0.80 (\pm 0.04 \text{ SE})$ as determined using the point frame method. Peak vascular LAI determined using the LAI-2000 Plant Canopy Analyzer (LI-COR Inc., Lincoln, NB, USA) was similar at $0.66 (\pm 0.15)$. The fen soil consisted of a layer of peat varying from approximately 40 cm (lawns) to 60 cm (tussocks) over silt loam mineral soil (Table 1) (Hayne, 2009), and completely freezes during the winter season. By mid August 2009, the peat layer had thawed with a maximum thaw depth of $47.4 (\pm 0.8)$ cm and $62.4 (\pm 0.8)$ cm for the lawn and tussock communities.

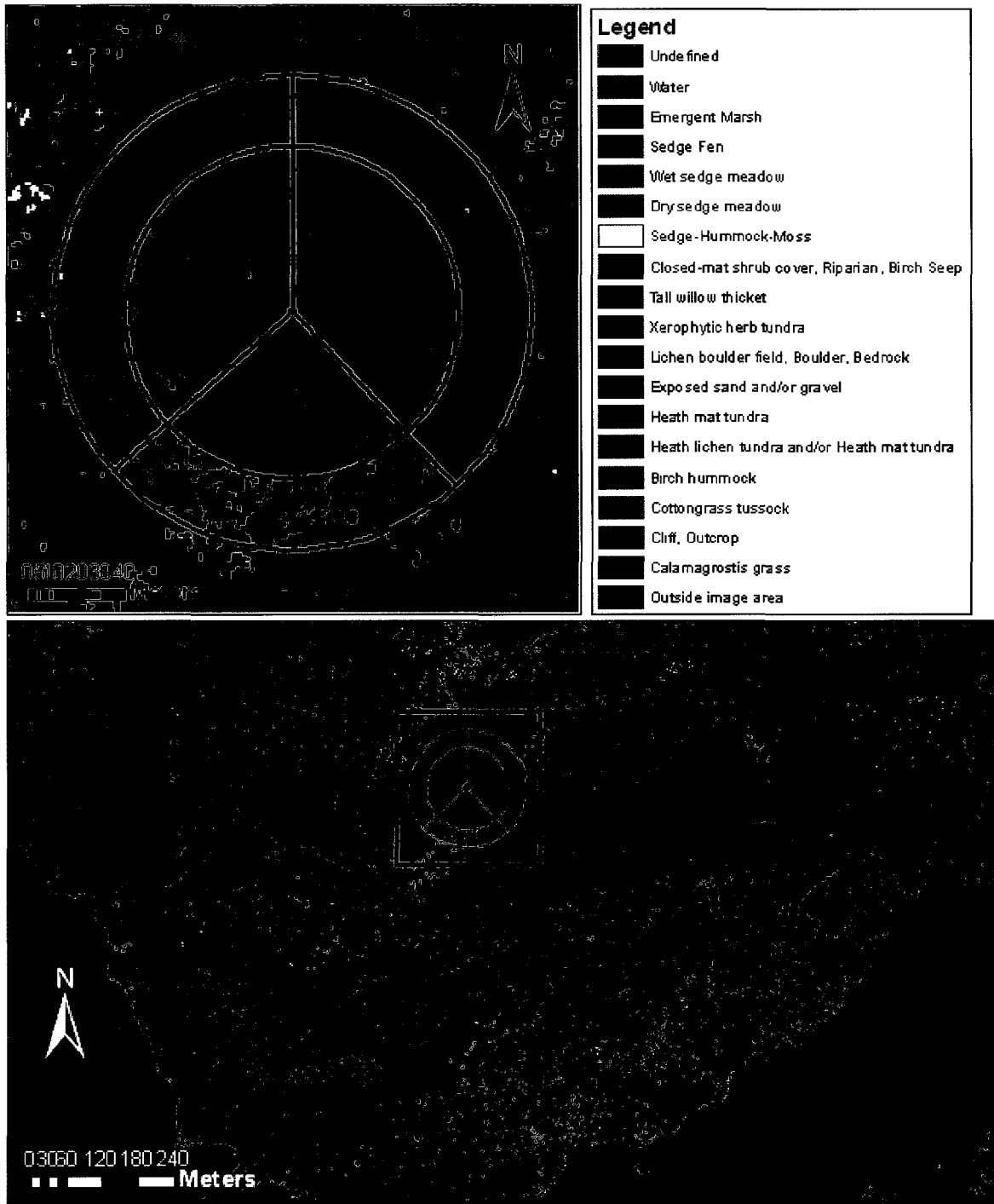


Figure 2. Vegetation map (edited from Obst, 2008) showing the location of micrometeorological tower within the wet fen at Daring Lake, NT. Inner ring represents radius of 70 m and outer ring a radius of 100 m. Three sectors are delineated: 0° - 135° (sedge fen dominated by lawn topography to NE, rocky upland area to SE); 135° - 225° (sedge fen with tussock topography, small, open water bodies and rocky upland area); 225° - 360° (sedge fen and shrub peat mound areas).



Figure 3. Top panel – NE aerial view of Darling Lake, NT including Yamba Lake in top left. Yellow circle gives approximate location of micrometeorological tower. Bottom panel – Micrometeorological setup with a view to the north. Lawn and tussock topography is shown in foreground.

3.2 Experimental Design

Both micrometeorological and chamber techniques were used to quantify CO₂ and CH₄ exchange between the fen and the atmosphere during a period from July 11th (DOY 192) to August 15th (DOY 227) 2009. The eddy covariance (EC) technique was used to measure ecosystem-scale C fluxes on a continuous basis while chamber measurements were made to investigate small scale spatial variations in these exchanges. In order to determine the relationships between ecosystem CO₂, CH₄, and environmental variables (biotic and abiotic), we needed continuous measurements (30 minute averages) of wind velocity and direction, air and soil temperature and moisture, photosynthetically active radiation, and water table depth. In order to determine the relationships between CO₂ and CH₄, microtopography, and environmental variables at the small plot-scale, we needed to measure air and soil temperature and moisture, photosynthetically active radiation, leaf area index, species composition and distribution, and thaw layer depth at the same time as CO₂ and CH₄ measurement. The EC tower (Figure 3) was located at 64° 51' 52" N and 111° 33' 59" W (NAD 27) approximately 100 m from the southern edge of the fen (Figure 2). Sixteen permanent collars were installed along a boardwalk within the fetch of the micrometeorological tower (Figure 4). The permanent locations of the 16 collars were assigned randomly along the boardwalk at the beginning of the study period. Eight collars (PVC SDR-35 sewer pipe inner diameter 29.5 cm and an area of 683.5 cm²) were installed in lawn (L) and tussock (T) communities. The lawn collars were 12 cm tall and inserted 5 cm into the soil to form a good seal with the surrounding saturated peat. The tussock collars were 20 cm tall and inserted approximately 15 cm to reach a depth that was generally saturated in order to prevent diffusion of CO₂ and CH₄ gas from the bottom

of collar. A knife was used to cut into the peat around the collar exterior and the vegetation was guided up through the centre of the collar before insertion. All collars had a groove in the top rim which was filled with water to form a seal between the chamber and the collar during sampling to minimize gas leaks.

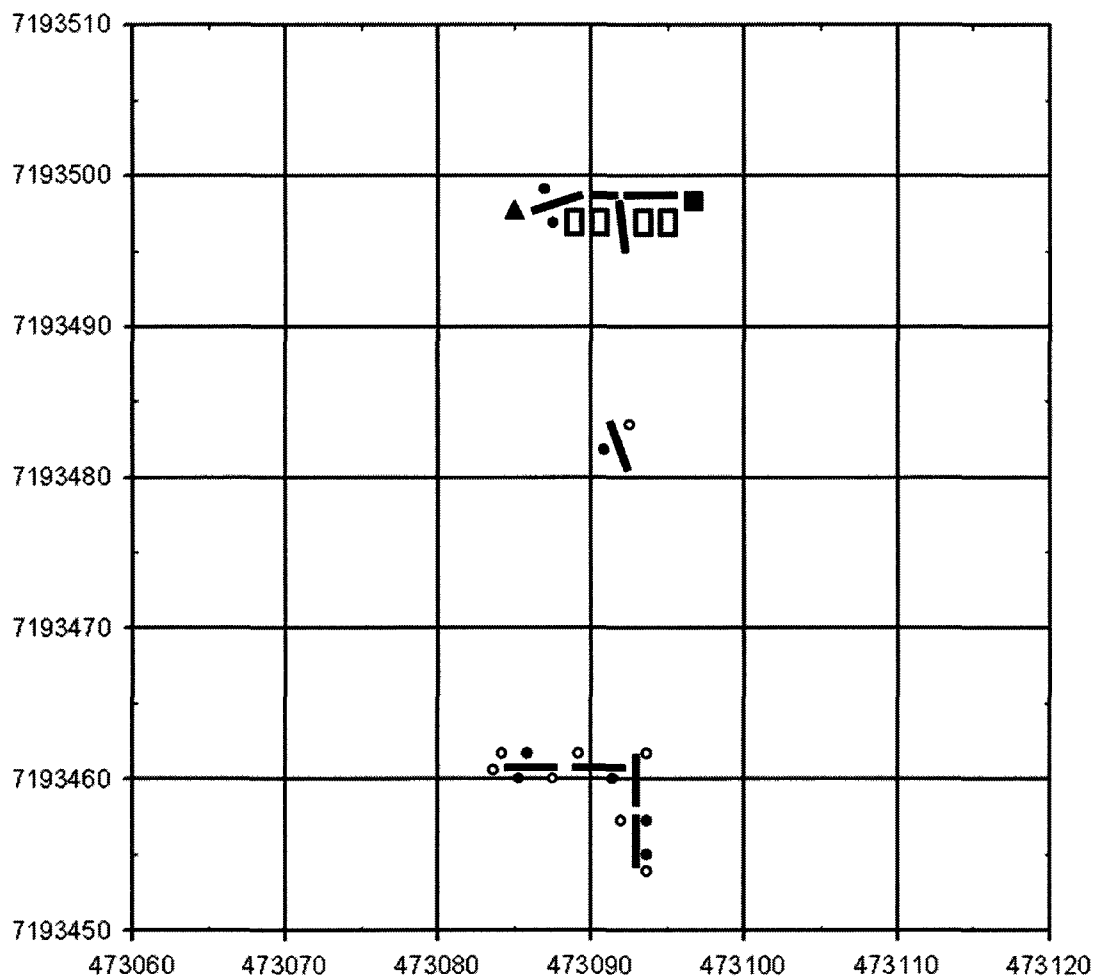


Figure 4. Plot locations of 16 permanent collars installed at Daring Lake, NT, 2009. Closed circles represent lawns and open circles represent tussocks. The closed black square represents micrometeorological tower, open squares represent solar panels, and closed triangle represents the generator. UTM coordinate system in Easting and Northing, Map 12N (North America). Locations are within 2 meter accuracy.

3.3 Data collection

3.3.1 NEE Chamber System

NEE was measured using a portable, closed, flow-through, non-steady state chamber system. The system consisted of the collar, a clear acrylic chamber lid (0.0197 m³) connected by tubing to an external infrared gas analyzer (IRGA) (LI-840, LI-COR Inc., Lincoln, NB, USA) via a pump. NEE was measured by sealing the chamber to the collar and measuring the change in CO₂ and H₂O concentrations within the chamber volume over a 2 min interval. In order for a relationship between NEE, light and temperature to be achieved, NEE was measured under four different light levels: full light using a clear, uncovered chamber, partial shade using a layer of 50% shading cloth over the chamber, more shade using two layers of 50% shading cloth, and opaque conditions using a heavy duty black plastic garbage bag over the chamber. Under opaque conditions, ecosystem respiration of CO₂ (ER_F) was measured; while, gross ecosystem production (GEP_{max}) was estimated as the difference between full light NEE (NEE_{max}) and ER_F measurements. Incoming photosynthetically active radiation (PAR) was measured using a quantum sensor (model LI-190, LI-COR Inc., Lincoln, NB, USA) mounted upon a tripod and subjected to the same shading conditions as the chamber. PAR received by the vegetation within the chamber was adjusted to 92% of sensor PAR to account for attenuation caused by the clear acrylic of the chamber (Kim *et al.*, 2004). Mounted within the chamber was a mixing fan, which continually mixed air within the chamber to prevent a concentration gradient from developing at the top of the chamber lid, a Peltier cooler, which was activated if chamber temperature elevated above ambient air temperature by 2 °C to maintain near ambient conditions, and a fine-wire

thermocouple, which measured the air temperature within the chamber. Bev-a-line inflow and outflow tubing were attached to the chamber lid and connected to the portable IRGA system. A pump circulated air in the system at 2 L min^{-1} with a subsample of air drawn into the IRGA at 0.7 L min^{-1} . A CR23X data logger (Campbell Scientific, Inc., Edmonton, AB, Canada) recorded date, time, CO_2 and H_2O concentrations, air temperature, and PAR at 1 Hz. The system was powered by a 12 V battery. All data was downloaded and stored on a computer at the end of each sampling day.

NEE measurements were made on days when incoming PAR was on average greater than $700 \mu\text{mol m}^{-2} \text{ s}^{-1}$. This allowed for a light response curve to be developed in relation to NEE, PAR, and T. During the 2009 field campaign, measurements on all collars were carried out on 13 days. The sampling order of 16 collars was randomized each day.

3.3.2 Opaque Chamber System

Static opaque chambers (0.0219 m^3) were used to measure respired CO_2 (ER_S) and CH_4 exchange in dark conditions which prevents the fixation of CO_2 through photosynthesis. These measurements were made by sealing a simple acrylic chamber to the collar and measuring the change in CO_2 and CH_4 concentration within the chamber volume over a 20 min interval. During this time, gas samples were taken at 0, 5, 10, 15, and 20 min. First, a 60 ml syringe connected by Bev-a-line tubing to the chamber was manually pumped 4-5 times to mix the chamber air before withdrawing a 27 ml sample from a septa attached to a 3-way stopcock. The gas sample was then injected into a pre-evacuated vial (Labco International Inc., Houston, TX, USA). Vials contained small amounts of magnesium perchlorate, a desiccant, to remove any moisture within the

sample. The gas samples were stored up to 2 months and transported to Carleton University's Biometeorology laboratory where CH₄ and CO₂ concentrations were determined using a gas chromatograph (CP 3800, Varian, CA, USA). The gas chromatograph was equipped with a methanizer and flame-ionization detector (FID) operating at 350 °C and 300 °C, respectively, both using helium carrier gas at a rate of 30 ml min⁻¹. Haysep N 80/100 pre-column (0.32 cm diam. × 50 cm length) and Poropak QS 80/100 mesh analytical columns (0.32 cm diam. × 200 cm length) were used in the column oven maintained at 50 °C to achieve gas separation from the samples. Three replicates of 5 standard gas concentrations (between 439.2 and 15212.6 ppm for CO₂ and between 1.08 and 19.94 ppm for CH₄ along with He blanks) were used to maintain quality control and establish a linear relationship between gas concentrations and chromatogram area (Hayne, 2009).

ER_S measurements were made on both clear and cloudy days when NEE measurements were not feasible. During the 2009 field campaign, measurements were carried out on 16 days. The sampling order of the 16 collars was randomized each day.

3.3.3 Environmental Variables

During chamber measurements, several environmental variables were measured within close proximity to each collar. Thermocouples permanently installed at 2, 5 and 10 cm soil depths and were measured using a digital thermometer (HH81 A, Omega, Laval, QC, Canada). Average soil volumetric water content (0-20 cm VWC) (m³ m⁻³) was measured by inserting a probe (Hydrosense, Campbell Scientific Inc., Logan, UT, USA) vertically to a depth of 20 cm from the soil surface. VWC was also measured continuously every 30 min at 5 and 10 cm depths within two lawn and two tussock

communities with an additional measurement at 20 cm in each tussock community (logger: EM5b, probe: Echo EC-5, Decagon Devices Inc., New Hampshire, WA, USA).

The point frame method was used to assess vegetation characteristics at the peak of biomass (beginning of August). Forty-four pin drops were made at the intersection of grid lines within a 4 x 4 cm grid, set over each collar. For each pin drop, the number of times green leaves touched the pin was recorded along with the plant functional type or species. If no vascular vegetation was touched but the pin contacted moss, this was noted separately. For each collar, % vascular cover, % moss cover and vascular leaf area index (LAI) was calculated. Total vascular LAI was calculated by dividing the total number of vascular vegetation “hits” by the total number of pin drops.

Thaw depth was recorded approximately every 10 days by inserting a steel rod 10 times into the peat at random locations along the fen boardwalk.

Water table depth was recorded, in reference to the lawn surface, using a float and potentiometer apparatus within a perforated polyvinyl chloride (PVC) pipe. Water table depth was also measured manually to establish a relationship between potentiometer readings and the water table depth.

3.4 Ecosystem Exchange of CO₂ and CH₄

3.4.1 Eddy Covariance Measurements of CO₂ and CH₄

Fluxes of CO₂ and CH₄ were obtained from eddy covariance instrumentation mounted upon the fen tripod which was erected in 2006. The instrumentation included a 3D sonic anemometer (R3-50, Gill Institute, Lymington, UK), and a CO₂/H₂O open-path infrared gas analyzer (IRGA) (LI-7500, LI-COR Inc., Lincoln, NE, USA) mounted at 2.5 m height from the peat surface. CH₄ mol fraction was measured using a closed-path fast

methane gas analyzer (FMGA) (907-0001-0002, Los Gatos Research, Mountainview, CA, USA) with air pulled through 3.5 m polyethylene coated tubing with an inner diameter of 4 mm (Dekabon Type 1300, Dekoron, Furon Brands, Aurora, Ohio, USA) by a pump (N920, KNF, Trenton, NJ, USA) approximately 10 L min^{-1} . This flow rate resulted in an effective sampling rate of 1.5 Hz by the FMGA. Velocity in 3 dimensions, air temperature, CO_2 , and H_2O mol density, and CH_4 mol fraction were measured at a rate of 10 Hz and stored on a data logger (CR1000, Campbell Scientific, Logon, UT, USA).

The eddy covariance system was powered using batteries charged using a combination of solar power and a generator. Continuous operation of the FMGA only occurred at the beginning and end of the field campaign (11 days). The charge controller failed early during the field campaign such that the FMGA was run directly off the generator for daytime periods.

3.4.2 Environmental Variables

Throughout the study period, the following environmental variables were recorded and stored at 30 min intervals: precipitation using a tipping bucket rain gauge (TE525m, Texas Electronics, Dallas, TX, USA), upwelling and downwelling photosynthetically active radiation (PAR) using quantum sensors (LI-190SA, LI-COR Inc., Lincoln, NB, USA), air temperature and humidity using a probe in a gill radiation shield (HMP45C, VaisalaOyj, Helsinki, Finland), atmospheric pressure using a barometer (PTB101B, VaisalaOyj, Helsinki, Finland), and wind speed using a propeller anemometer and vane (Wind Monitor, R. M. Young, Traverse City, IM, USA). These variables were measured at a nearby meteorological tower (Lafleur and Humphreys, 2008). On the tower at the fen, a four-component net radiometer (CNR1, Kipp&Zonen B.V., Delft, the

Netherlands) measured incoming and outgoing solar and long wave radiation. Copper-constantan thermocouples were installed at depths of 0.05, 0.10, 0.20 and 0.60 m within the peat profile.

3.5 Dissolved Organic Carbon

At the beginning of the field campaign, sampling wells were installed at the inlet and outlet to the fen to measure hydraulic head. Each pair of wells was installed 15 meters up/downstream from each other at the outlet and 20 meters up/downstream at the inlet. At the inlet, 3 pairs of wells were installed 30 meters apart (in the approx. N-S direction) from each other for a total of 6 wells. At the outlet, 3 pairs of wells installed only 5 meters apart because the outlet was smaller in width than the inlet. Wells consisted of perforated PVC pipe cut to a length of 1.5 meters and installed to maximum thaw depth. Wells were measured on 4 days approximately 10 days apart. During measurements, hydraulic head was recorded for each pair of wells using a theodolite. At this time, a 60 ml water sample was taken using a syringe. Samples were filtered and transferred to 100 ml bottles and stored frozen. Samples were analyzed for DOC at McGill University on a Shimadzu 5050 Total Organic Carbon analyzer. On each sampling day, the wells were pushed down into the peat to the maximum extent of thaw depth.

3.6 Data Analysis

3.6.1 Chamber Flux Calculation

CO₂ and CH₄ flux (F) for both the NEE and opaque static chamber systems was calculated using Equation 1,

$$F = \frac{V}{A} \frac{P}{RT} \frac{dx}{dt} \quad (1)$$

where flux of CO₂ and CH₄ are in units of μmol m⁻² s⁻¹ and nmol m⁻² s⁻¹ respectively and is determined from a linear rate of change in gas species mixing ratio (dx/dt), chamber area (A) and volume (V) in m² and m³ respectively, barometric pressure (P) in Pa, the gas constant (R) 8.314 J K⁻¹ mol⁻¹, and air temperature (T) in Kelvin. Negative fluxes signify ecosystem uptake of CO₂ or CH₄, while positive fluxes signify the release of CO₂ or CH₄ from the ecosystem.

3.6.2 NEE of CO₂ and CH₄ Flux Calculation

The eddy covariance (EC) method measures turbulent exchange of energy and trace gases such as CO₂ and CH₄ (Baldocchi, 2003). Eddy flux is determined as the covariance between instantaneous deviation in vertical wind speed (w') from the mean value (\bar{w}) and instantaneous deviation in the scalar of interest (s') from the mean value (\bar{s}),

$$F = \overline{p_a w' s'} \quad (2)$$

where the flux is multiplied by the mean air density (p_a). Several mathematical operations and assumptions, including Reynolds decomposition, are involved in deriving practical equations for computing flux from physically complete equations of the turbulent flow (Baldocchi, 2003). For the EC system described in this study, 30 min CO₂ fluxes were computed from vertical velocity and CO₂ mixing ratio as described by Lafleur and Humphreys (2008). The Webb-Pearman-Leuning procedure was applied to the 30 min CH₄ fluxes to account for density fluctuations caused by humidity variation

(Webb *et al.*, 1980). Corrections for energy closure or for high frequency flux losses were not applied.

NEE was calculated as the sum of 30 min CO₂ flux and the rate in change of CO₂ stored in the air column below the EC instrumentation (Lafleur and Humphreys, 2008). Quality control criteria described by Lafleur and Humphreys (2008) were used to remove fluxes that were physically or theoretically unsupported. In particular, this included removing fluxes at night when u^* was below 0.1 m s⁻¹ and during rainfall or when the diagnostic signal on the open-path IRGA indicated the path was obstructed. NEE is negative while GEP exceeds ER during daylight hours and is positive when photosynthesis ceases during the night (defined as PAR less than 20 $\mu\text{mol m}^{-2} \text{s}^{-1}$) and during the day when ER exceeds GEP.

3.6.3 Light-Temperature Response

The relationship between NEE and PAR and T is described by the following,

$$NEE = \frac{GP_{\max} \alpha PAR}{GP_{\max} + \alpha PAR} + R_{10} Q_{10}^{\frac{T-T_{ref}}{10}} \quad (3)$$

where the first term on the right-hand side of Equation 3 relates GEP to photosynthetically active radiation (PAR) through a rectangular hyperbolic relationship. The second term on the right describes the exponential relationship between ecosystem respiration (ER) and air temperature (T) within the chamber. GP_{\max} is the maximum photosynthetic uptake of CO₂ at saturating light; while, α is the effective quantum yield. R_{10} is ER at a reference temperature (T_{ref}) of 10 °C, and Q_{10} is the relative increase in ER for every 10 °C increase in temperature and is generally near 2 (Lloyd & Taylor, 1994).

3.6.4 DOC Flux Calculation

Through the use of Darcy's law, which relates the instantaneous discharge rate of a fluid through a medium to the viscosity of a fluid and the pressure drop over a given distance, it is possible to determine the flow rate and compute the inputs and outputs of DOC within a peatland catchment. A simplified version of Darcy's law is,

$$Q = \kappa A \frac{dh}{dz} \quad (4)$$

where Q is the discharge rate ($\text{m}^3 \text{s}^{-1}$), κ is permeability (saturated hydraulic conductivity) of peat (m s^{-1}), A is the cross-sectional area (m^2), and dh/dz is the difference in hydraulic head from one point to another (m m^{-1}).

DOC flux for the growing season was determined using an average daily flux rate calculated for the entire study period and is explained as follows. As κ was not measured, a value of 10^{-4} m s^{-1} was applied, which is between the generally accepted values of peat permeability (10^{-2} and 10^{-5}) (Bear, 1972). Cross-sectional area was determined for the inlet and outlet, respectively, as the total width of the inlet (240 m) and outlet (40 m) multiplied by the average depth of water table above frost table for the 6 wells at each location for each sampling period. dh/dz for the inlet and outlet was determined as the average difference between the hydraulic head for each of the 3 pairs of sampling wells. An average Q for the inlet and outlet during the 3 sampling periods was determined and was multiplied by the average concentration (mg l^{-1}) of DOC from the 6 wells at each location during the sampling period. The flux of DOC was determined as the difference between the discharge rate at the outlet and inlet. A negative value indicated DOC storage, while a positive value indicated DOC loss. As only three sampling periods occurred, in order to determine the growing season DOC flux, the three periods were

averaged to determine an overall daily storage rate which was extrapolated for the entire growing season. This method likely represents an underestimation of the total DOC flux as measurements were not typically made during or immediately after large rain events.

3.6.5 Flux Footprint

Flux footprint (footprint distance) is defined as the area upwind where atmospheric flux is generated and measured by instrumentation downwind. Using an eddy covariance tower, it is a measure of the influence of an area to an observed vertical turbulent flux. Footprint distance is also known as fetch (Schuepp *et al.*, 1990). The dimensions for the flux footprint representing the area from which 90% of the flux originates were calculated using FSAMwin.exe (Schmid, 1994). Input parameters included the height of the EC instrumentation (2.5 m), roughness length (0.02 m), stability (MoninObukhov length, L) and the ratio of the standard deviation of lateral velocity to friction velocity (σ_v/u_*).

3.6.6 Gap-filling and C budget Calculations

In order to determine the growing season CH₄ emission, it was necessary to determine a functional relationship between CH₄ flux and its primary environmental drivers which could be used for extrapolation and gap-filling. A relationship between temperature and frictional velocity has been well documented in previous studies (Friborg *et al.*, 2000; Wille *et al.*, 2008) and are included in the model following their approaches as,

$$CH_4 Flux = a \times b \frac{T - T_{ref}}{10} \times c^{u^* - u^*_{ref}} \quad (5)$$

where CH₄ flux is the measured flux, *a*, *b*, and *c* are the parameters fit using non-linear least squares regression with 5 cm soil temperature (*T*) and friction velocity (*u**) as the independent variables and *T_{ref}* and *u*_{ref}* are the mean values during the measurement period. A combination of linear interpolation and empirical modelling was used to gap-fill NEE as described by Laflour and Humphreys (2008). For short periods with gaps of one or two half hours, linear interpolation was used; however, for longer periods, variations in 30-min NEE were modelled using the functional relationship described in Equation 3. Following the procedure of Laflour and Humphreys (2008), modelled values were adjusted for seasonal variations in ER and GEP caused by phenology, moisture limitations, nutrient supply, etc, were applied by fitting predicted ER and GEP to observed fluxes using a moving window. For a more detailed explanation see Laflour and Humphreys (2008).

To determine the growing season C budget, modelled growing season daily NEE was summed and losses of C through CH₄ emission (modelled with Equation 5), and DOC export (determined using Equation 4) were subtracted. To determine the radiative forcing potential of the fen, methodology outlined by the IPCC (2007) was used to give a GWP for the growing season. IPCC (2007) states that CH₄ has, on a per gram of C basis, 72 and 21 times the GWP of CO₂ over the 20 year and 100 year timescale, respectively.

3.7 Statistical Analysis

All statistical analysis of data was performed using JMP (J.M.P.8 Statistical Analysis Software, 2008). One-way analysis of variance (ANOVA) was used to

determine differences in vegetation and microclimate characteristics among lawn and tussock variables. Post-hoc multiple comparisons were computed using the Tukey's Honest Significant Difference test (HSD). The influence of vegetation community (lawns and tussocks) and time on CO₂ and CH₄ fluxes was assessed using repeated-measure analysis of variance (RM ANOVA). Spearman's correlation was used to test for significant relationships between environmental variables, CO₂, and CH₄ flux, and least squares linear regression was used to characterize the dependence of fluxes on biotic and abiotic variables. Tests were significant when $p < 0.05$.

4.0 RESULTS

4.1 Site Characteristics

Vegetation and soil characteristics of lawns and tussocks are listed in Table 1. The average height difference between lawns and tussocks was approximately 15 cm. Both tussocks and lawns had 100% *Sphagnum* moss cover and there were no significant differences in total vascular LAI or vascular cover between the two communities. There was some difference in the species composition between the two communities with significantly greater LAI for *Andromeda polifolia* and significantly less LAI for the sedges on the tussocks; although, the dominant vascular species for both lawns and tussocks were sedge species.

Table 1. Soil and vegetation characteristics of the lawn and tussock environments. Values in brackets are the standard error of the mean (± 1 SE) for the 8 tussock and 8 lawn collars. Values with different superscripts denote significant differences between communities ($p < 0.05$). * Source (Hayne, 2009).

	<i>Lawns</i>	<i>Tussocks</i>
Soil Texture	Peat over Silt Loam	
Depth of Organic Layer (cm)*	40-50	50-60
Average Organic Matter Content 0-25 cm depth (kg m ⁻²)*	21.56 (1.26)	
Average Leaf Area Index (live leaf area per unit ground (m ² m ⁻²))	0.77 (0.03) ^a	0.83 (0.07) ^a
Average Leaf Area Index – <i>Andromeda polifolia</i> (live leaf area per unit ground (m ² m ⁻²))	0.06 (0.03) ^a	0.31 (0.03) ^b
Average Leaf Area Index – sedges (live leaf area per unit ground (m ² m ⁻²))	0.69 (0.03) ^a	0.51 (0.04) ^b
Vascular Cover (%)	48.3 (1.09) ^a	55.27 (3.37) ^a
Moss Cover (%)	100 (0) ^a	100 (0) ^a
Dominant Vascular Species	<i>Carex</i> spp. <i>Eriophorum</i> spp.	<i>Carex</i> spp. <i>Eriophorum</i> spp.

Tussock tops remained well above the water table for the duration of the sampling period. The water table gradually decreased from a high of 4 cm to approximately 14 cm below the lawn surface with some fluctuations associated with small precipitation events (Figure 5). Consequently, there were significant differences between mean VWC for the lawns and tussocks at depths of 5 and 10 cm and integrated over 0-20 cm (Table 2 & Figure 5). The 0-20 cm VWC gradually decreased throughout the study period for tussocks while, there was no clear trend in the lawns as the water table remained within this 20 cm surface layer (Figure 5). Due to the high heat capacity of water, soil temperature at depths of 2, 5, and 10 cm remained cooler in the lawns than in the tussocks throughout the study (Figure 6 & Table 2). Both lawns and tussocks showed considerable variations in 2 cm soil temperature through the sampling period as air temperature varied (Figure 6). Mean daily air temperature and soil temperature at 2 cm reached peak values in mid to late July (DOY~199 – 205) (Figure 6). Thaw depth gradually increased during the field season (Figure 6) with a maximum thaw depth of 47.4 cm below the lawn surface and 62.4 cm below the tussock surface (Table 2).

Table 2. Environmental characteristics of the lawn and tussock communities. Values in brackets are ± 1 SE. Values with different superscripts denote significant differences between communities ($p < 0.05$).

	<i>Lawns</i>	<i>Tussocks</i>
Mean soil temperature at 2 cm	14.7 (0.3) ^a	15.7 (0.3) ^b
Mean soil temperature at 5 cm	11.3 (0.2) ^a	12.8 (0.3) ^b
Mean soil temperature at 10 cm	7.9 (0.1) ^a	9.3 (0.2) ^b
Mean VWC ($\text{m}^3 \text{m}^{-3}$) (0-20 cm)	86.2(1.2) ^a	41.4 (2.0) ^b
Mean VWC ($\text{m}^3 \text{m}^{-3}$) 5 cm	76.9 (0.4) ^a	34.3 (0.1) ^b
Mean VWC ($\text{m}^3 \text{m}^{-3}$) 10 cm	87.5 (0.01) ^a	32.8 (0.1) ^b
Maximum thaw depth (cm)	47.4 (0.8)	62.4 (0.8)

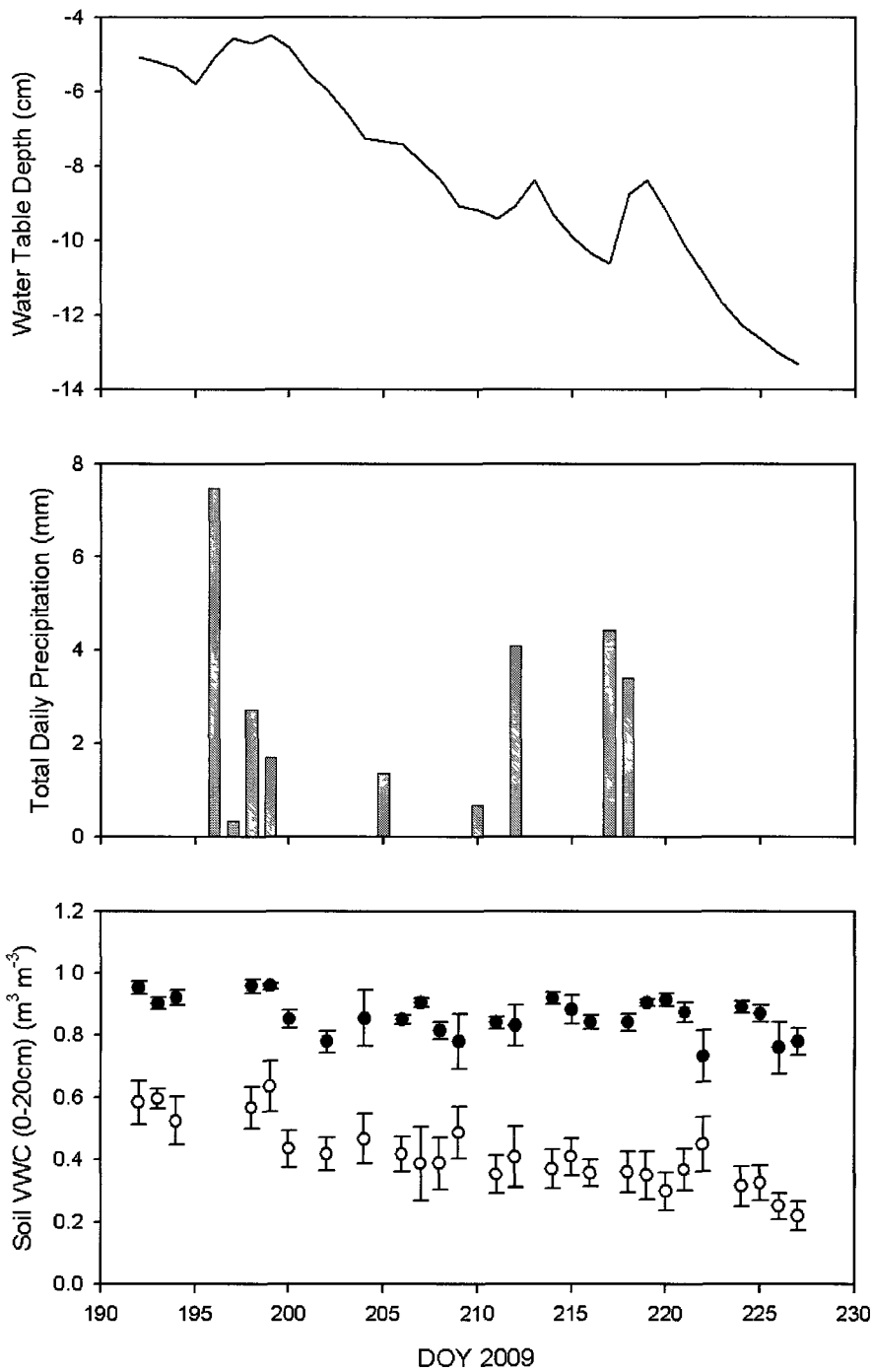


Figure 5. Daily average water table depth relative to the lawn surface, total daily precipitation, and average soil volumetric water content (VWC) for the 0 – 20 cm layer of lawns (closed circles) and tussocks (open circles) at Daring Lake, NT from July 11th to August 15th, 2009. Error bars represent ± 1 standard error (± 1 SE).

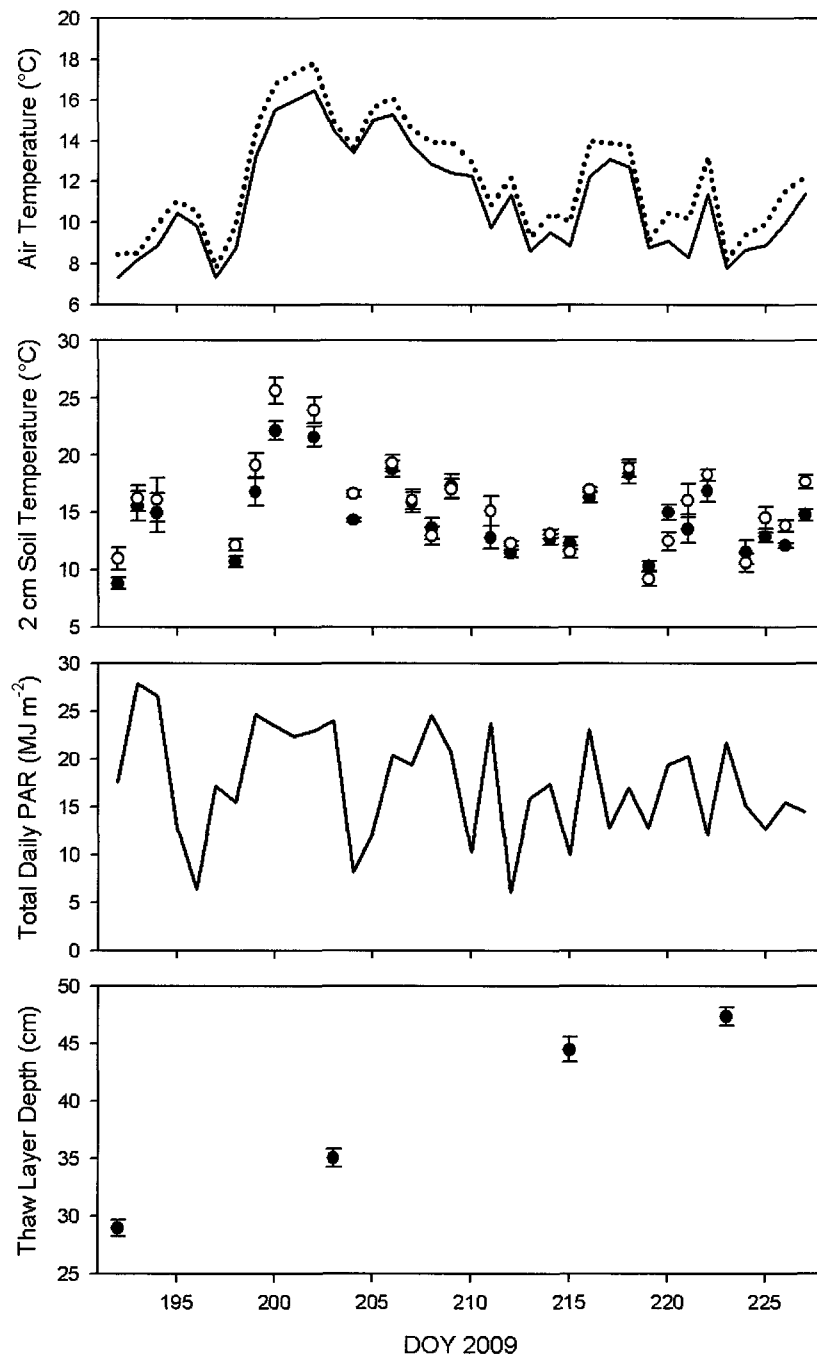


Figure 6. Average daily air temperature (solid line), average daily daytime air temperature (PAR > 10 W m⁻²) (dotted line), average soil temperature at 2 cm depth for lawns (closed circles) and tussocks (open circles), daily photosynthetically active radiation (PAR), and thaw layer depth at Daring Lake, NT from July 11th to August 15th, 2009. Error bars represent ±1 SE. The number of samples for each 2 cm soil temperature symbol is 8. The number of samples for each thaw layer depth symbol is 15.

4.2 Carbon Exchange

4.2.1 Spatial Variations in CO₂ Fluxes

NEE_{max}, GEP_{max}, and ER_F were not significantly different among lawns and tussocks (RM ANOVA (Treatment): $F_{1, 14} = 0.01$ $p = 0.91$; $F_{1, 14} = 0.43$ $p = 0.52$; $F_{1, 14} = 0.67$ $p = 0.43$, respectively) (Table 3). However, ER_F was significantly greater than ER_S (ANOVA: $F_1 = 93.96$, $p = 0.0001$) (Table 3) possibly because the NEE chamber system was preferentially used on sunnier, warmer days. As a result, the average 2 cm soil temperature measured during the ER_F measurements was 16.8 (± 0.3) °C vs. 13.5 (± 0.2) °C for the ER_S measurements. Nonetheless, like ER_F, ER_S was not significantly different between lawns and tussocks (RM ANOVA (Treatment): $F_{1, 14} = 0.06$, $p = 0.81$).

Variability in NEE was well described using Equation 3 for both tussocks and lawns (Table 4 & Figure 7). Similarly, GP_{max} and R₁₀ were not significantly different among lawns and tussocks (Table 4). The value of R₁₀ was lower than the average ER_F (Table 3 & Table 4) as expected because field measurements were made when near surface air and soil temperatures were typically well above 10 °C (Figure 6). Q₁₀ was approximately 1.3 and considerably lower than the typical value of 2 (Lloyd & Taylor, 1994) possibly because chamber air temperature may not represent the temperature influencing both above and below ground respiration processes.

Table 3. Average NEE and component fluxes for the two vegetation communities. NEE_{max} is the net ecosystem exchange of CO_2 for PAR greater than $1000 \mu mol m^{-2} s^{-1}$. GEP_{max} is the average gross ecosystem production for PAR greater than $1000 \mu mol m^{-2} s^{-1}$. ER is the average ecosystem respiration in the dark measured using the flow-through chambers (ER_F) and the static chambers (ER_S). Values in brackets represent ± 1 SE. Values with different superscripts denote significant differences between communities ($p < 0.05$).

	<i>Lawns</i>	<i>Tussocks</i>
NEE_{max} ($\mu mol m^{-2} s^{-1}$)	-1.93 (0.09) ^a	-1.87 (0.11) ^a
GEP_{max} ($\mu mol m^{-2} s^{-1}$)	-3.92 (0.11) ^a	-4.02 (0.13) ^a
ER_F ($\mu mol m^{-2} s^{-1}$)	1.99 (0.07) ^a	2.15 (0.10) ^a
ER_S ($\mu mol m^{-2} s^{-1}$)	1.38 (0.04) ^a	1.37 (0.05) ^a

Table 4. Parameters for Equation 3 describing the response of NEE to PAR and chamber air temperature for the two communities. GP_{max} is maximum gross photosynthesis, α is the initial slope of the curve, R_{10} is ecosystem respiration at a reference temperature of 10 °C, n is the number of observations, Q_{10} is rate of increase in ER for a 10 °C increase in temperature, and RMSE is the root mean square error. Values in brackets represent ± 1 SE. Values with different superscripts denote significant differences between communities ($p < 0.05$).

	<i>Lawns</i>	<i>Tussocks</i>
GP_{max} ($\mu mol m^{-2} s^{-1}$)	-6.17 (0.46) ^a	-6.27 (0.56) ^a
α	-0.007 (0.0007) ^a	-0.008 (0.001) ^a
R_{10} ($\mu mol m^{-2} s^{-1}$)	1.37 (0.09) ^a	1.54 (0.11) ^a
n	396	400
Q_{10}	1.36 (0.07) ^a	1.33 (0.07) ^a
RMSE	0.757	1.014

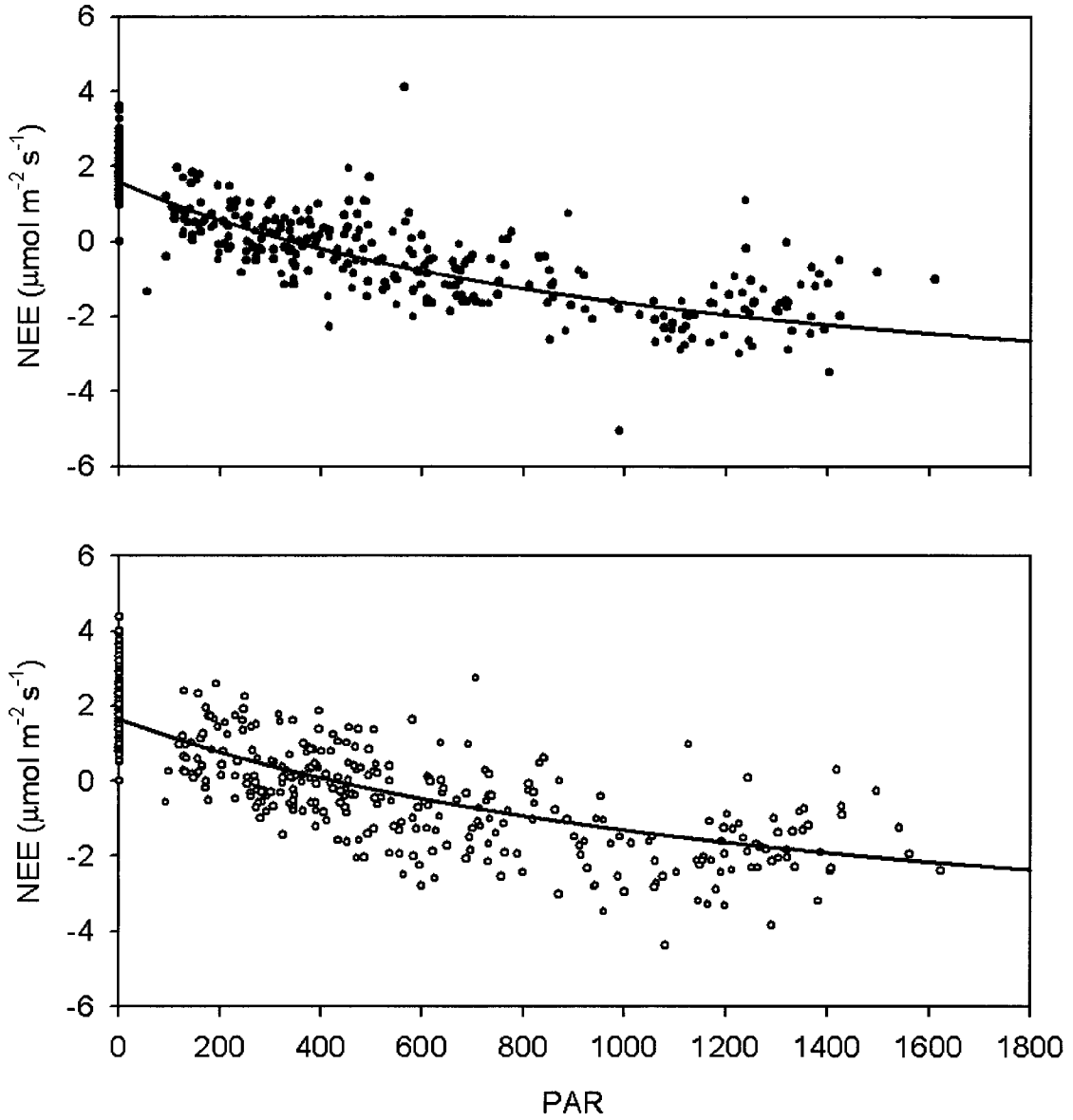


Figure 7. The top and bottom panels show the relationship between net ecosystem exchange of CO₂ (NEE) and photosynthetically active radiation (PAR) for lawns and tussocks, respectively. The light response curves are shown as solid lines. Curves (solid lines) are determined using Equation 3 with parameters listed in Table 4.

Although there was no significant difference in CO₂ exchange between the two community types, there was considerable variation in the average NEE_{max} and component fluxes among the collars. Overall, vegetation characteristics appeared to play an important role in determining variations in NEE_{max} and GEP_{max} among collars. LAI significantly correlated with both NEE_{max} ($r = -0.48$, $p = 0.04$) and GEP_{max} ($r = -0.61$, $p = 0.01$) but not ER_F ($r = 0.26$, $p = 0.32$). Stronger relationships were found for NEE_{max} ($r = -0.81$, $p = 0.0001$) and GEP_{max} ($r = -0.66$, $p = 0.006$) with % vascular cover (Figure 8). Consequently, because LAI and vascular % cover did not significantly differ between lawns and hummocks, it was not surprising that CO₂ sequestration (GP_{max} and GEP_{max}) and thus NEE_{max} also did not differ. ER_F did not significantly correlate directly with any vegetation characteristics but was found to significantly correlate to GEP_{max} ($r = -0.61$, $p = 0.01$). Although these two fluxes are not independent, this may indicate that ER is largely related to variations in productivity directly through autotrophic respiration processes and through decomposition of fresh substrates. None of the CO₂ fluxes measured with the flow-through chamber were significantly correlated to soil temperature or moisture variables. This suggested that cooler and wetter conditions did not reduce the growth (GEP) of these species well adapted to saturated conditions.

In contrast to ER_F, ER_S was found to significantly and positively correlate with soil temperature at 2 cm ($r = 0.59$, $p = 0.02$) possibly because sampling occurred on a greater number of days (16 vs. 13). ER_S did not vary significantly with any biotic variable and similar to ER_F, it had a significant negative correlation with GEP_{max} ($r = -0.59$, $p = 0.02$).

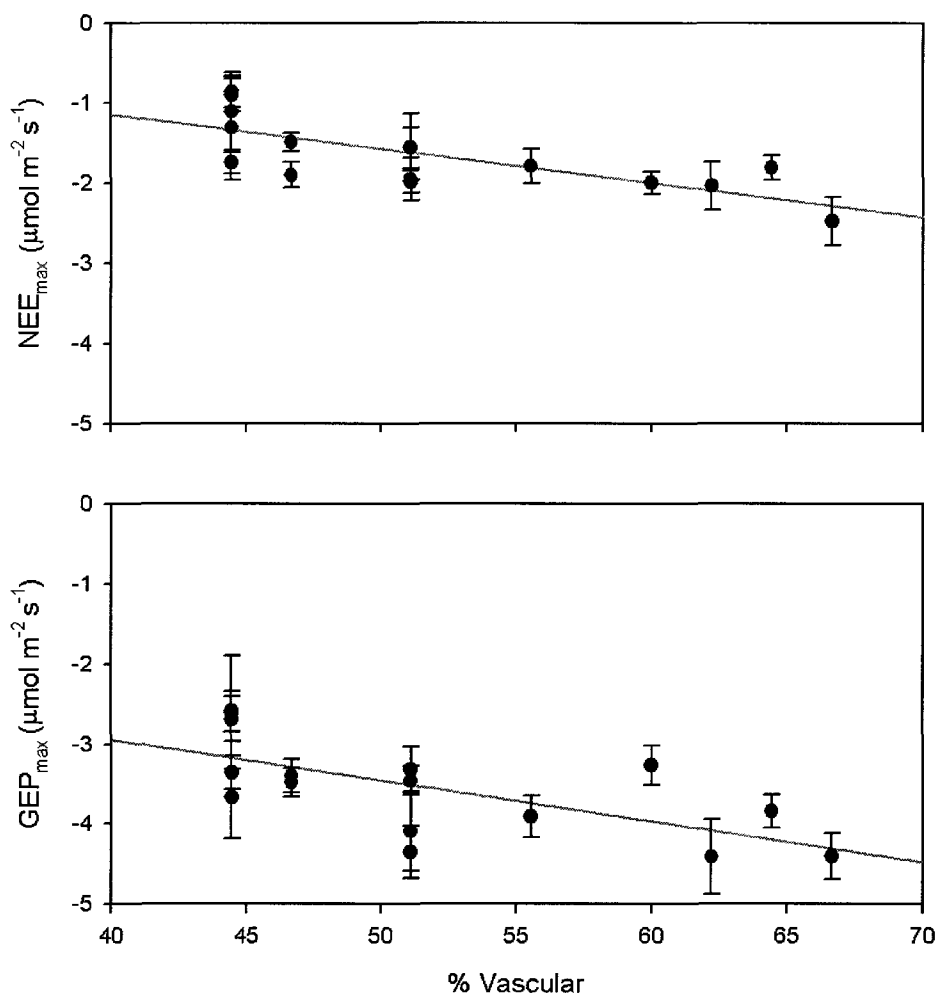


Figure 8. The relationship between net ecosystem exchange of CO₂ (NEE_{max}) (top panel) and gross ecosystem exchange of CO₂ (GEP_{max}) (bottom panel) to % vascular. Error bars represent ± 1 SE. The number of samples for each symbol is 13. Lines are given for significant linear regressions (NEE_{max} = -0.04 (% Vascular) + 0.55, $r^2 = 0.56$; GEP_{max} = -0.05 (% Vascular) - 0.92, $r^2 = 0.43$).

4.2.2 Spatial Variations in CH₄ Fluxes

CH₄ flux was found to be significantly different among lawns and tussocks (RM ANOVA (Treatment): $F_{1, 14} = 8.03$, $p = 0.01$). The range in observed CH₄ fluxes was nearly twice as large in lawns than in tussocks, and, when assessed, the average CH₄ flux was significantly greater in lawns ($58.21 \pm 2.10 \text{ nmol m}^2 \text{ s}^{-1}$) than in tussocks ($34.82 \pm 1.52 \text{ nmol m}^2 \text{ s}^{-1}$) (Table 5). Wetter collar sites were associated with higher CH₄ fluxes (Figure 9) ($r = 0.66$, $p = 0.005$). When examining the spatial variations within the two communities, lawn CH₄ flux was not significantly correlated to any abiotic variable; however, tussock CH₄ flux was significantly positively correlated to soil temperature at 2 cm depth ($r = 0.71$, $p = 0.04$) (Figure 10). CH₄ flux did not significantly correlate to ER_S ($r = 0.45$, $p = 0.08$), ER_F ($r = 0.003$, $p = 0.991$), NEE_{max} ($r = -0.21$, $p = 0.44$) or GEP_{max} ($r = -0.27$, $p = 0.31$) when the full set of collars was investigated. However, there was a significant positive correlation between CH₄ flux and ER_S within tussocks ($r = 0.76$, $p = 0.03$) but not for lawns ($r = 0.47$, $p = 0.23$) (Figure 11). CH₄ flux did not relate to any biotic variable when examining lawn and tussock communities; however, when the full set of collars was assessed, CH₄ had a significant positive correlation to sedge LAI ($r = 0.61$, $p = 0.01$) and a significant negative correlation to bog rosemary LAI ($r = -0.51$, $p = 0.04$).

Table 5. The range and mean CH₄ flux for the lawn and tussock communities. Values in brackets represent ± 1 SE. Values with different superscripts denote significant differences between communities ($p < 0.05$). The number of samples for lawns and tussocks is 132.

		<i>Lawns</i>	<i>Tussocks</i>
CH ₄ flux (nmol m ⁻² s ⁻¹)	Minimum	7.85	1.84
	Maximum	164.76	80.24
	Mean (SE)	58.21 (2.10) ^a	34.82 (1.52) ^b

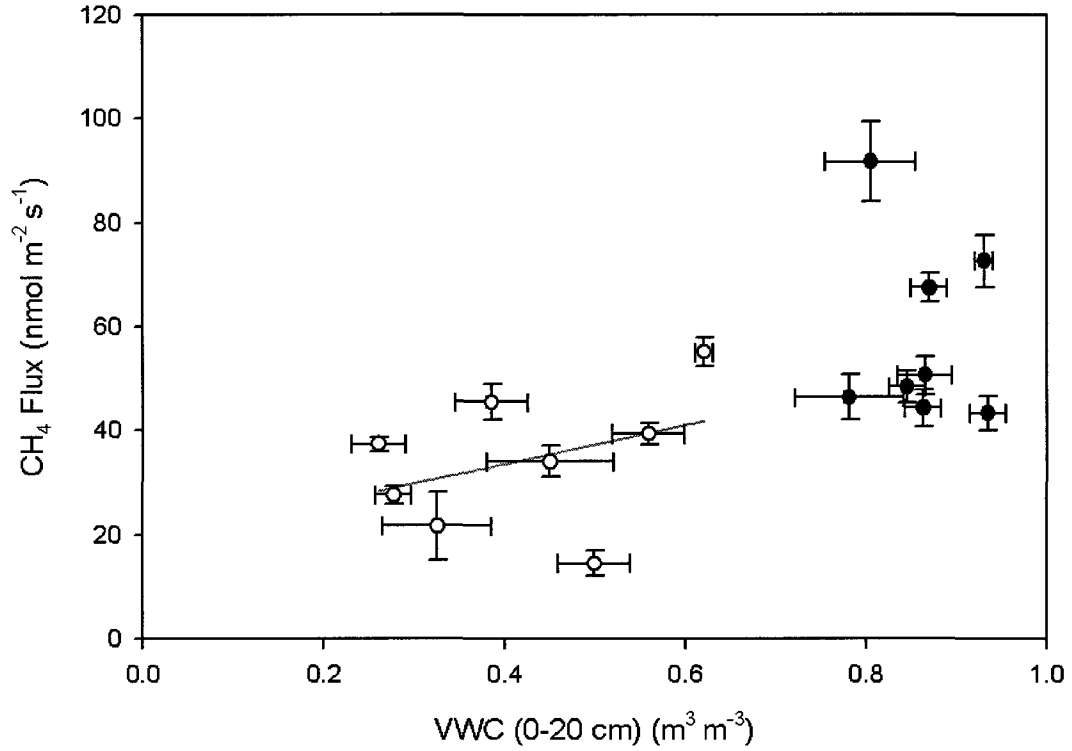


Figure 9. Relationship between CH₄ Flux and volumetric water content (VWC) for lawns (dark circles) and tussocks (open circles). Error bars represent ± 1 SE. The number of samples for each symbol is 16. Lines are given for significant linear regressions (CH₄ Flux = 37.35(VWC) + 18.62, r² = 0.24).

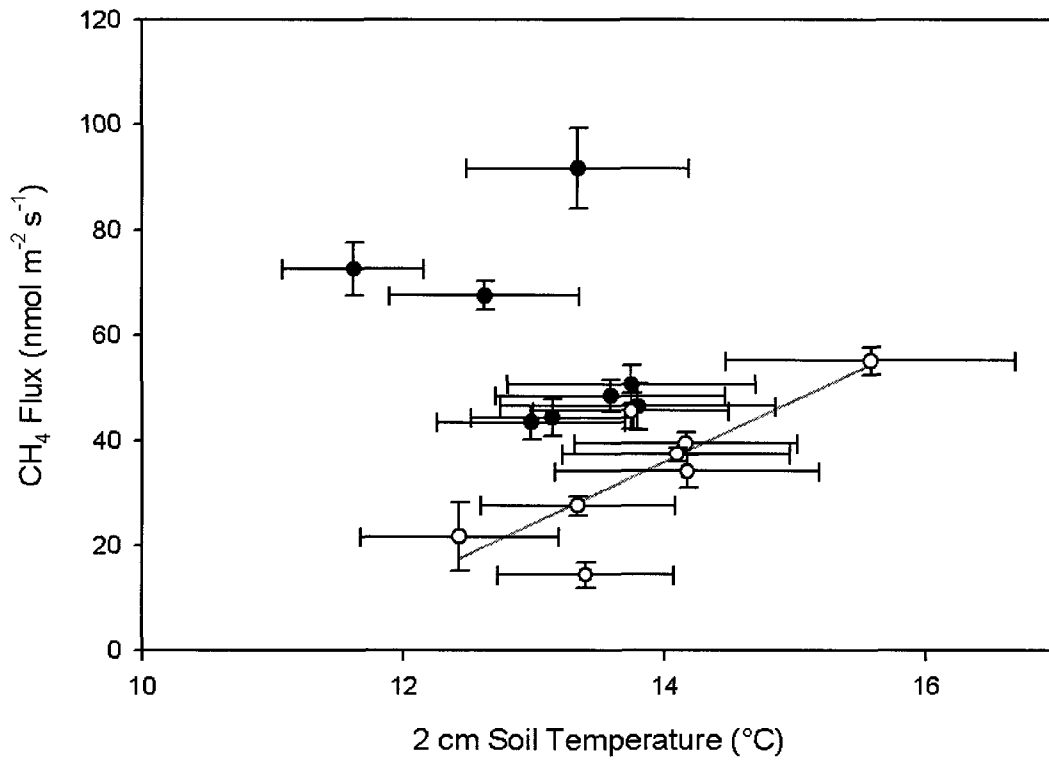


Figure 10. Relationship between 2 cm soil temperature and CH₄ flux for lawns (dark circles) and tussocks (open circles). Error bars represent ± 1 SE. The number of samples for each symbol is 16. Lines are given for significant linear regressions ($\text{CH}_4 \text{ Flux} = 11.72 (\text{Temperature}) - 128.1, r^2 = 0.66$).

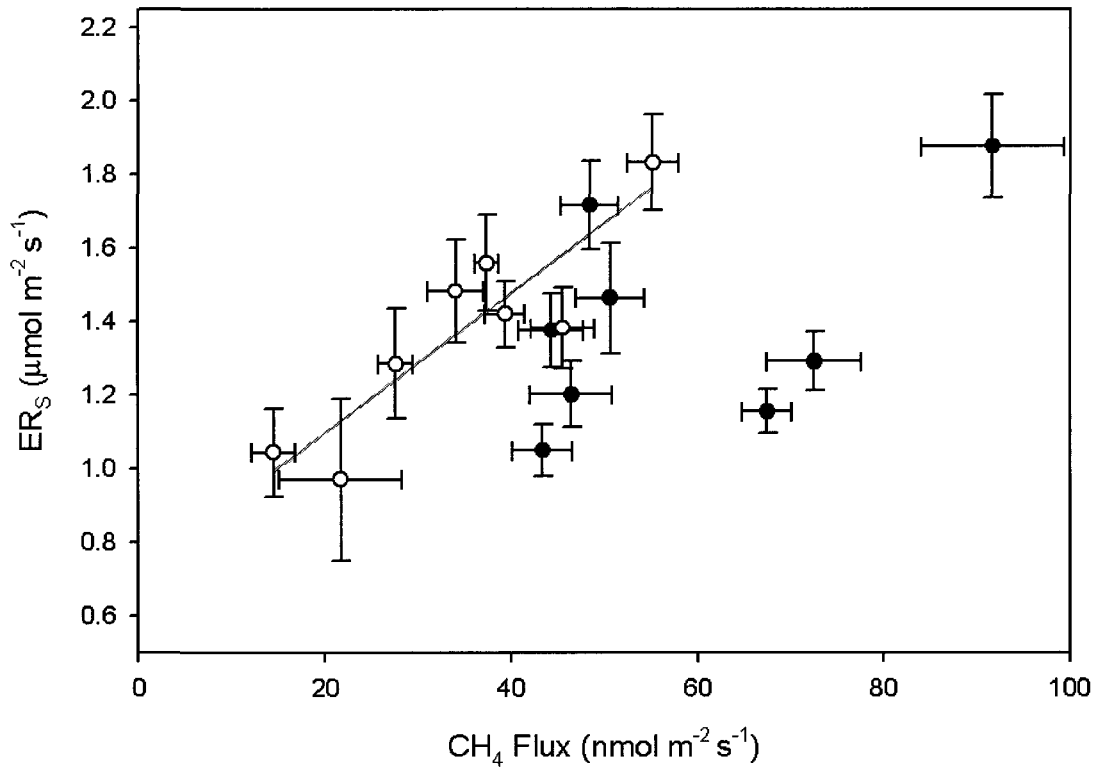


Figure 11. The relationship between ecosystem respiration (static chamber) (ER_S) and CH_4 flux for lawns (dark circles) and tussocks (open circles). Error bars represent ± 1 SE. The number of samples for each symbol is 16. Lines are given for significant linear regressions ($ER_S = 0.02 (CH_4 \text{ Flux}) + 0.72$, $r^2 = 0.80$).

4.3.1 Temporal Variations in CO₂ Fluxes

Temporal variations in the various CO₂ fluxes are shown in Figure 12. For both lawns and tussocks, CO₂ uptake increased from DOY 193 to 206 after which NEE_{max} and GEP_{max} decreased in magnitude from DOY 211 to 227. During the period with maximum uptake (DOY 206-211), precipitation was minimal, water table decreased approximately 5 cm to a depth of 10 cm below the soil surface (Figure 5), and daily average air temperatures reached their maximum for the study period (Figure 6).

ER_F was relatively constant through the sampling period but increased briefly on DOY 200 and 202 when static chamber measurements were not made (i.e. no ER_S measurements). The interaction between lawn and tussock communities and time (RM ANOVA (Time)) was found to be significant for NEE_{max} ($F_{10,5} = 53.64$, $p = 0.0002$), GEP_{max} ($F_{10,5} = 7.79$, $p = 0.01$), and ER_F ($F_{10,5} = 71.64$, $p = 0.0001$). However, only ER_F trends were different for tussocks and lawns over time (RM ANOVA (Interaction): $F_{10,5} = 12.98$, $p = 0.006$) (Figure 12). In contrast, ER_S did not vary significantly over time (RM ANOVA (Time): $F_{14,1} = 107.32$, $p = 0.08$) and there was a similar lack of temporal variation for lawns and tussocks (RM ANOVA (Interaction): $F_{14,1} = 6.90$, $p = 0.29$). This lack of variation may be due to more similar environmental conditions during ER_S sampling on cloudy days and having not sampled as often during the large loss period around DOY 200-205 when air and soil temperatures were greatest (Figure 6 & Figure 12).

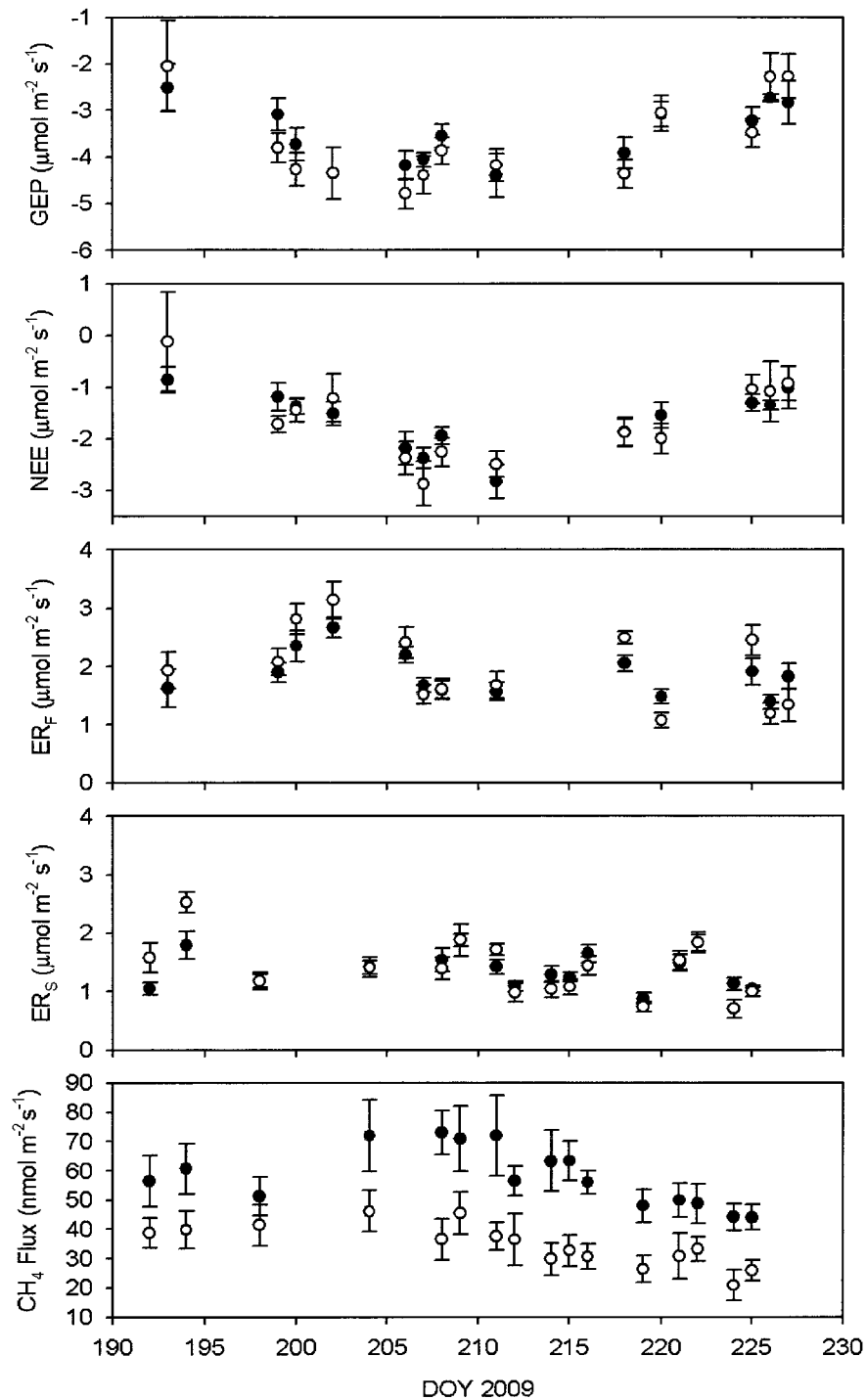


Figure 12. The average daily flux for lawns (closed circles) and tussocks (open circles) using the flow-through and opaque static chamber systems. Gross ecosystem production (GEP); net ecosystem exchange (NEE); ecosystem respiration (flow-through chamber) (ER_F); ecosystem respiration (static chamber) (ER_S). Error bars represent ± 1 SE. The number of samples for each symbol is 8.

NEE_{max}, GEP_{max}, and ER_F significantly correlated with PAR and soil temperature at 10 cm depth over the study period (Table 6). Both photosynthesis and respiration rates tended to increase for warmer sunnier conditions although uptake increased to a greater extent than loss such that NEE_{max} was greater on these days. NEE_{max} did not significantly correlate to any other abiotic variable; whereas, GEP_{max}, ER_F, and ER_S were found to significantly correlate to temperature at 2 and 5 cm depths and also with air temperature (Table 6). There were no significant correlations between ER_F to water table depth or VWC; however, when lawns and tussocks were treated separately there was a significant correlation between ER_F and water table depth and VWC (lawns: $r = 0.47$, $p = 0.0001$ and $r = -0.21$, $p = 0.04$, respectively and tussocks: $r = 0.39$, $p = 0.0001$ and $r = 0.29$, $p = 0.004$, respectively) (Figure 13), indicating that there were similar abiotic controls on ER_F respiration within lawns and tussocks, but their relationships were different. This different response to water table and VWC may have caused lawn and tussock ER_F to vary differently over time (RM ANOVA (interaction): $F_{10, 5} = 12.98$, $p = 0.006$) (Figure 12).

Lawn and tussock ER_S correlated significantly to temperatures at 2 and 5 cm depths, air temperature, and CH₄ flux ($r = 0.41$, $p = 0.0001$ and $r = 0.60$, $p = 0.0001$ respectively) (Table 7 & Figure 14). Lawn ER_S had a significant negative correlation to VWC while tussock ER_S had a significant positive correlation to VWC (Table 7 & Figure 14). Overall, ER_F and ER_S were found to be enhanced by warmer, moist, but not saturated soil conditions for both communities.

Table 6. Spearman's rho correlation coefficients showing significant relationships between environmental variables and CO₂ fluxes with p-values given in brackets. Net ecosystem exchange (NEE_{max}); gross ecosystem production (GEP_{max}); ecosystem respiration (flow-through chamber) (ER_F); ecosystem respiration (static chamber) (ER_S).

	NEE_{max}	GEP_{max}	ER_F	ER_S
Temperature (°C) at 2 cm depth		-0.26 (0.0002)	0.52 (0.0001)	0.62 (0.0001)
Temperature (°C) at 5 cm depth		-0.23 (0.0009)	0.41 (0.0001)	0.48 (0.0001)
Temperature (°C) at 10 cm depth	-0.32 (0.0001)	-0.47 (0.0001)	0.34 (0.0001)	
Air Temperature (°C)		-0.45 (0.0001)	0.59 (0.0001)	0.48 (0.0001)
Volumetric water content (0-20 cm) (m ³ m ⁻³)				
Water table depth (cm)				
Photosynthetically active radiation (μmol m ⁻² s ⁻¹)	-0.18 (0.01)	-0.36 (0.0001)	0.26 (0.0002)	

Table 7. Spearman's rho correlation coefficients showing significant relationships between environmental variables and ecosystem respiration (static chamber) (ER_S), for lawn and tussock communities with p-values given in brackets.

	ER_S Lawn	ER_S Tussock
Temperature (°C) at 2 cm depth	0.60 (0.0001)	0.65 (0.0001)
Temperature (°C) at 5 cm depth	0.38 (0.0001)	0.60 (0.0001)
Temperature (°C) at 10 cm depth		
Air Temperature (°C)	0.51 (0.0001)	0.45 (0.0001)
Volumetric water content (0-20 cm) (m ³ m ⁻³)	-0.22 (0.01)	0.25 (0.005)
Water table (cm)		
CH ₄ Flux (nmol m ⁻² s ⁻¹)	0.41 (0.0001)	0.60 (0.0001)

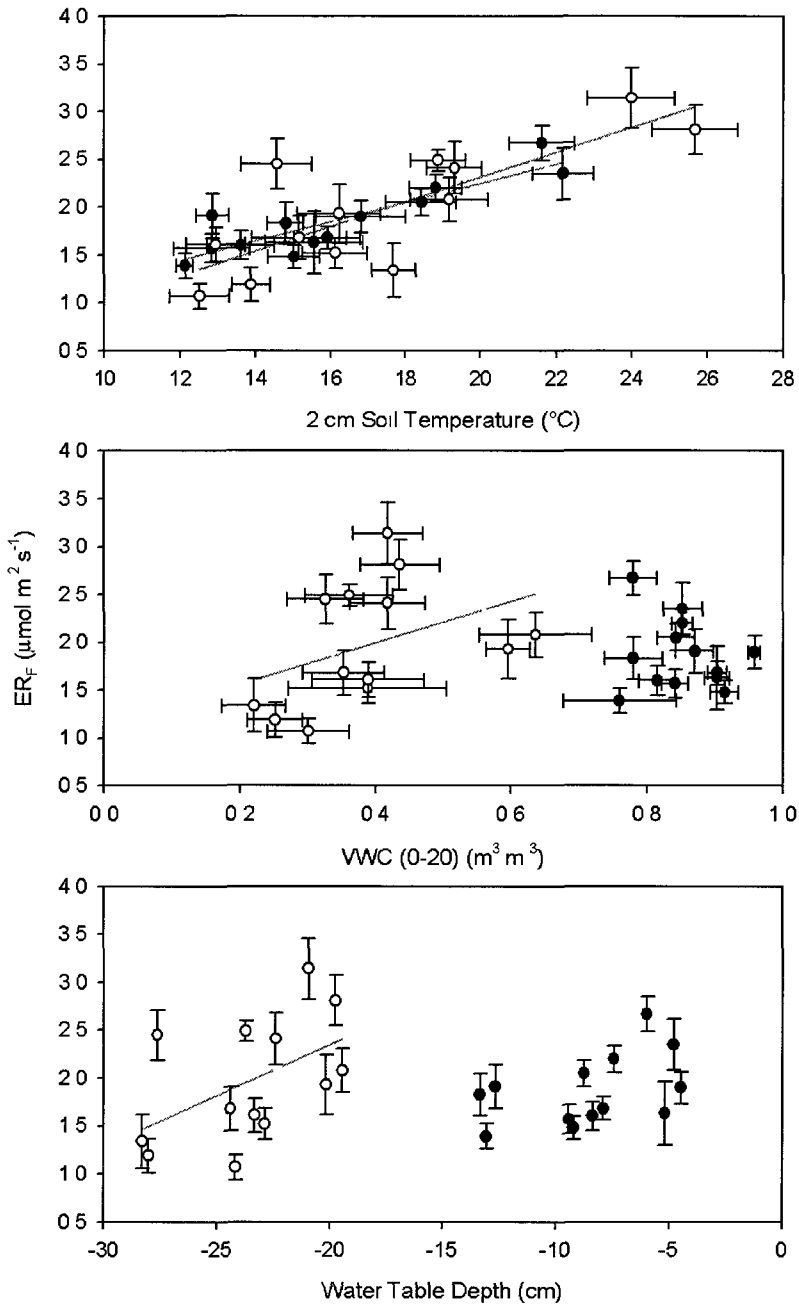


Figure 13. The relationship between ecosystem respiration (flow-through chamber), ER_F , and temperature at 2 cm depth (top panel), average volumetric water content (VWC) (middle panel), and water table depth (bottom panel). Closed circles represent lawns and open circles represent tussocks. Error bars represent ± 1 SE. The number of samples for each symbol is 8. Lines are given for significant linear regressions. Top panel lawns ($ER_F = 0.1 (\text{Temperature}) + 0.24$, $r^2 = 0.77$) and tussocks ($ER_F = 0.13 (\text{Temperature}) - 0.27$, $r^2 = 0.64$); middle panel ($ER_F = 2.16 (\text{Temperature}) + 1.13$, $r^2 = 0.25$); bottom panel ($ER_F = 0.11 (\text{Temperature}) + 2.89$, $r^2 = 0.25$).

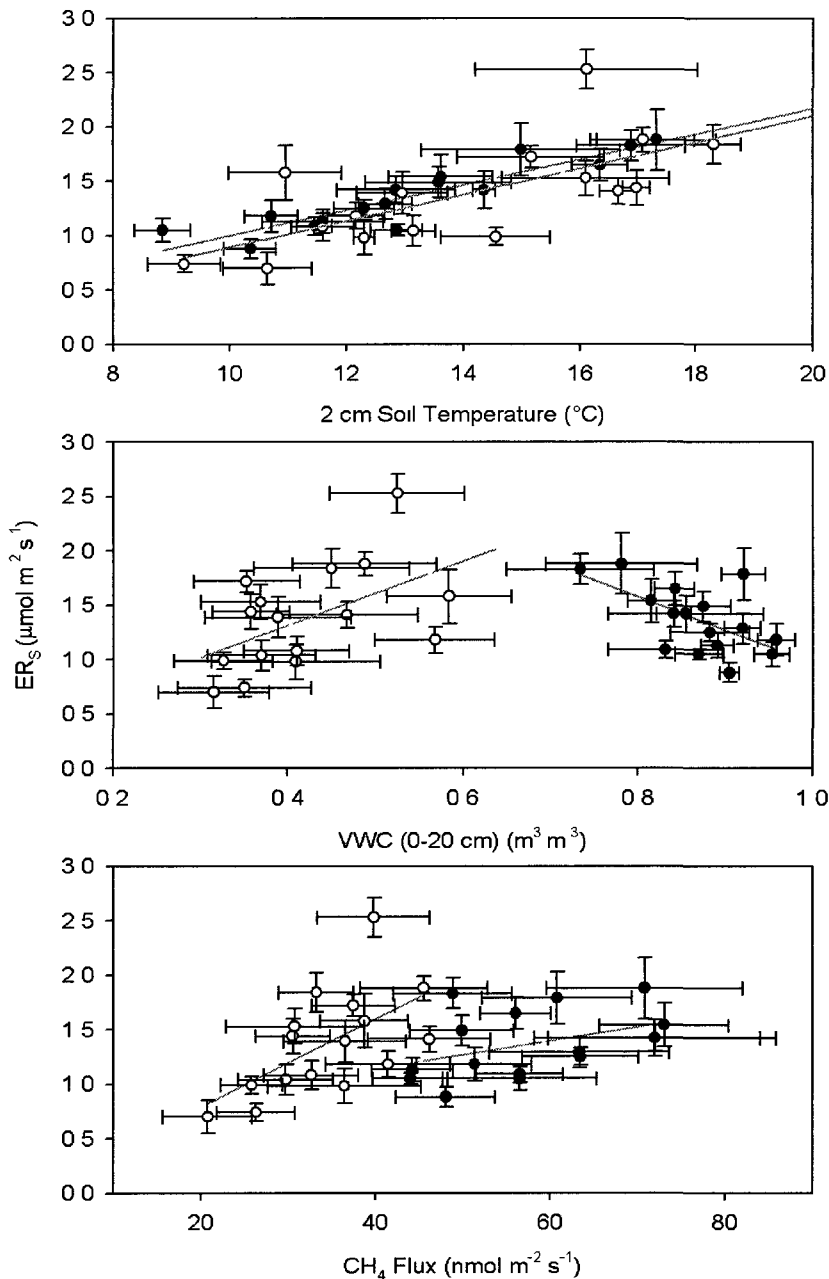


Figure 14. The relationship between ecosystem respiration (static chamber) (ER_S) and temperature at 2 cm depth (top panel), average volumetric water content (VWC) (middle panel), and CH_4 Flux (bottom panel). Closed circles represent lawns and open circles represent tussocks. Error bars represent ± 1 SE. The number of samples for each symbol is 8. Lines are given for significant linear regressions. Top panel (L: $ER_S = 0.12$ (Temperature) - 0.17, $r^2 = 0.82$; T: $ER_S = 0.07$ (Temperature) + 0.41, $r^2 = 0.37$), middle panel (L: $ER_S = -3.04$ (VWC) + 4.01, $r^2 = 0.36$; T: $ER_S = 2.54$ (VWC) + 0.14, $r^2 = 0.27$), bottom panel (L: $ER_S = 0.01$ (CH_4 Flux) + 0.62, $r^2 = 0.28$; T: $ER_S = 0.04$ (CH_4 Flux) - 0.02, $r^2 = 0.36$).

4.3.2 Temporal Variations in CH₄ Fluxes

Similar to ER_s, CH₄ fluxes did not vary significantly over time (RM ANOVA (Time): $F_{14,1} = 7.38$, $p = 0.28$) and this lack of temporal variation was common for lawns and tussocks (RM ANOVA (Interaction): $F_{14,1} = 26.78$, $p = 0.15$). However, Figure 12 shows that CH₄ fluxes, particularly for lawns, peaked around the same time as GEP_{max} and NEE_{max} after which, CH₄ fluxes decreased. CH₄ fluxes correlated positively and significantly with air temperature and water table within and among lawns and tussocks (Table 8). Tussock CH₄ fluxes were positively correlated to VWC ($r = 0.38$, $p = 0.0001$); whereas, lawn CH₄ fluxes were not ($r = 0.003$, $p = 0.997$). Lawns had mostly saturated conditions throughout the field study (Figure 7) and precipitation had little effect on CH₄ fluxes. In comparison, as tussock VWC decreased over time (Figure 5) so too did rates of CH₄ flux (Figure 12). CH₄ fluxes correlated significantly and positively with soil temperature at 10 cm depth within lawns; however, not within tussocks (Table 8 & Figure 15). This may be a result of lawns being saturated at 10 cm depth for most of the field season (Figure 5) and thus this depth is near the zone of maximum CH₄ production. Tussock CH₄ fluxes instead correlated significantly and positively to soil temperature at shallower depths (2 and 5 cm) (Table 8 & Figure 15) where temperatures were significantly higher (Table 2). Overall, CH₄ fluxes within lawns and tussocks seem to increase with warmer air and soil conditions, greater VWC, and higher water table. Lawns emitted significantly more CH₄ (Table 5) likely due to less CH₄ oxidation within a reduced aerobic zone and possibly due to warmer temperatures at the depth where the peat was saturated (as this depth was effectively closer to the surface).

Table 8. Spearman's rho correlation coefficients showing significant relationships between environmental variables and CH₄ flux for lawn and tussock communities separately and combined with significant p-values given in brackets.

	<i>Lawn</i>	<i>Tussock</i>	<i>Lawn and Tussock</i>
Temperature (°C) at 2 cm depth		0.30 (0.0008)	
Temperature (°C) at 5 cm depth		0.29 (0.001)	
Temperature (°C) at 10 cm depth	0.20 (0.02)		
Air Temperature (°C)	0.25 (0.005)	0.20 (0.03)	0.19 (0.003)
Volumetric water content (0-20 cm) (m ³ m ⁻³)		0.38 (0.0001)	0.53 (0.0001)
Water table (cm)	0.21 (0.02)	0.29 (0.0009)	0.56 (0.0001)

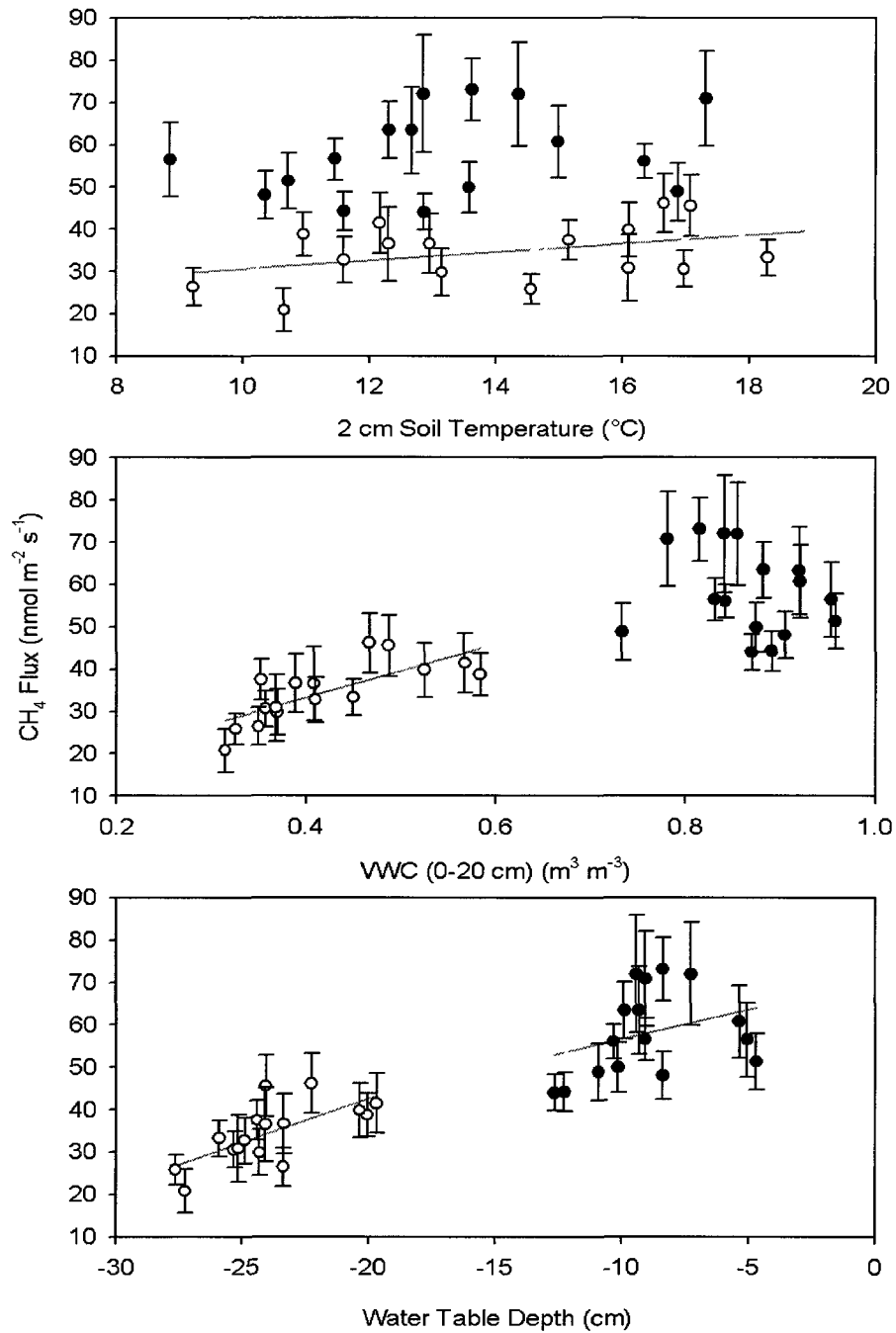


Figure 15. The relationship between CH_4 flux and temperature at 2 cm depth (top panel), average volumetric water content (VWC) (middle panel), and water table depth (bottom panel). Error bars represent ± 1 SE. The number of samples for each symbol is 8. Lines are given for significant linear regressions. Top panel ($\text{CH}_4\text{Flux} = 1.01 (\text{Temperature}) + 20.5$, $r^2 = 0.15$), middle panel ($\text{CH}_4\text{Flux} = 63.16 (\text{VWC}) + 7.97$, $r^2 = 0.57$), bottom panel (L: $\text{CH}_4\text{Flux} = 1.39 (\text{WT}) + 70.54$, $r^2 = 0.17$; T: $\text{CH}_4\text{Flux} = 2.07 (\text{WT}) + 52.94$, $r^2 = 0.47$).

4.4 General Seasonal Trends in CH₄ and CO₂ Exchange

Seasonal variations in daily daytime CH₄ flux and NEE measured using chamber and EC techniques showed similar patterns but relatively large differences in magnitude (Figure 16). Seasonal peaks of CH₄ release and CO₂ uptake occurred around the same time (DOY 201 – 215) (July 20 – Aug 3) during the study. This period saw seasonal highs for air temperature, 5 cm soil temperature, and average daily PAR (Figure 6).

Maximum daytime losses of CH₄ from the fen, measured by the EC system were approximately 40 - 55 nmol m⁻² s⁻¹ during mid-summer. Methane fluxes before and after this time declined to a low of approximately 20 nmol m⁻² s⁻¹ (Figure 16). Generally, chamber CH₄ fluxes from the sedge lawn and tussock areas were considerably larger ranging from 20 – 80 nmol m⁻² s⁻¹. However, the EC fluxes may have been reflecting contributions from communities other than the lawn and tussock areas such as the shrub mounds NW of the tower (Figure 3) where CH₄ emissions were negligible (data shown in Figure 16 from Piquette (2010)), which constituted approx 27% of the area within sector 3 (70 - 100 m).

Maximum daytime uptake of CO₂ measured by the EC system peaked with fluxes of approximately -4 to -5.5 μmol m⁻² s⁻¹ during mid-summer. CO₂ fluxes before and after this time declined to a low of approximately -2 μmol m⁻² s⁻¹. Overall, the magnitude of chamber NEE fluxes from the sedge lawn and tussock areas were considerably smaller ranging from approximately -1 to -3 μmol m⁻² s⁻¹ while NEE on the peat shrub mounds was considerably larger at -7 to -8 μmol m⁻² s⁻¹ (Piquette, 2010).

Day to day variations in daily average CH₄ flux were relatively large compared to the day to day variations in NEE (Figure 16). The factors that influence this short-term variability in day-to-day CH₄ and CO₂ flux are discussed in the following section.

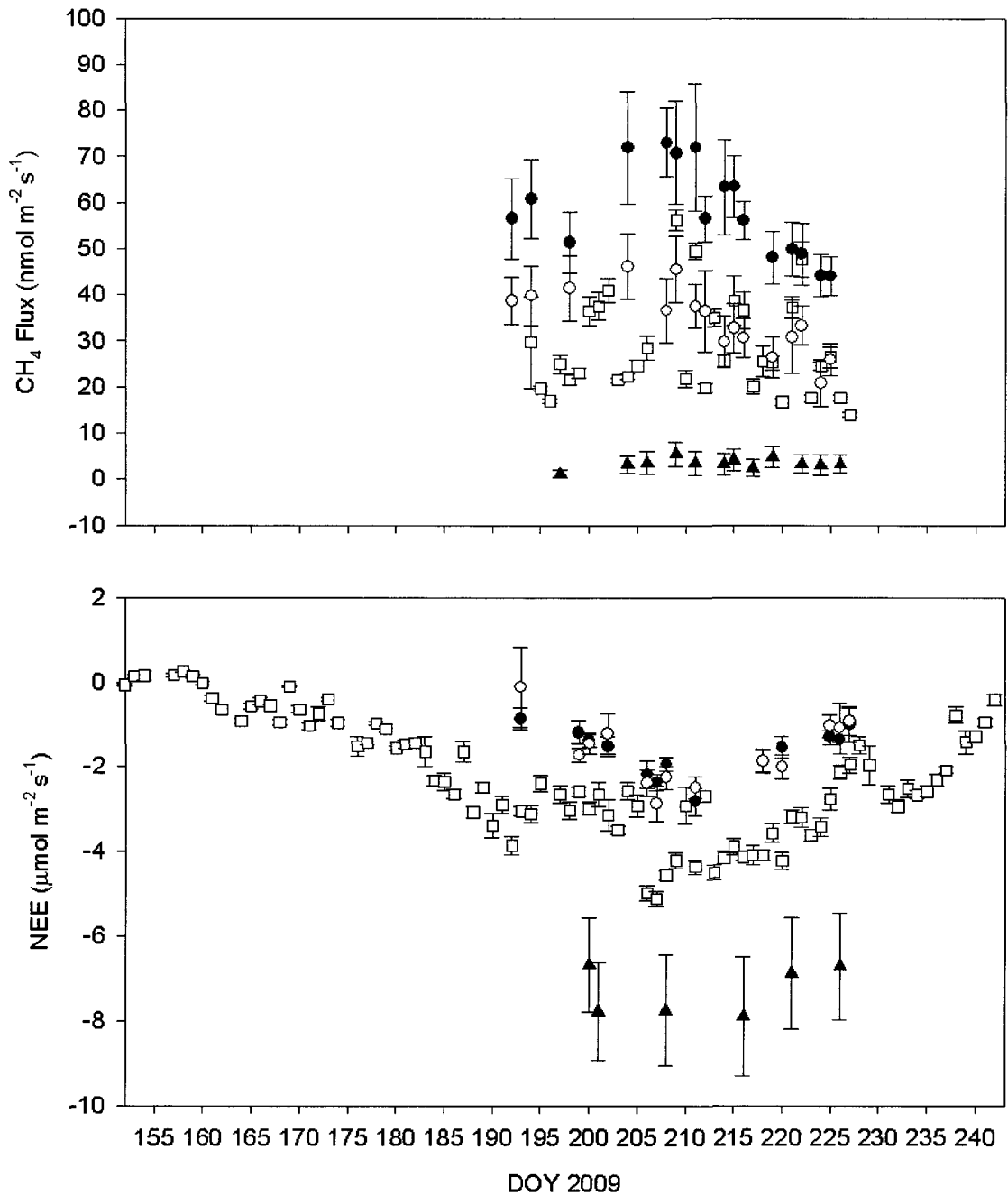


Figure 16. Daily daytime (10 am - 6 pm) average eddy covariance and chamber measurements of CH_4 flux and net ecosystem exchange CO_2 (NEE). Eddy covariance fluxes are shown for days when there were at least 6 half hours with good quality measurements. Chamber fluxes are means of 8 different collar measurements for each plotted day. Error bars represent ± 1 SE. Chamber fluxes are represented by closed circles for lawns, open circles for tussocks, triangles for shrub peat mounds, and open squares represent tower fluxes.

4.5.1 Daily Variation in Ecosystem CH₄ and CO₂ Exchange

Daily daytime CH₄ flux measured using the EC system had a significant positive relationship with 5 cm soil temperature described here using an exponential relationship where $\text{CH}_4 \text{ Flux} = 18.16 * 3.43^{((T_{\text{temp}} - 10)/10)}$ (RMSE = 4.95, p = 0.01) and a significant negative relationship with u* fitted using a linear regression where $\text{CH}_4 \text{ Flux} = -6.57(u^*) + 4.53$ ($r^2 = 0.3$, p = 0.01) (Figure 17). Note, there was no significant correlation between 5 cm soil temperature and u*. In comparison, daily daytime NEE was not related to those two variables but had a significant negative relationship with PAR ($r = -0.45$, p = 0.0009) (Figure 18), illustrating an increase in CO₂ uptake rates with sunnier conditions. This relationship between NEE and PAR was improved when grouped by air temperature (temperature < 12°C ($r = -0.31$, p = 0.12), temperature > 12°C ($r = -0.52$, p = 0.006), illustrating a greater dependence of NEE on PAR when temperature was high (Figure 18).

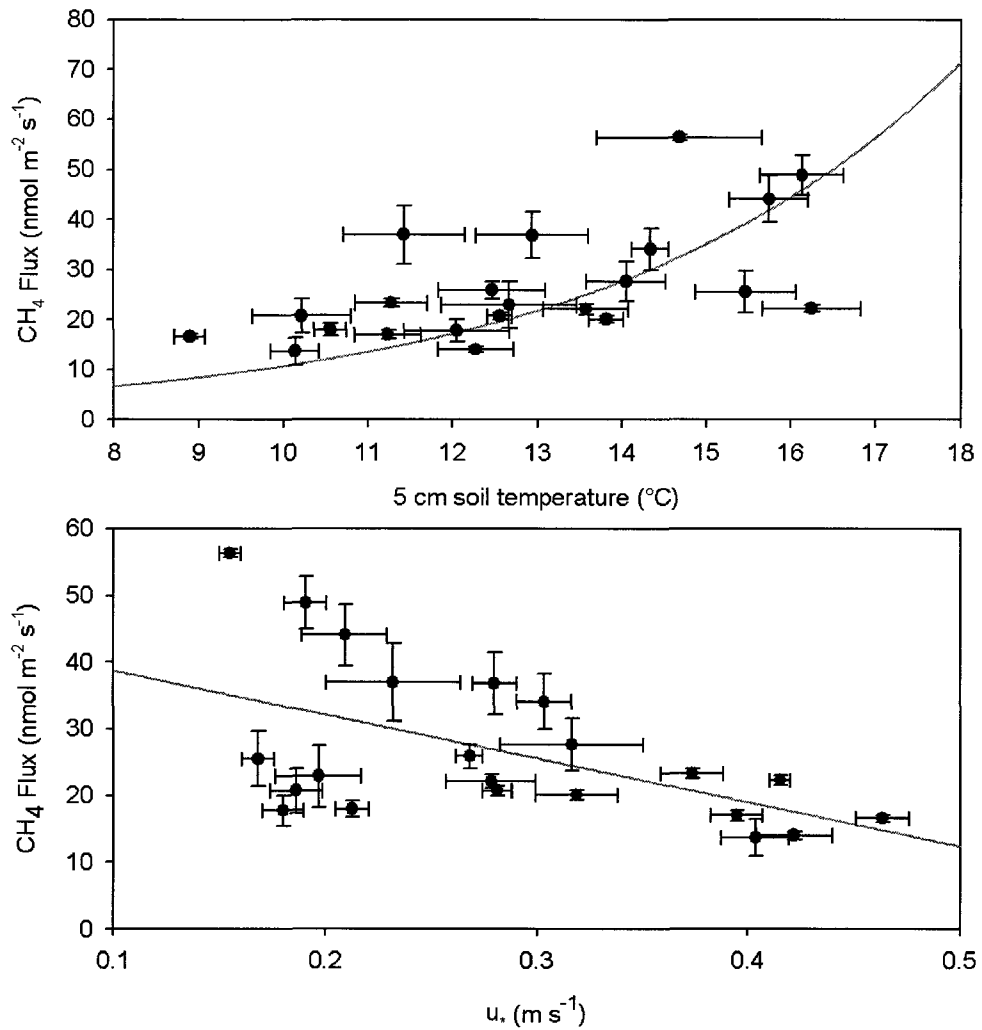


Figure 17. The relationship between daily daytime (10am – 6pm) CH₄ flux and 5 cm soil temperature (top panel) and friction velocity (u_*) (bottom panel). Error bars represent ± 1 SE. The number of 30 min fluxes for each symbol ranges from 6 to 16.

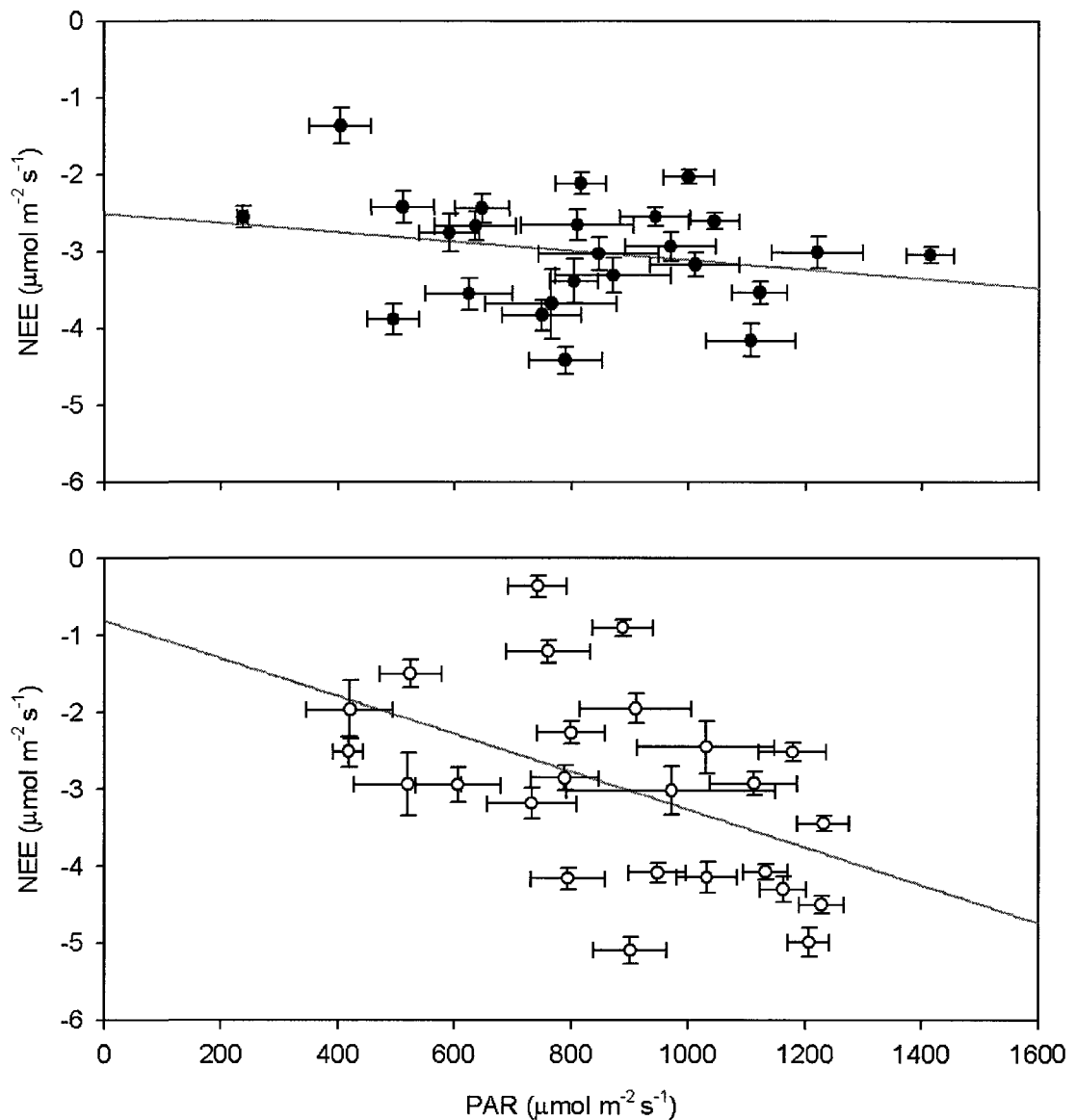


Figure 18. The relationship between daily daytime (10am – 6pm) net ecosystem exchange of CO_2 (NEE) and photosynthetically active radiation (PAR). The top panel illustrates the relationship for air temperature below 12°C and the bottom panel is for air temperature above 12°C . Lines are given for significant linear regressions. Top Panel: $(\text{NEE} = -0.0006 (\text{PAR}) - 2.52, r^2 = 0.05)$ and bottom panel: $(\text{NEE} = -0.003 - 0.81, r^2 = 0.25)$. Error bars represent ± 1 SE. The number of 30 min fluxes for each symbol ranges from 6 to 16.

4.5.2 Diurnal Variation in Ecosystem CH₄ and CO₂ Flux

Figure 19 shows the average diurnal variation in 30 min CH₄ flux during three different characteristic turbulence conditions. The first column in Figure 19 shows diurnal variation of CH₄ flux during days with consistently turbulent conditions, the second column are days with consistently calm conditions, and the third column are days with mixed conditions. During turbulent conditions, CH₄ flux was consistently low throughout the day (Figure 19, column 1) regardless of temperature; however, during relatively calm conditions, CH₄ varied with 5 cm soil temperature tending to peak in the evening (Figure 19, column 2). When u_* and temperature both varied diurnally, CH₄ flux also varied from low to high values depending on the magnitude of u_* and temperature (Figure 19, column 3). The effect of u_* and 5 cm soil temperature on 30 min CH₄ flux is also shown in Figure 20. When temperature remained below 12 °C, CH₄ flux tended to be low (typically less than 30 nmol m⁻² s⁻¹). Above 12 °C, CH₄ flux was more variable with values as high as 50 to 75 nmol m⁻² s⁻¹ when u_* was low (less than 0.24 m s⁻¹) but still above 0.1 m s⁻¹. Above u_* of 0.24 m s⁻¹, CH₄ flux was similar regardless of temperature (Figure 20). Figure 21 again shows how this u_* threshold of 0.24 m s⁻¹ influences the relationship between CH₄ flux and 5 cm soil temperature. Only when u_* is low does CH₄ flux notably increase with temperatures above 12 °C.

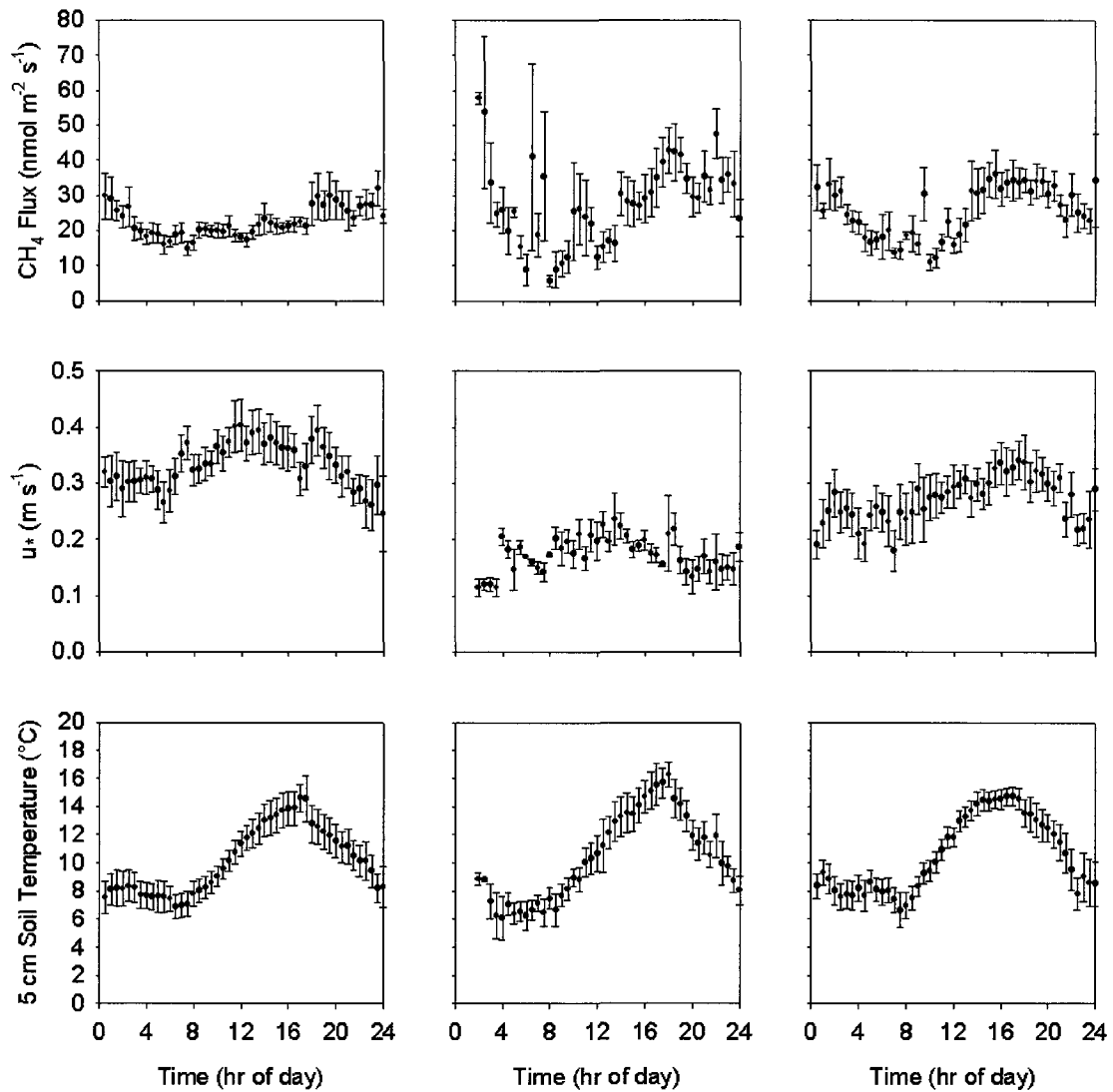


Figure 19. Diurnal variation of CH₄ flux, friction velocity (u_*), and 5 cm soil temperature for days with different turbulence conditions. Column 1 represents whole days ($14 < \text{half-hour measurements} < 49$) when mean u_* was above 0.24 m s^{-1} and the standard deviation (SD) was below 0.07 m s^{-1} , column 2 represents u_* below 0.24 m s^{-1} and the SD was below 0.07 m s^{-1} , and column 3 represents mixed u_* (all other days) with a SD above 0.07 m s^{-1} . Half-hour measurements with u_* below 0.1 m s^{-1} were not included. Error bars represent ± 1 SE. The number of 30 min measurements for each symbol ranges from 10 to 21.

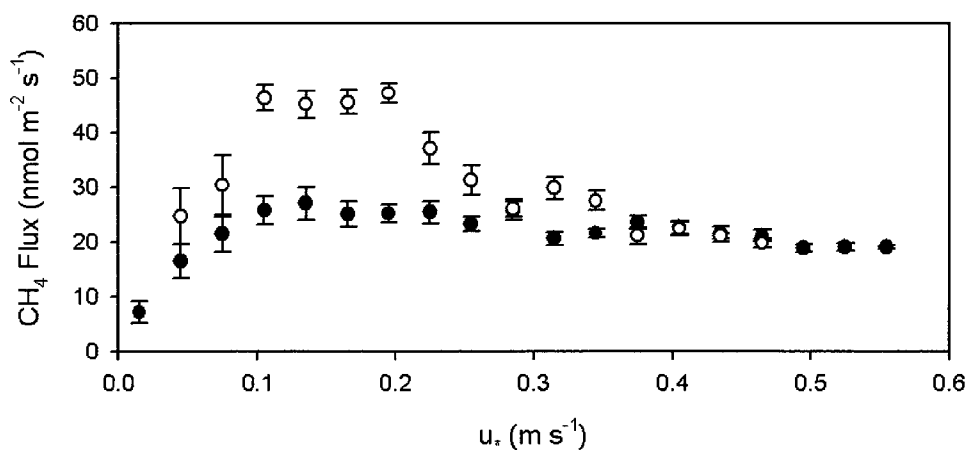


Figure 20. The relationship between 30 min CH₄ flux and frictional velocity, u*. Data are binned by u* (0.03 m s⁻¹ wide) and separated by temperature above (open circles) and below (closed circles) 12 °C. Error bars represent ±1 SE. The number of 30 min fluxes for each symbol ranges from 6 to 53.

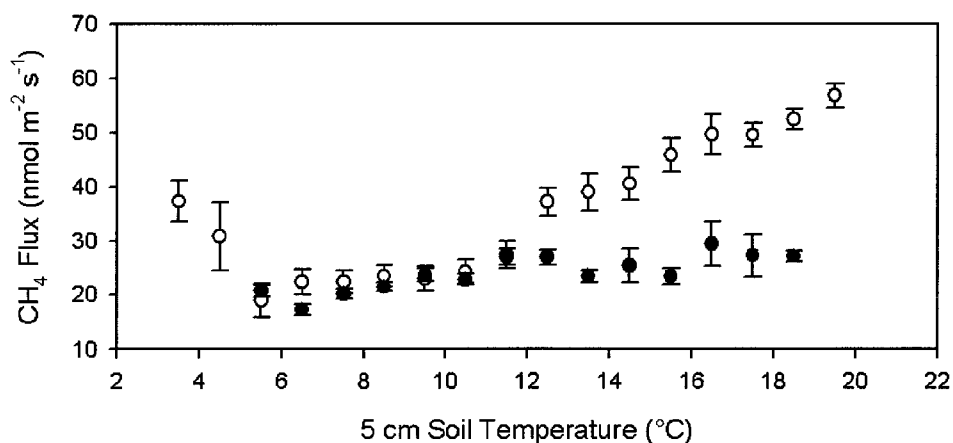


Figure 21. The relationship between 30 min CH₄ flux and 5 cm soil temperature. Data is binned by temperature (0.5 °C) and separated by u*. Open circles represent data below 0.24 m s⁻¹ and closed circles represent data above 0.24 m s⁻¹. Error bars represent ±1 SE. The number of 30 min fluxes for each symbol ranges from 5 to 58.

Based on the observation that CH₄ flux only responds to temperature variations above 12 °C and that this response depends on u* (Figure 20 & Figure 21), we identified two distinct groups of CH₄ fluxes when 5 cm soil temperature was above 12 °C. Group 1 consisted of fluxes above 30 nmol m⁻² s⁻¹, which were associated with low u*. Group 2 consisted of fluxes below 30 nmol m⁻² s⁻¹, which were associated with high u*. These two groups of 30 min CH₄ flux were tested for relationships with variables commonly associated with temporal variations in CH₄ exchange (Table 9 & Figure 22). CH₄ flux below 30 nmol m⁻² s⁻¹ correlated negatively to latent heat flux and PAR; whereas, CH₄ flux above 30 nmol m⁻² s⁻¹ correlated positively to VPD and 5 cm soil temperature (Table 9). For both groups combined, CH₄ fluxes correlated positively and significantly to VPD and 5 cm soil temperature and correlated negatively to PAR, friction velocity, and ecosystem conductance. No significant correlations were found for water table depth or stability.

Table 9. Spearman's rho correlation coefficients showing significant relationships between CH₄ flux and environmental variables for flux values above 12 °C. P- values are given in brackets and considered significant when p < 0.05.

	<i>Latent heat flux (W m⁻²)</i>	<i>PAR (μmol m⁻² s⁻¹)</i>	<i>VPD (kPa)</i>	<i>5 cm soil temperature (°C)</i>	<i>Friction velocity (m s⁻¹)</i>	<i>Ecosystem conductance (mol m⁻² s⁻¹)</i>
CH ₄ below 30 nmol m ⁻² s ⁻¹	-0.21 (0.006)	-0.23 (0.002)				
CH ₄ above 30 nmol m ⁻² s ⁻¹			0.22 (0.02)	0.25 (0.003)		
All CH ₄ flux		-0.22 (0.0001)	0.29 (<0.0001)	0.29 (<0.0001)	-0.32 (<0.0001)	-0.33 (<0.0001)

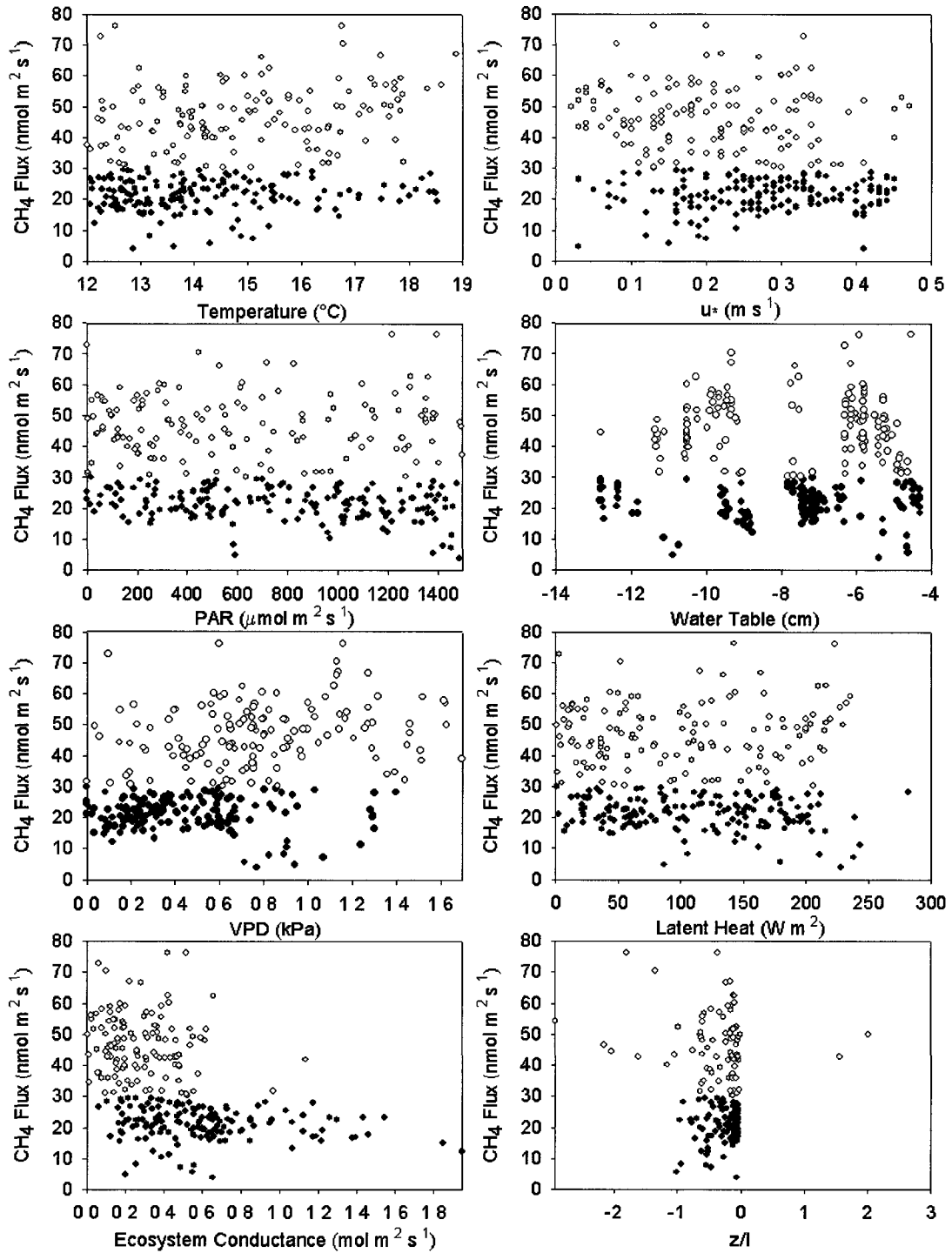


Figure 22. The relationship between 30 min CH₄ flux and all variables above 12 °C separated by CH₄ flux above and below 30 nmol m⁻² s⁻¹. Closed circles represent CH₄ flux below 30 nmol m⁻² s⁻¹ and open circles represent CH₄ flux above 30 nmol m⁻² s⁻¹.

Above the generally accepted u_* threshold of 0.1 m s^{-1} , nighttime NEE (CO_2 efflux) remained relatively constant particularly when 5 cm soil temperature remained below $8.5 \text{ }^\circ\text{C}$ (Figure 23). Greater CO_2 efflux was expected during warmer conditions as it influences both rates of plant and microbial respiration. Daytime 30 minute averages of NEE cannot be used to assess the influence of u_* because short-term variation is heavily influenced by PAR (Figure 24). This relationship between NEE and PAR is described using a rectangular hyperbolic relationship that highlights rapid increase in CO_2 sequestration at low light levels while at higher light levels, CO_2 uptake approaches an asymptotic value (GP_{max}) as light saturation occurs.

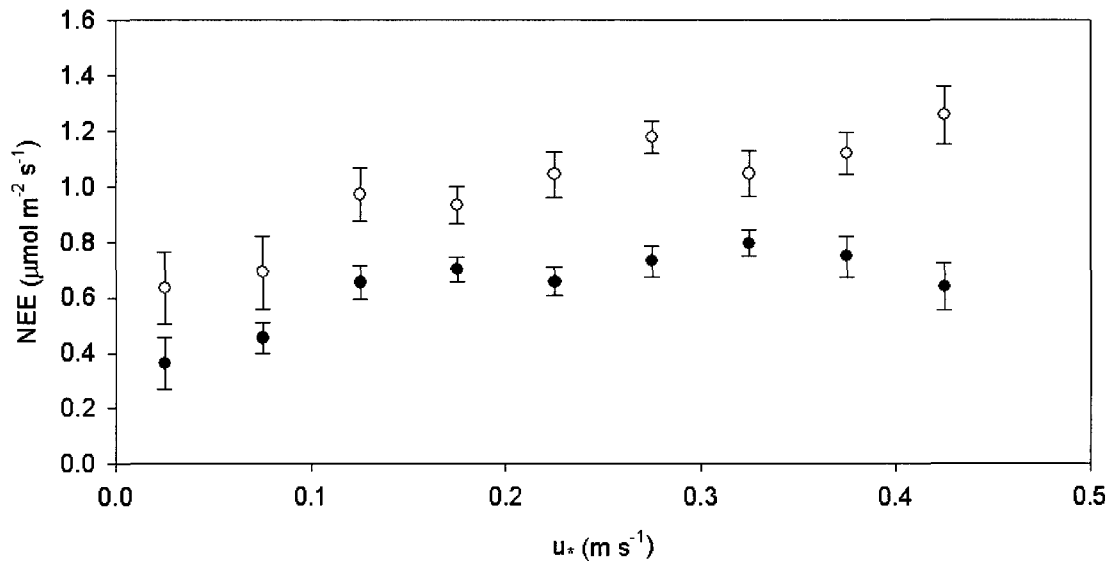


Figure 23. The relationship between nighttime (PAR less than $20 \mu\text{mol m}^{-2} \text{s}^{-1}$) net ecosystem exchange of CO_2 , NEE CO_2 , and frictional velocity, u_* . Data are binned by u_* (0.05 m s^{-1} wide) and separated by temperature above (open circles) and below (closed circles) $8.5 \text{ }^\circ\text{C}$. Positive values indicate net ecosystem carbon loss. Error bars represent $\pm 1 \text{ SE}$. The number of samples for each symbol ranges from 18 to 70.

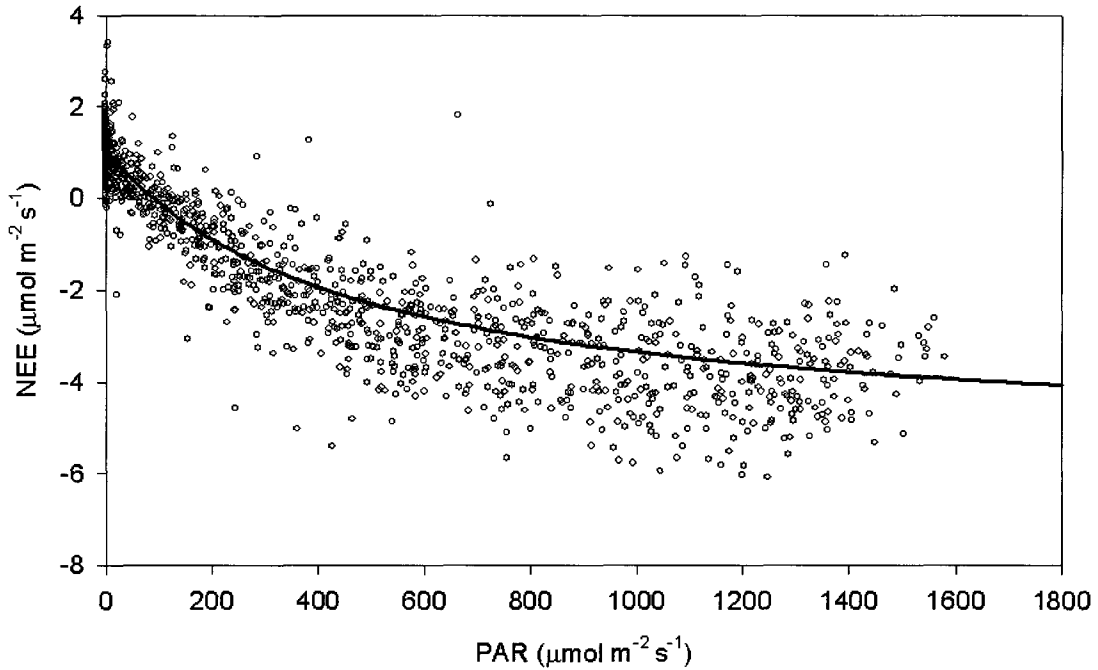


Figure 24. The relationship between net ecosystem exchange of CO₂, NEE, and photosynthetically active radiation, PAR for the study period. Symbols correspond to 30 minute averages of NEE which were above the frictional velocity threshold of 0.1 m s⁻¹ at night (PAR < 20 μmol m⁻² s⁻¹). The curved line corresponds to Equation 3 with parameters listed in Table 10. Negative values represent ecosystem uptake of carbon.

Table 10. Parameters for Equation 3 describing the response of NEE to PAR and average ecosystem air temperature for the study period. GP_{max} is maximum gross photosynthesis, α is the initial slope of the curve, R₁₀ is ecosystem respiration at a reference temperature of 10 °C, n is the number of observations, Q₁₀ is rate of increase in ER for a 10 °C increase in temperature*, RMSE is the root mean square error, and Temp is the average air temperature for the study period. Values in brackets indicate approximate standard error.

	GP_{max} ($\mu\text{mol m}^{-2}$ s^{-1})	α	R_{10} ($\mu\text{mol m}^{-2}$ s^{-1})	n	$RMSE$	$Temp$ (°C)
Sedge	-7.12	-0.01	0.89	1253	0.83	11.7
Fen	(0.16)	(0.0007)	(0.04)			

* The Q₁₀ value was set to 2, which is a commonly accepted value when assessing net ecosystem exchange at the ecosystem level.

4.6 Spatial Variation in Ecosystem CH₄ and CO₂ Flux

In addition to the influence of temporal variations in environmental factors such as turbulence, temperature, and light, variations in wind direction and footprint size influence the flux source area. For the spatial analysis of CH₄ and CO₂ flux, the area around the tower was divided into three distinct directional sectors based on landscape composition: sector 1, 0° - 135° (sedge fen dominated by lawn topography to NE, rocky upland area to SE); sector 2, 135° - 225° (sedge fen with tussock topography, small, open water bodies and rocky upland area); and sector 3, 225° - 360° (sedge fen and shrub peat mound areas) (Figure 2). While the area immediately around the tower was homogenous in all directions, all sectors became heterogeneous when the flux footprint included distances greater than 70 meters (Figure 2).

For all three sectors, high u_* resulted in large footprints and low CH₄ flux (Figure 25) presumably due the influence of greater turbulence rather than different source areas. For example, there was no tendency for fluxes to differ among the three directional sectors when footprints exceeded 70 m. At smaller footprint lengths and lower u_* , CH₄ fluxes tend to be slightly greater from sector 1 and slightly smaller from sector 2, which may be the result of slightly lower average soil temperatures associated with the sector 2 measurements (sector 2: 9.8 ± 0.3 °C vs. sector 1: 11.3 ± 0.3 °C) during the sampling period ($F_{1,132} = 11.32$, $p = 0.001$).

NEE also demonstrated similar trends and magnitudes when winds came from sectors 2 and 3, while sector 1 was significantly different, until a critical footprint distance of approximately 70 meters was reached (Figure 26 & Table 11). Significantly less CO₂ uptake (negative NEE) may have occurred in sector 1 due to slight differences

in spatial heterogeneity within the three sectors. Significantly greater CO₂ uptake tended to occur within sector 3 at distances greater than 70 m (sedge fen and dwarf birch shrub peat mound area) when compared to the other two sectors (Table 11). These tower results agree with the greater rates of CO₂ uptake measured using the chamber system in the shrub areas (Figure 16).

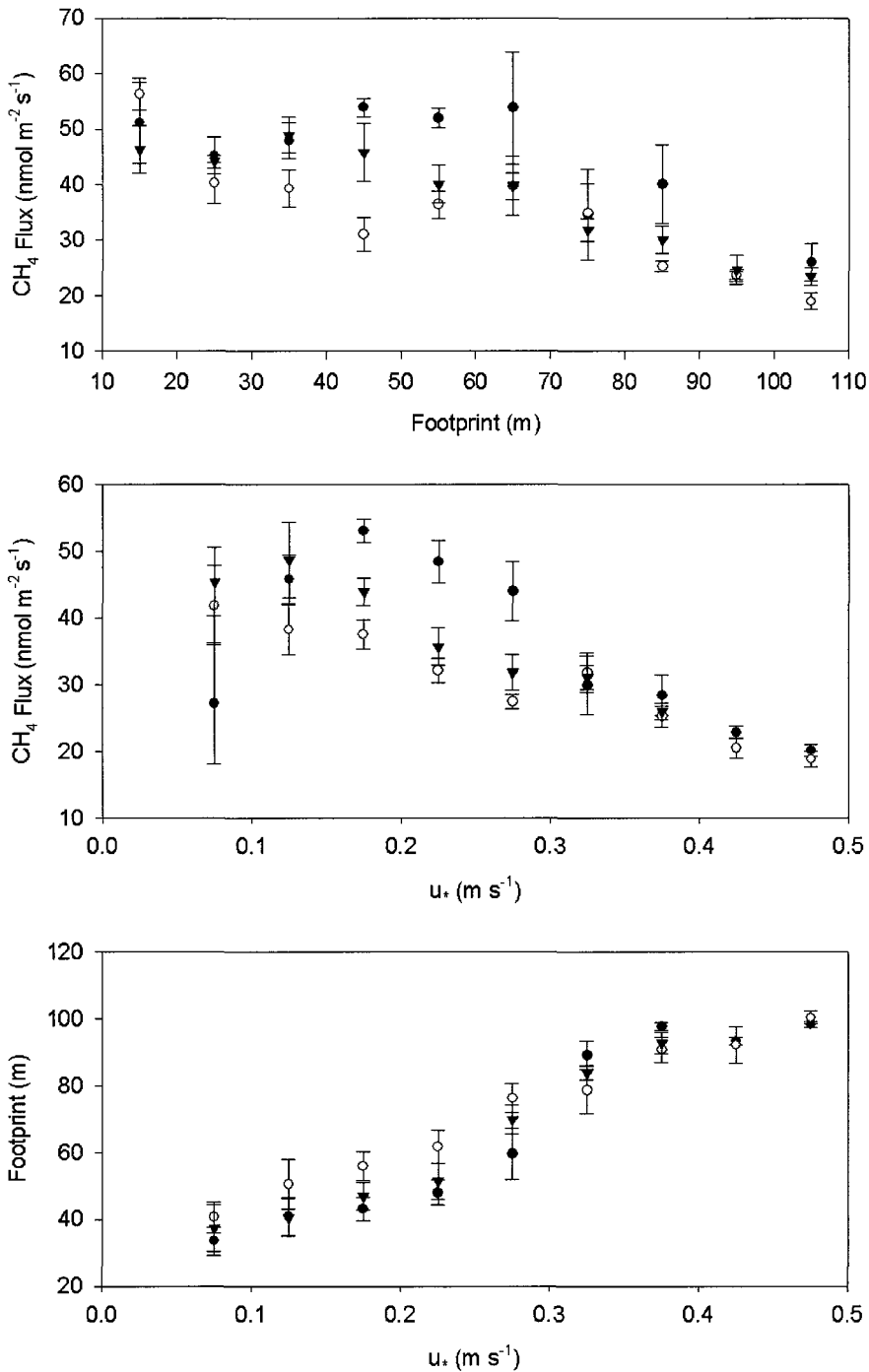


Figure 25. The relationship between 30 minute averages of CH₄ flux, friction velocity, u*, and footprint distance for three spatially different areas within the fetch of the eddy covariance tower. Closed circles represent sector 1 (0° - 135°), open circles represent sector 2 (135° - 225°), and closed triangles represent sector 3 (225° - 360°). Data are binned by footprint (10 m wide) and u* (0.05 m s⁻¹ wide). Error bars represent ±1 SE. The number of samples for each symbol ranges from 6 to 36.

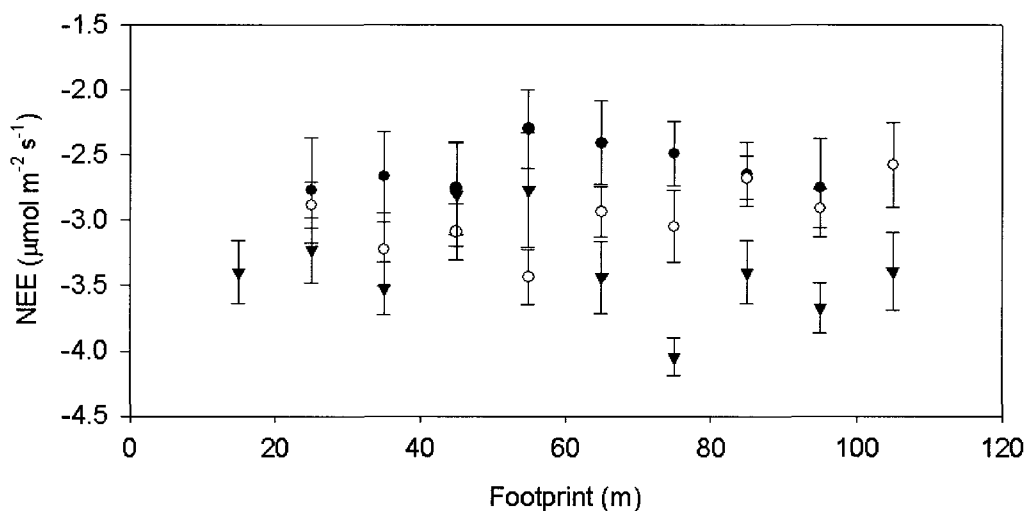


Figure 26. The relationship between net ecosystem exchange of CO₂, NEE, and footprint distance for three spatially different areas within the fetch of the eddy covariance tower. Closed circles represent sector 1 (0° - 135°), open circles represent sector 2 (135° - 225°), and closed triangles represent sector 3 (225° - 360°). Error bars represent ± 1 SE. The number of samples for each symbol ranges from 9 to 50.

Table 11. Average daytime (10am – 6pm) NEE for footprint distances from tower of 70 m or less and for distances greater than 70 m for the three sectors during the study period. Error associated with NEE is ± 1 SE. Numbers in brackets indicate the number of observations. Different superscript letters indicate significant differences within a column ($p < 0.05$). NEE, net ecosystem exchange of CO₂.

	<i>Average NEE < 70 m</i> ($\mu\text{mol m}^{-2} \text{s}^{-1}$)	<i>Average NEE > 70m</i> ($\mu\text{mol m}^{-2} \text{s}^{-1}$)
Sector 1	-2.55 ± 0.16 (86) ^a	-2.58 ± 0.15 (83) ^a
Sector 2	-3.13 ± 0.11 (74) ^b	-2.84 ± 0.10 (97) ^a
Sector 3	-3.25 ± 0.12 (73) ^b	-3.62 ± 0.11 (130) ^b

4.7 Growing Season C Budget and GWP

Daily total and cumulative NEE was computed for the full growing season (June 1 to August 31) after gap-filling as described in section 3.6.6 (Figure 27). The fen was a sink for CO₂ with overall estimated NEE for the 2009 growing season to be -66.3 g C m⁻².

Growing season CH₄ exchange was determined by first computing daily average CH₄ fluxes using days where data coverage was >25% (12 half-hour measurements) (n=27 days). Next, daily averages of CH₄ flux, 5 cm soil temperature, and u* were calculated in order to minimize variance associated with rapid changes in wind speed, direction, and footprint size. Modelled daily CH₄ flux was obtained from equation 5 with parameters listed in Table 12. A good agreement (r²= 0.69) between measured and modeled data was obtained (Figure 28). The overall estimated CH₄ emission for the 2009 growing season was 2390 mg C m⁻² or 2.4 g C m⁻² (Figure 29). The amount of C released as CH₄ was approximately 3.75% of that sequestered through ecosystem exchange of CO₂.

The average amount of DOC (mg l⁻¹) for the three sampling periods is listed in Table 13, along with the average slope and flow rates for the inlet and outlet. Average flux values for these three days were calculated using equation 4 with an estimated peat hydraulic conductivity of 10⁻⁴ m s⁻¹, a fen area of 42 hectares, and a varying hydraulic head (Table 14). The average of these three days was used to calculate the overall estimated DOC flux for the 2009 growing season. The estimated DOC flux was 0.9 g C m⁻². The amount of C released as DOC was approximately 1.33 % of that sequestered through NEE.

Overall, the fen was a sink of approximately 63.0 g C m^{-2} during the growing season of 2009 at Daring Lake. Emission of CH_4 and loss of DOC accounted for approximately 5 % of the overall growing season C taken up as CO_2 (Table 15). With these relatively small CH_4 emissions and large CO_2 uptake, the growing season C budget for the fen represented a negative forcing effect on atmospheric warming over both the 20 year and 100 year timescales (Table 15).

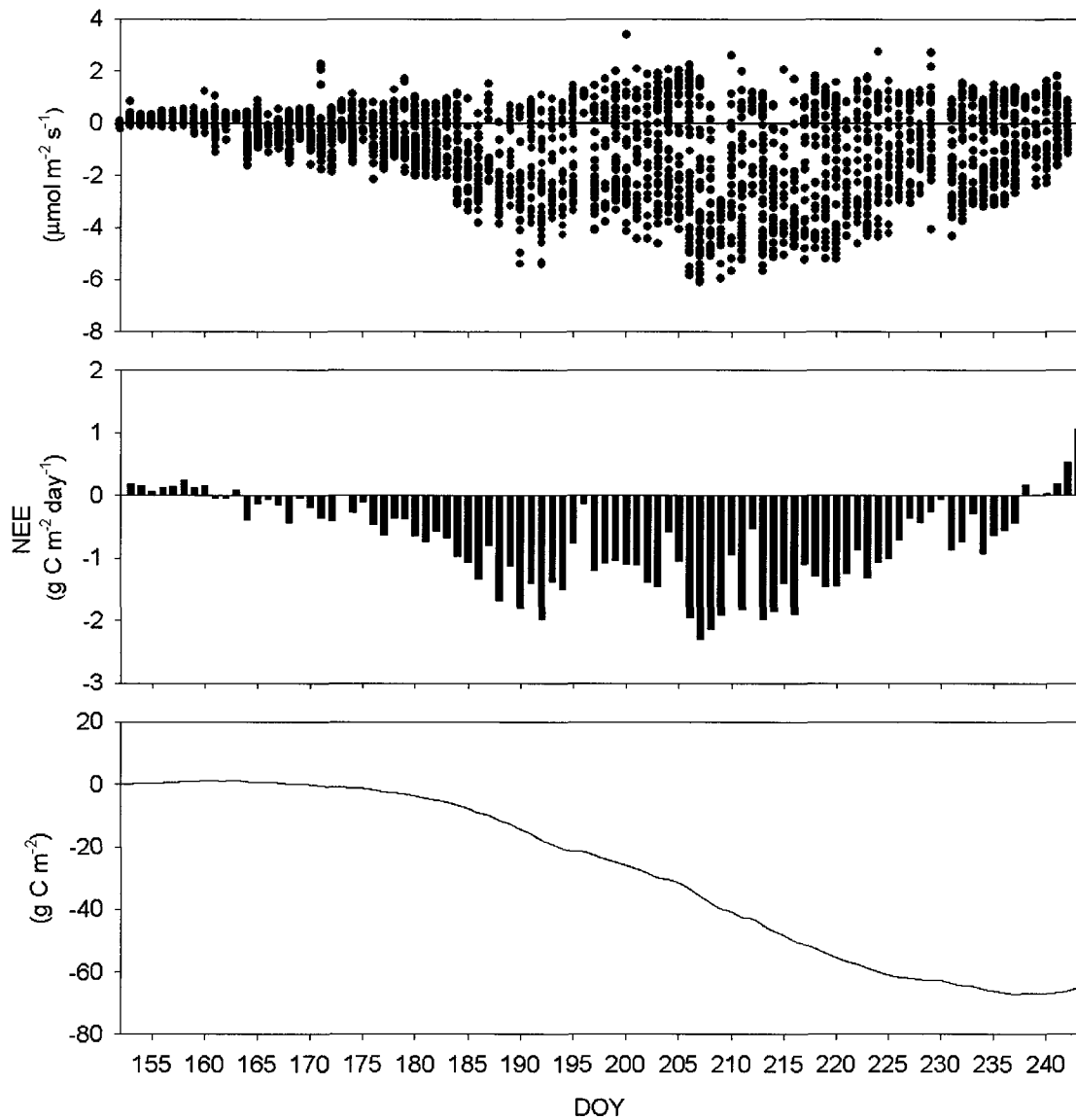


Figure 27. Half-hour measured net ecosystem exchange (NEE) (top), gap-filled daily NEE (middle) and cumulative NEE (bottom) for 1 June to 31 August 2009. Positive values represent a net C loss to the atmosphere while negative values represent a net C accumulation by the ecosystem.

Table 12. CH₄ input and model parameters for the growing season of 2009 using Equation 5. T_{ref}, average temperature for the sampling period, u*_{ref}, average frictional velocity for the sampling period, a, b, c are fit parameters, RMSE, root-mean standard error, r², correlation coefficient, n, number of samples. Errors associated with fit parameters are ± SE. The number of daily averages used was 27.

<i>Parameters</i>	
T _{ref} (°C)	8.57
u* _{ref} (m s ⁻¹)	0.23
a (mg m ⁻² day ⁻¹)	25.2 ± 1.31
b (°C)	2.07 ± 0.51
c (m s ⁻¹)	0.17 ± 0.09
RMSE	5.0
r ²	0.69

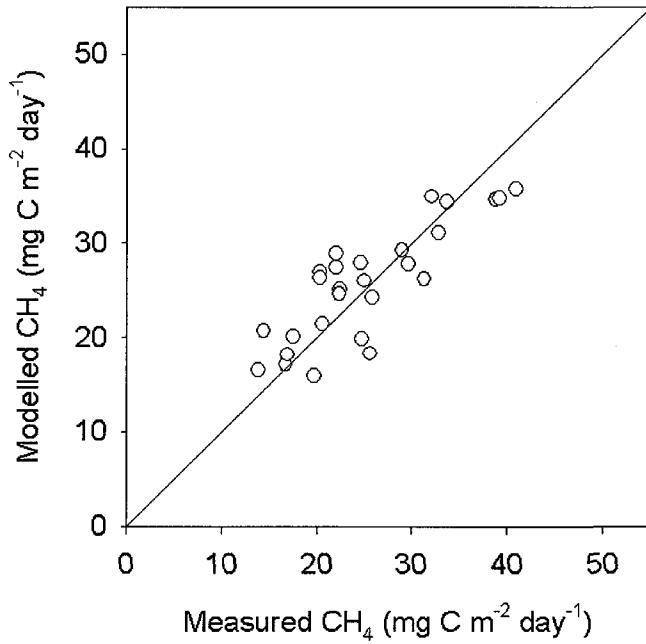


Figure 28. Daily integrated mean values of eddy covariance CH₄ emission versus modelled emission rates from Equation 5 and modelled parameters from Table 12. CH₄, methane.

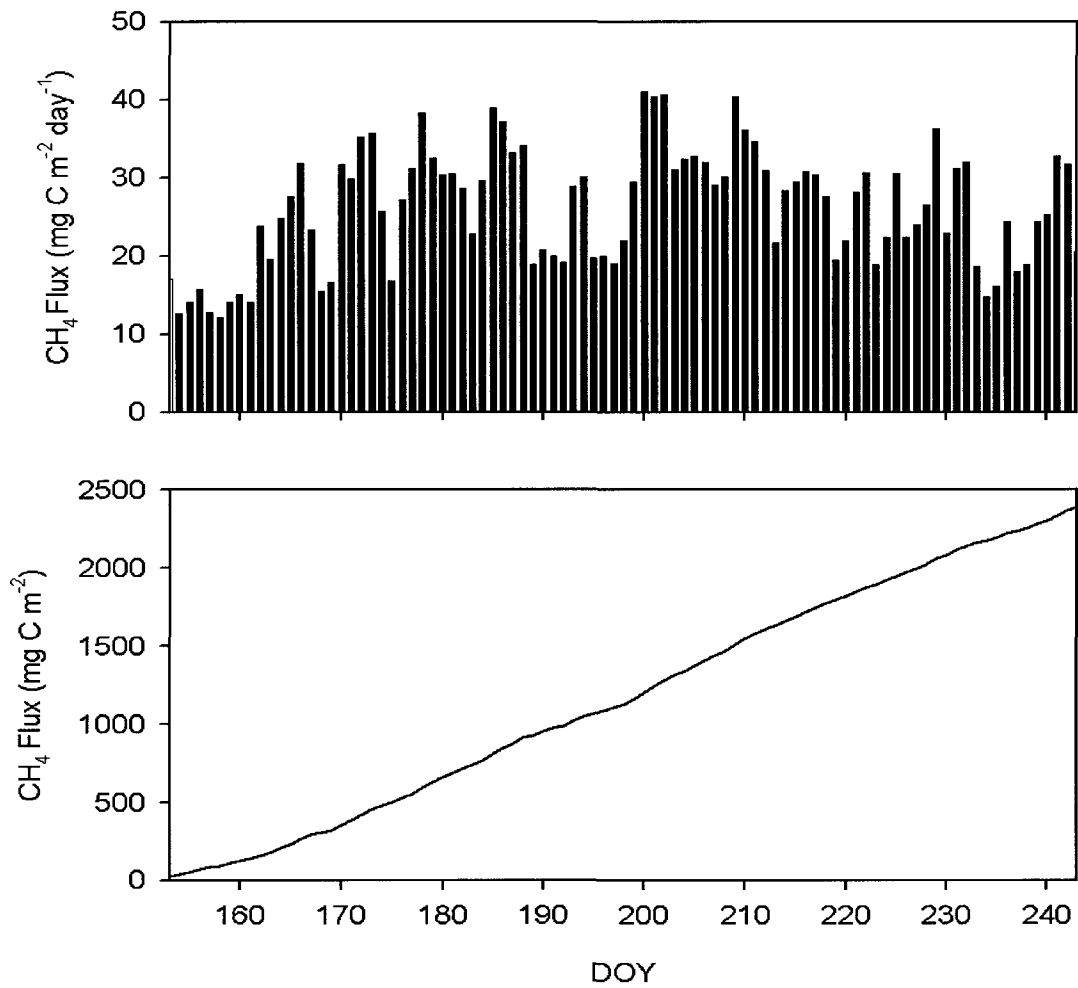


Figure 29. Daily CH₄ flux (middle) and cumulative CH₄ flux (bottom), modelled, for 1 June to 31 August 2009. Positive values result in net C loss to atmosphere. CH₄, methane.

Table 13. Average dissolved organic carbon (DOC), slope (dh/dz), and flow rates for three measurement periods during summer of 2009, Daring Lake. Values within brackets indicate standard error of the mean. The number of samples for each measurement is 3.

	<i>DOY 203</i>	<i>DOY 213</i>	<i>DOY 223</i>
Inlet Concentration (mg C l ⁻¹)	52.35 (4.09)	48.93 (3.93)	42.35 (5.51)
Inlet slope (dh/dz)	0.0015	0.0006	0.0002
Inlet flow (cm ³ s ⁻¹)	0.96	0.90	0.82
Outlet Concentration (mg C l ⁻¹)	27.00 (2.04)	27.53 (2.73)	24.96 (3.77)
Outlet slope (dh/dz)	0.028	0.029	0.027
Outlet flow (cm ³ s ⁻¹)	3.46	3.51	3.09

Table 14. Average ecosystem storage change of dissolved organic carbon, DOC, for three measurement periods during the summer of 2009, Daring Lake. Values within brackets indicate standard error of the mean. Positive values indicate loss of DOC from the ecosystem. The number of samples for each measurement is 6.

	<i>DOY 203</i>	<i>DOY 213</i>	<i>DOY 223</i>	<i>Average Daily Rate</i>
Ecosystem Storage Change DOC (g C m ⁻² day ⁻¹)	8.88×10^{-3}	1.08×10^{-2}	8.74×10^{-3}	9.47×10^{-3} (0.0028)

Table 15. GWP and modelled carbon balance for the growing season (June 1 – August 31) 2009 at Daring lake, NT. Positive numbers indicate ecosystem carbon loss and negative numbers indicate ecosystem carbon uptake and negative forcing potential to warm atmosphere.

	<i>Fen CO₂</i>	<i>Fen CH₄</i>	<i>Fen DOC</i>	<i>Fen Total</i>
Carbon Balance (g C m ⁻²)	-66.3	2.4	0.9	-63.0
GWP (20 yr horizon) (g CO ₂ m ⁻²)	-243.3	229.4		-13.8
GWP (100 yr horizon) (g CO ₂ m ⁻²)	-243.3	66.9		-176.3

5.0 DISCUSSION

This research builds on the considerable body of literature on land-atmosphere interactions in arctic wetlands and in particular, sedge fen tundra. For the first time, to my knowledge, concurrent ecosystem scale fluxes of CO₂ and CH₄ are reported for this type of arctic ecosystem. These results highlight how factors such as vegetation, moisture, temperature and light influence these components of the C budget and in particular, how the importance of these factors change as fluxes are integrated over larger spatial scales.

5.1 CO₂ Fluxes

On an ecosystem level, PAR and temperature were found to be important factors controlling daily and 30 min variations in NEE as these factors influence rates of photosynthesis and respiration. Photosynthesis is primarily controlled by the amount of incoming solar radiation and to a lesser extent temperature (Vourlitis *et al.*, 2000). As PAR increases, photosynthetic activity increases to a saturation point where an increase in PAR no longer promotes the plant's ability to photosynthesize at an optimum rate. After this point, temperature often becomes an important factor influencing the magnitude of 30 min NEE (Vourlitis and Oechel, 1999; Kwon *et al.*, 2006) and may explain the increase in scatter in NEE around the temperature-light response curve as PAR increases (Figure 24). When temperatures increase, ER, which is a function of autotrophic and heterotrophic respiration, may respond through increased microbial activity and plant respiration resulting in an exponential rise in CO₂ release (Vourlitis and Oechel, 1999; Kwon *et al.*, 2006). The temperature-light response curve in this study was associated with a coefficient of determination of 0.76, indicating that only 24% of

the variation in NEE could not be explained by variations in PAR and temperature. This was similar to the relationship developed for a sedge fen landscape with very similar site characteristics at Happy Valley, Alaska ($r^2 = 0.70 - 0.75$) (Vourlitis *et al.*, 2000). In contrast, the r^2 values for upland tundra at Daring Lake (Lafleur and Humphreys, 2008) were less ($r^2 = 0.56 - 0.66$) in 2004 to 2006. The greater proportion of variation in NEE explained by PAR and temperature in the sedge fen ecosystems compared to the upland tundra may be due to differences in species composition but also due to the relatively consistent moisture conditions of these sedge fen ecosystems. Upland tundra NEE may respond more dramatically to rainfall events for example.

In this study, daily CO₂ uptake increased more with sunnier conditions when it was warmer but other studies suggest that temperature change may have a minimal effect on CO₂ uptake, as arctic plants have a broad range at which optimum photosynthesis can occur (Vourlitis and Oechel, 1999; Vourlitis *et al.*, 2000).

Although many studies show the importance of seasonal variations in soil moisture or water table on CO₂ exchange (Vourlitis and Oechel, 1999; Vourlitis *et al.*, 2000; Corradi *et al.*, 2005; Kwon *et al.*, 2006; Merbold *et al.*, 2009), there was no evidence of these factors playing a role in temporal variations in ecosystem CO₂ exchange. The lack of a wetness control may be due to minimal water table drawdown from the beginning (5 cm below surface) to the end (13 cm below surface) of the study period, resulting in a hydraulic head difference of only 8 cm, while in these other studies, maximum variation was larger (e.g. 20 cm in the study by Vourlitis and Oechel (1999)).

In contrast, at the small plot scale, chamber measurements of CO₂ exchange highlighted the importance of vegetation characteristics and soil moisture as well as light and temperature on both spatial and temporal variations in CO₂ changes.

Overall, GEP, ER, and NEE did not differ between lawns and tussocks for the study period. While there were significant differences in soil temperature and VWC between the two communities, total LAI and % cover did not differ. Instead, spatial variations in NEE and GEP on a per collar basis were significantly related to LAI and % cover while ER related to GEP illustrating that the simple designation of tussock vs. lawn could not explain the considerable spatial variability in CO₂ exchange at this site. Other wetland studies have found differences in C fluxes that could be related to both microtopography and vegetation characteristics. Riutta *et al.* (2007) suggested that GEP differences within 5 similar communities containing both lawns and tussocks in a northern boreal fen were determined in part by significant differences in % vascular cover and also by differences in water table depth where a lower water table resulted in increased ER. However, Riutta *et al.* (2007) also noted a strong relationship between GEP and vascular respiration, supporting the conclusion that a portion of ER is driven by changes in GEP. Sullivan *et al.* (2008) suggested that higher GEP in tussocks vs. lawns in a high arctic fen was directly related to greater LAI and plant biomass. Christensen *et al.* (2000) reported higher net CO₂ uptake (more negative NEE) in tussocks compared to lawns which is in contrast to the observations by Heikkinen *et al.* (2002) in a low arctic wet tundra landscape and Strack *et al.* (2006) within a wet fen northern ecosystem where lawns had greater net CO₂ uptake.

Temporal variations in plot scale measurements of GEP, ER, and NEE were directly related to temporal variations in PAR, air temperature, soil temperature, water table depth, and VWC. It is interesting to note that ER within lawn and tussocks at Daring Lake had opposite significant relationships to VWC, but increases in ER in both microsites related to increases in soil temperature. This may have occurred because lawns were already moist enough for optimal ER and additional water may have reduced rates of aerobic respiration while tussocks required more moisture for optimal ER. Other field and laboratory studies have proposed a relationship between soil respiration and VWC with greatest CO₂ effluxes occurring at some optimum moderate VWC and decreasing respiration at higher or lower VWC (Bunnell *et al.*, 1997, Reth *et al.*, 2005, Strack and Price, 2009). However, the nature of this relationship is difficult to isolate due to concurrent variations in other variables such as soil temperature, substrate amount, pH-value, and nutrient status (Reth *et al.*, 2005). Increases in temperature most likely increased plant and soil respiration as the water table and VWC decreased throughout the study. Sullivan *et al.* (2008) also showed that soil drying increased ER in saturated lawn microtopography. However, as water table increased, ER in hummocks decreased but as VWC was not reported by Sullivan *et al.* (2008), it is difficult to suggest the reasons for this discrepancy. In a WT and temperature manipulation experiment in an Alaskan sedge fen tundra ecosystem, increases in soil temperature and decreases in water table were related to increases in ER (Oechel *et al.*, 1998). Vourlitis *et al.* (2000) suggested that variations in WT, independent of temperature, may act as the dominant factor that may cause these ecosystems to switch from being a C sink to being source of C.

5.2 CH₄ Fluxes

In contrast to CO₂ exchange, CH₄ emissions were significantly different between lawns and tussocks. The spatial as well as temporal variations in these fluxes were also related to many of the same abiotic controls important in CO₂ exchange. Overall, the significantly cooler, wetter, lawns resulted in significantly higher CH₄ flux (almost twice) compared to the elevated, warm, dry tussocks. As total CH₄ emissions depend in part on production in anaerobic soil conditions and consumption in aerobic soil conditions, it is not surprising that greater rates of CH₄ emission are common in microsites with greater VWC. For example, CH₄ emissions were greatest within saturated lawn microtopography in a hummocky fen in the high Arctic (Christensen *et al.*, 2000). Christensen *et al.* (1995) found greater rates of CH₄ emission in wet tussock habitats vs. mesic habitats in Siberian and European tundra environments.

The factors influencing CH₄ transport are just as important as production and oxidation in overall emission (Lai, 2009). The presence of vascular vegetation with aerenchymatous tissue, such as sedges, which can develop deep rooting systems into the anaerobic zone, provides a conduit for CH₄ to the surface (Grondahl *et al.*, 2008; Lai, 2009). Vegetation characteristics have been shown to influence spatial differences in CH₄ flux at a number of arctic sites (Christensen *et al.*, 1995; Christensen *et al.*, 2000; Grondahl *et al.*, 2008; Hayne, 2009). Methane emission has also been linked to ecosystem productivity at waterlogged sites where sedge root exudates and fresh plant material available for decomposition supply the necessary substrate for methanogenesis to occur (Bellisario *et al.*, 1999; Christensen *et al.*, 2000). In this study, CH₄ flux was positively related to sedge LAI when the tussock and lawn collars were combined into a

single group, indicating the potential for CH₄ emission to be influenced by these plants. However, since there was no relationship between CH₄ emission and ecosystem productivity in this study, this suggests that sedges may have had a greater influence on transport than production.

Spatial differences in temperature can affect the rate at which methanogenesis occurs; however, it is tightly related to soil moisture (Lai, 2009). Generally, a positive relationship exists between temperature and microbial production of CH₄; however, oxidation rates of CH₄ may influence CH₄ emission when the water table is below the surface (Treat *et al.*, 2007). Christensen (2000) found in five distinct Arctic tundra environments that within-season variability of CH₄ flux at wet sites were primarily controlled by soil temperature; however, at sites that were generally dry, CH₄ flux was primarily controlled by position of water table.

In general, temporal variations in CH₄ emissions were positively related to temperature, VWC, and WT; however, these relationships were not always consistent between tussocks and lawns. While tussocks had a positive relationship with VWC, lawns did not. Due to the small drop in WT over the study period, VWC remained relatively high and constant in lawns, while tussocks experienced more variation in moisture. As a result, the depth of the aerobic zone was much more variable in tussocks and may have led to more variable rates of CH₄ oxidation, potentially resulting in variable rates of CH₄ emissions. CH₄ emission was greater when the WT was closer to the surface which is in accordance with typical relationships observed in field studies (Christensen *et al.*, 2000). Bellisario *et al.* (1999) observed a similar relationship between CH₄ and WT in a boreal peatland where the range of WT (15 cm) among sites

was very similar to this study. For permanently, or close to permanently, waterlogged zones, plant productivity has been suggested to be the main control of CH₄ emission as plants provide substrate for methanogenesis and ventilation associated with plant CH₄ transport (Whiting and Chanton, 1993; Bellisario *et al.*, 1999; Christensen *et al.*, 2000). For drier sites, a positive relationship between plant productivity and CH₄ emission is not necessarily valid as WT may override other biotic and abiotic controls (Bubier and Moore, 1994; Waddington *et al.*, 1996; Christensen *et al.*, 2000). At Daring Lake, GEP was not measured concurrently with CH₄ emissions but when examining the average CH₄ flux for each collar, there was no relationship with the average GEP. However, concurrent measurements of CH₄ flux and ER_S were positively correlated in time for tussocks and combined lawns and tussocks; however, no significant relationship was observed for CH₄ and ER_S in lawns. It is possible that this links autotrophic respiration and thus plant productivity to CH₄ emissions, however, this is confounded by temporal variations in abiotic factors (temperature, VWC, WT, and PAR) that promote both CO₂ and CH₄ production.

While there have been many arctic studies examining CO₂ exchange, ecosystem scale controls on CH₄ flux dynamics in the Arctic remain uncertain (Sachs *et al.*, 2008). Ecosystem scale CH₄ flux studies have been conducted in a limited number of arctic and northern boreal ecosystems (Friborg *et al.*, 2000; Hargreaves *et al.*, 2001; Sachs *et al.*, 2008; Wille *et al.*, 2008; Gazovic *et al.*, 2010; Long *et al.*, 2010); however, most of these have taken place in either wet polygonal tundra or in treed fens.

At the Daring Lake fen, temperature and friction velocity controlled variation in daily and 30 min CH₄ emissions. The positive relationship between temperature and CH₄

emission reflects the direct dependence of microbial activity on temperature (Wille *et al.*, 2008). This relationship has been well documented in numerous CH₄ emission studies (Friborg *et al.*, 2000; Hargreaves *et al.*, 2001; Wille *et al.*, 2003; Sachs *et al.*, 2008; Long *et al.*, 2010).

Water table position has been identified as another environmental variable controlling methane emission (Friborg *et al.*, 2000) and was clearly the case for the small plot-scale CH₄ fluxes at Daring Lake. This can be explained through regulation of methane production and consumption in the aerobic and anaerobic layers of the peat profile, with increasing consumption resulting in decreasing CH₄ emission as the aerobic/anaerobic ratio increases (Wille *et al.*, 2008). However, in contrast to the chamber measurement results, variations in water table did not relate to daily variation in ecosystem scale CH₄ emissions. This is similar to other studies where water table remained at or just below peat surface (Hargreaves *et al.*, 2001; Wille *et al.*, 2008). This is also seen at sites where the water table was significantly below the peat surface (40 – 60 cm) throughout the study period (Long *et al.*, 2010). A relationship between ecosystem scale CH₄ fluxes and water table was observed at a high-arctic fen in Greenland where water table varied from above the fen surface to 80 cm below the surface during the study period (Friborg *et al.*, 2000). The water table at the beginning of our measurement period was located below the peat surface (5 cm). If measurements had been made when the water table was above the surface in the early spring, it is plausible that a relationship between CH₄ and WT may have existed, however, the tendency for temperature to increase while water table drops through the growing season may confound such a relationship.

Thaw depth has been identified as another abiotic factor controlling methane emission (Friborg *et al.*, 2000). In our study, thaw depth was not a determinant of CH₄ emission indicating that, while increases in temperature did increase available C at depth, dominant methane production is likely to have originated from the upper portion of the soil horizon. It is likely that the decreasing amount of biologically available C substrate at depth used for energy production via methanogenesis was the controlling variable limiting production of CH₄ in this area for microorganisms well adapted to cold environments (Wille *et al.*, 2008). Several studies from Siberian arctic tundra report no relationship between thaw depth and CH₄ emission (Sachs *et al.*, 2008; Wille *et al.*, 2008).

Atmospheric pressure drop resulting in bubble ebullition has also been identified as a factor controlling methane emission (Kellner *et al.*, 2005, Tokida *et al.*, 2007); however, in our study, there was no observed relationship. Kellner *et al.* (2005) indicate that a drop in pressure may cause episodic release of CH₄ gas that was entrapped in peat cavities and stuck to pore walls, though adhesion, where over time they accumulate and grow. A pressure drop would cause an enlargement of the volume of gas, potentially resulting in release; however, Tokida *et al.* (2007) report that due to the episodic behavior of ebullitive CH₄ flux, it is difficult to quantify.

In addition to temperature, turbulence in the near-surface boundary layer, quantified by u_* , was a second important driver of CH₄ flux at our site. CH₄ fluxes increased with u_* until approximately 0.1 m s^{-1} and then decreased when u_* increased beyond 0.24 m s^{-1} . To date, no other studies have reported exactly this relationship. The increase in CH₄ emissions with increasing u_* is consistent with observations by Fan *et al.*

(1992) who reported similar results from a mixed tundra landscape with high surface coverage of water within the fetch. Hargreaves *et al.* (2001) described similar findings between momentum flux and CH₄ emissions for periods up to one day within a Finnish Lapland tundra site with 70 percent open standing water. Sachs *et al.* (2008) and Wille *et al.* (2008) also reported that u^* was an important driver of CH₄ flux for Siberian arctic polygonal tundra and both of these studies also reported the presence of open water bodies. A positive relationship between CH₄ emission and u^* for sites with open water is driven through changes in the near surface turbulent layer by diffusive and turbulent transfer across the water-air interface, with results from lake studies suggesting direct dependence of gas transfer on wind speed (Wille *et al.*, 2008). Also, bubbles of CH₄ that adhere to plant surfaces under the water may be released by agitation of plants, wave action, and under-water turbulence caused by increases in wind velocity (Sachs *et al.*, 2008). In a northern Canadian moderately treed fen with a WT greater than 40 cm below the surface, Long *et al.* (2010) also found CH₄ emissions to increase with u^* . Increases in CH₄ emission associated with increases in u^* in non-inundated surfaces, dominated by thick moss layers, may be a result of a thinning laminar boundary layer causing a high concentration gradient between the soil and the turbulent boundary layer, ultimately resulting in an increase in diffusive flux of CH₄ to the surface (Sachs *et al.*, 2008). Hargreaves *et al.* (2001) found increases in CH₄ emissions following calm periods (Sachs *et al.*, 2008). However, it is suggested that storage flushing may only play a role on shorter timescales, and over longer time scales, the rate of CH₄ emission may decrease.

Our results show a negative relationship between CH₄ emission and u^* greater than 0.24 m s^{-1} , which is contrary to observations by Long *et al.* (2010) in a non-

inundated ecosystem. At Daring Lake, sustained high u_* was associated with consistently low CH_4 fluxes while calmer conditions (but still with u_* above 0.1 m s^{-1}) resulted in higher but much more variable CH_4 fluxes as variations in temperature only influenced CH_4 emissions when u_* remained below 0.24 m s^{-1} . Although u_* was related to footprint size, there was no clear relationship between source area and CH_4 emissions. One possibility is that under sustained turbulence, diffusion/ebullition rates match production rates, while under calmer conditions, particularly when $u_* < 0.1 \text{ m s}^{-1}$, CH_4 has the potential to accumulate within the peat (more so during warmer conditions) establishing a greater below to above ground concentration gradient such that when u_* increases slightly, greater diffusion, ebullition and plant mediated transport is possible. This reasoning is supported by Sachs *et al.* (2008) who suggest that atmospheric parameters exhibit superior control over CH_4 release when compared to temperature related production and emission and that the production and emission of CH_4 are not closely linked on short timescales. Sachs *et al.* (2008) observed with congruent CH_4 chamber and eddy covariance measurements that a slight disturbance of sediments beneath a floating chamber resulted in a quick five-fold CH_4 concentration increase. This observation would imply that a substantial amount of free-phase CH_4 is stored within the soil profile and that rates of CH_4 production, transport, and emission proceed at varying rates dependent upon dominant biotic and abiotic controls.

A number of studies have compared chamber and eddy covariance flux magnitudes of either CH_4 or CO_2 within the same ecosystem (Griffis *et al.*, 2000; Twine *et al.*, 2000; Aurela *et al.*, 2007; Rinne *et al.*, 2007; Fox *et al.*, 2008; Sachs *et al.*, 2008). Both sampling techniques have potential uncertainties associated with them (Fox *et al.*,

2008; Grondahl *et al.*, 2008; Sachs *et al.*, 2008; Schrier-Uijl *et al.*, 2010). Chamber measurement techniques have the potential to alter air pressure and air and soil temperature during sampling within the chamber (Kutzbach *et al.*, 2007; Sachs *et al.*, 2008), while the effects of atmospheric turbulence on CH₄ release and production are inhibited (Sachs *et al.*, 2008). Eddy covariance fluxes may be affected by heterogeneous soil characteristics and surface cover, turbulence properties, flow distortion, sensor separation, and instrument error (Schrier-Uijl *et al.*, 2010). A lack of energy balance closure, which is not uncommon (Corradi *et al.*, 2005), may result in underestimation of actual fluxes (Twine *et al.*, 2000). While chambers are excellent over short timescales in small, well defined microtopography, measurements can have great spatial variability within similar vegetated areas resulting from vegetation patchiness and differences in soil composition, temperature, and moisture (Grondahl *et al.*, 2008). Eddy covariance measurements may also incorporate other microtopographic areas not sampled using chamber analysis. As such, a good representative sample of all heterogeneous areas when attempting to quantitatively ‘match’ chamber and eddy covariance fluxes is necessary (Schrier-Uijl *et al.*, 2010).

Results from Daring Lake show that average daily (10am – 6pm) ecosystem-scale NEE was more negative (greater uptake of CO₂) than average chamber NEE, while average daily CH₄ emission at the ecosystem-scale was lower (less release of CH₄) than average chamber CH₄ emission. Aurela *et al.* (2007) found in a boreal sedge fen that CO₂ fluxes from both chamber and eddy covariance methods had similar magnitudes, while chamber CO₂ flux was slightly lower (less uptake) on average than eddy covariance measurements. Griffis *et al.* (2000) in a sub-arctic sedge fen found that

chambers had the potential to considerably underestimate CO₂ fluxes. In addition, Twine *et al.* (2000) found that grassland eddy covariance measurements may underestimate CO₂ fluxes by 10 – 30%, while Fox *et al.* (2008) reported that chamber NEE had the potential to be 60% more negative than eddy covariance measurements and could potentially overestimate CO₂ uptake in heterogeneous arctic tundra. Schrier-Uijl *et al.* (2010) found a difference of 51% when average CH₄ field emissions from chambers and eddy covariance were assessed. However, when representative landscape elements were taken into account, the difference between chamber and eddy covariance CH₄ flux became less (13%).

5.3 Carbon Exchange Rates at the Daring Lake Fen and other Arctic Sites

The growing season pattern of CO₂ flux observed in 2009 was very similar to findings by Lafleur and Humphreys (2008) and to other eddy covariance and plot scale results obtained in arctic environments (Vourlitis and Oechel, 1999; Christensen *et al.*, 2000; Vourlitis *et al.*, 2000; Corradi *et al.*, 2005; Kwon *et al.*, 2006; Sullivan *et al.*, 2008). The season began with small net daily losses of CO₂ after snowmelt but gradually increased until maximum CO₂ uptake was reached about 3 weeks after summer solstice (DOY 206 to 214) and then decreased thereafter. The mid-summer daily flux during 2009 ranged between -0.8 and -2.2 g C m⁻² day⁻¹ with an average of -1.5 ± 0.1 g C m⁻² day⁻¹ (\pm SE). The magnitude of CO₂ exchange at the Daring Lake fen falls in the middle of observations from a number of other arctic sedge-dominated ecosystems (Vourlitis and Oechel, 1999; Vourlitis *et al.*, 2000; Corradi *et al.*, 2005; Kwon *et al.*, 2006). For example, the ecosystem GP_{max} in this study, $-7.1 \mu\text{mol m}^{-2} \text{s}^{-1}$, is very similar to the value obtained for a sedge fen in Alaska ($-6.7 \mu\text{mol m}^{-2} \text{s}^{-1}$ to $-8.0 \mu\text{mol m}^{-2} \text{s}^{-1}$), while a moist

tussock shrub ecosystem located within 2.5 km reported a higher GP_{\max} value of $-8.2 \mu\text{mol m}^{-2} \text{s}^{-1}$ to $-12.3 \mu\text{mol m}^{-2} \text{s}^{-1}$ (Vourlitis *et al.*, 2000). The daily maximum CO_2 uptake ($-2.2 \text{ g C m}^{-2} \text{ day}^{-1}$) at the Daring Lake fen was smaller than the daily maximum CO_2 gain ($-5.4 \text{ g C m}^{-2} \text{ day}^{-1}$) observed by Kwon *et al.* (2006) in a 5 year study of a sedge fen ecosystem in Alaska. Overall, the ecosystem average of $-1.5 \text{ g C m}^{-2} \text{ day}^{-1}$ at Daring Lake is very similar to the average flux observed in an Alaskan sedge fen ecosystem ($-1.3 \text{ g C m}^{-2} \text{ day}^{-1}$ to $-1.9 \text{ g C m}^{-2} \text{ day}^{-1}$) (Vourlitis *et al.*, 2000), more negative (more CO_2 uptake) than $-0.5 \text{ g C m}^{-2} \text{ day}^{-1}$ reported by Corradi *et al.* (2005) in a wet tussock grassland in north-east Siberia, and more negative than -0.5 to $-0.6 \text{ g C m}^{-2} \text{ day}^{-1}$ reported by Vourlitis and Oechel (1999) over a two year study in a moist tussock ecosystem in the Happy Valley of Alaska. Griffis *et al.* (2000) reported a small daily average ecosystem CO_2 flux of $-0.7 \text{ g C m}^{-2} \text{ day}^{-1}$ for the growing season in a very similar sedge fen to Daring Lake located in the low Arctic near Churchill, Manitoba. The water table at the Churchill site was considerably lower during peak biomass period (DOY 173 – 220) and may have resulted in increased ER and less negative GEP, resulting in the smaller magnitude for NEE. In fact, during mid-summer at the Churchill fen, there was even less CO_2 uptake with average ecosystem NEE of $-0.3 \text{ g C m}^{-2} \text{ day}^{-1}$.

Plot scale GP_{\max} of $-6.2 \mu\text{mol m}^{-2} \text{s}^{-1}$ and $-6.3 \mu\text{mol m}^{-2} \text{s}^{-1}$ for lawns and tussocks, respectively, were in good agreement with ecosystem GP_{\max} ($-7.1 \mu\text{mol m}^{-2} \text{s}^{-1}$), while average daytime field measurements of NEE were less negative ($-2.0 \text{ g C m}^{-2} \text{ day}^{-1}$ and $-1.9 \text{ g C m}^{-2} \text{ day}^{-1}$ lawns and tussocks, respectively) than the average daytime ecosystem flux ($-2.9 \text{ g C m}^{-2} \text{ day}^{-1}$). Our results were similar to a study by Sullivan *et al.* (2008), where under light saturating conditions ($\text{PAR} > 1000 \mu\text{mol m}^{-2} \text{s}^{-1}$) the range of mid-day

CO₂ flux in hummocks was -0.7 g C m⁻² day⁻¹ to -2.2 g C m⁻² day⁻¹ and in lawns was -1.1 g C m⁻² day⁻¹ to -2.0 g C m⁻² day⁻¹ at a Greenland fen with a similar microtopography and vascular species composition to Daring Lake. Another chamber flux study in a high arctic sedge fen ecosystem in Greenland with tussock and lawn topography report a larger range in NEE (-2.2 g C m⁻² day⁻¹ to -0.4 g C m⁻² day⁻¹), with larger uptake rates associated with tussock topography and smaller rates associated with lawns (Christensen *et al.*, 2000). The magnitude of our lawn and tussock CO₂ flux results are quite large when compared to the averages of -0.24 g C m⁻² day⁻¹ hummocks and 0.05 g C m⁻² day⁻¹ for hollows reported by Griffis *et al.* (2000) in the Churchill low arctic sedge fen. Differences in species composition, duration of the study period, and WT may account for the differences in observed NEE.

Seasonal patterns in daily ecosystem and small plot scale CH₄ emissions were similar to the pattern observed by Riutta *et al.* (2007) and to other eddy covariance and plot scale studies in northern and arctic sedge fen dominated ecosystems (Christensen *et al.*, 2000; Friberg *et al.*, 2000; Corradi *et al.*, 2005; Wille *et al.*, 2008). In contrast, at a high arctic wet tundra ecosystem, no significant variation in seasonal CH₄ emission was observed (Sachs *et al.*, 2008). The beginning of the study started off with approximate CH₄ emissions of 25 mg CH₄ m⁻² day⁻¹ and increased to maximum mid-summer values between 55 mg CH₄ m⁻² day⁻¹ and 69 mg CH₄ m⁻² day⁻¹ and then decreased to similar values observed at the beginning of the study. These emissions were almost twice as large as those observed by Sachs *et al.* (2008) in a high arctic wet tundra ecosystem (35 mg CH₄ m⁻² day⁻¹), in a Siberian arctic polygonal tundra ecosystem (30 mg CH₄ m⁻² day⁻¹, Wille *et al.* 2008), and in a low arctic Finnish fen (38 mg CH₄ m⁻² day⁻¹, Hargreaves *et*

al., 2001). However, Daring Lake CH₄ emissions were almost half the reported CH₄ emission in a high arctic Greenland fen (120 mg CH₄ m⁻² day⁻¹, Friborg *et al.*, 2000) and in a northern boreal treed fen (103.6 mg CH₄ m⁻² day⁻¹, Long *et al.*, 2010).

Plot scale measurements were also quite variable within and among sites. The range of CH₄ emission for lawns at Daring Lake was between 11 mg CH₄ m⁻² day⁻¹ and 227 mg CH₄ m⁻² day⁻¹ with an average of 80 mg CH₄ m⁻² day⁻¹ over the study period; while, tussock fluxes were considerably lower with a range between 3 mg CH₄ m⁻² day⁻¹ and 110 mg CH₄ m⁻² day⁻¹ with an average of 48 mg CH₄ m⁻² day⁻¹. Contrary to results at Daring Lake, a few northern and arctic sedge fen chamber studies have reported no significant difference between lawn and tussock CH₄ emission (Corradi *et al.*, 2005; Riutta *et al.*, 2007). Corradi *et al.* (2005) reported a higher average CH₄ emission from a Siberian wet tussock grassland of 195.8 ± 80.7 mg CH₄ m⁻² day⁻¹, while Riutta *et al.* (2007) also reported higher CH₄ emissions of approximately 240 mg CH₄ m⁻² day⁻¹ during the peak of growing season in a northern Finnish fen. In a high arctic fen, characterized by lawn and tussock microtopography similar to the Daring Lake fen, Christensen *et al.* (2000) reported a comparable average lawn CH₄ flux of 218 mg CH₄ m⁻² day⁻¹ and average tussock CH₄ flux of 68 mg CH₄ m⁻² day⁻¹ which was slightly higher than our reported averages yet within our observed CH₄ flux range. Overall, summer CH₄ emissions were consistent with the range of average summer CH₄ flux (-1.3 to 255 mg CH₄ m⁻² day⁻¹) summarized by Liblik *et al.* (1997) for other northern and arctic plot scale studies.

5.4 Growing Season Carbon Budget and GWP

Estimated growing season (June 1 – August 31, 92 days) flux of CO₂ and CH₄, and DOC runoff were -66.3, 2.4, and 0.9 g C m⁻², with an overall C budget of -63.0 g C m⁻². This cumulative net CO₂ exchange is similar to two Alaskan sedge fen tundra campaigns (CH₄ and DOC were not measured) (-76.8 g C m⁻², 92days; -70 g C m⁻², 92 days) (Vourlitis *et al.*, 2000; Kwon *et al.*, 2006, respectively). However, it is important to note that there is considerable year-to-year variability in growing season NEE. For example, NEE varied from -46.4 g C m⁻² to -70 g C m⁻² over a 5 year period in an Alaskan sedge fen tundra campaign (Kwon *et al.*, 2006) and from -39.9 to -55.2 g C m⁻² over 2 years in an Alaskan moist tussock ecosystem (Vourlitis and Oechel, 1999). Over a nine week study (63 days) in 2004, a Siberian high-arctic fen reported almost half the uptake of CO₂ (-33.8 ± 6.0 g C m⁻²) reported at Daring Lake in 2009 (Grondahl *et al.*, 2008); while, during a similar eight and a half week time period (60 days), a Siberian arctic sedge wetland ecosystem was a much bigger sink (-100 g C m⁻²) (Corradi *et al.*, 2006).

Total CH₄ emitted by the Daring Lake fen (June 1 to August 31, 92 days, 2.4 g C m⁻²) was within the range of growing season fluxes reported in a northern Siberian wet tundra ecosystem (June 1 to September 30, 122 days, 1.9 g C m⁻²) (Sachs *et al.*, 2008), in a Siberian wet polygonal tundra ecosystem (June 9 to September 19, 103 days, 1.9 g C m⁻²) (Wille *et al.*, 2008), and in a Greenland high-arctic wet fen (June 1 to September 1, 93 days, 3.7 g C m⁻²) (Friborg *et al.*, 2000).

Due to the scarcity of DOC flux investigation in arctic peatland environments, there lacks a suitable comparison to the Daring Lake study; however, in a subarctic Alaskan catchment, Carey (2003) found the yearly flux to be approximately twice our reported growing season value (1.6 g C m^{-2} vs. 0.9 g C m^{-2}). Given that 69% of DOC export occurred during the spring snowmelt period (Carey, 2001), it is likely that DOC flux at Daring Lake could be much larger if continuous measurements of outflow were made during summer capturing rainfall events and if spring freshet and fall storm periods were included.

Carbon budget comparisons are complicated due to the abiotic and biotic variables which are sensitive to site-specific characteristics. Variations in these variables can result in dramatically different C budgets within and among sites and year to year. While many studies do not include a complete C budget, and the inclusion of CH_4 and DOC fluxes may not change the overall C sink/source magnitude of an ecosystem, the inclusion of these smaller fluxes can be very important where the sink/source magnitude is close to zero. In our study, CH_4 emission and DOC loss represented approximately 5 % of the total amount of C stored through NEE during the growing season. In comparison, in a boreal ombrotrophic peatland, annual DOC export (8.2 g C m^{-2}) was approximately 12 % of the annual amount of C taken up through CO_2 exchange (-71 g C m^{-2}) (Fraser *et al.*, 2001). In a British upland peat catchment, annual DOC loss was 6% while CH_4 emission accounted for approximately 13% of annual C taken up through CO_2 exchange, resulting in a C budget decrease from approximately -55 g C m^{-2} to -36 g C m^{-2} annually (Worrall *et al.*, 2003). Friberg *et al.* (2003) estimated that CH_4 emissions accounted for approximately 6.5% of C taken up through CO_2 exchange in a Siberian

boreal wetland. Wille *et al.* (2008) estimated that CH₄ emissions represented 14% of the annual C budget of a Siberian wet polygonal ecosystem.

Although estimates of the annual C budget of the Daring Lake fen are beyond the scope of this study, it is expected that including spring and fall periods would increase the % contribution of CH₄ and DOC exchange as NEE becomes positive during these periods (Lafleur and Humphreys, 2008). Panikov (1999) report winter and spring fluxes to be an important part of the annual CH₄ and CO₂ budget, with some studies reporting 5 to 50% of yearly flux during these periods. Elberling *et al.* (2008) suggest that large bursts of CO₂ and CH₄ during spring thaw indicate the importance of winter soil respiration and microbial action, while the autumn period when snowfall covers and insulates the ground, keeping soil warm, will extend periods of high ER and CH₄ production furthering the importance of non-growing season fluxes on annual C budgets.

The inclusion of a GWP budget, at the 20 year and 100 year timescale, and its associated radiative forcing potential on the atmosphere should be viewed and interpreted with caution. The GWP methodology (IPCC, 2007) and its calculated radiative forcing potential to either warm or cool the atmosphere is highly dependent upon time horizon selection (Frolking *et al.*, 2006). Uptake and emission (CO₂ and CH₄) reported using GWP methodology in C cycling studies are generally treated as isolated perturbations or pulses to constant atmospheric concentrations; however, GWP should be determined over the lifetime of an ecosystem, as peatlands do not store or emit greenhouse gases in an isolated annual pulse; rather, they persistently emit CH₄ and variably, spatially and temporally, either emit or store CO₂ (Frolking *et al.*, 2006). Frolking *et al.* (2006) used atmospheric budget models and time series estimates to assess the impact of sustained or

variable greenhouse gas emissions on radiative forcing potential over the lifetime of an ecosystem. Frohking *et al.* (2006) report that constant CH₄ emissions from northern peatlands maintain atmospheric concentrations, while a change in CH₄ emission will result in a net positive radiative forcing over a few decades and then will neutralize; while, constant C sequestration via CO₂ exchange results in a constant negative radiative forcing over an ecosystem's lifetime. For northern peatland, a net positive radiative forcing effect will occur for approximately the first 50 years, while diminishing positive radiative forcing effects are seen over the next hundred to several millennia, dependent upon C sequestration rates, and thereafter, the peatland will have net negative radiative forcing effect (cooling) on the atmosphere (Frohking *et al.*, 2006).

6.0 CONCLUSION

Arctic peatland ecosystems store vast quantities of C, much of which is stored in perennially frozen soil. Enhanced mineralization of this C as a result of climate change is a potentially significant positive feedback to the global climate system. Recently, much investigation into the biotic and abiotic controls that drive the dynamic processes that control the amount of C that is either stored or released within wetland environments has taken place outside of Canada (Christensen *et al.*, 1995; Christensen *et al.*, 2000; Friberg *et al.*, 2000; Friberg *et al.*, 2003; Corradi *et al.*, 2005; Grondahl *et al.*, 2008; Sullivan *et al.*, 2008; Wille *et al.*, 2008), but there have been very few studies in Canada's low or high Arctic (Welker *et al.*, 2004; Oberbauer *et al.*, 2007; Hayne, 2009; Wilson and Humphreys, 2010), facilitating the need for investigation into spatial and temporal controls on C flux dynamics in an area expected to see dramatic climatic change in the near future.

This study examined temporal and spatial variations in CO₂ and CH₄ fluxes within a Canadian low Arctic peatland to test the following hypotheses:

- 1) *During the study period, the sedge fen is a C sink with more C taken up as CO₂ than lost as CH₄ and DOC.*

The Daring Lake fen was a C sink of 63 g C m⁻² over the growing season. The relative C budget components at the Daring Lake fen were within the range observed at other sedge-dominated arctic systems but smaller in magnitude to other C budget studies within wetland environments at lower latitudes. CH₄ and DOC losses were small relative to growing season CO₂ uptake (5%) but are expected to be of greater importance on an

annual basis. In order to accurately determine the sink/source magnitude of an area, measurements during the spring, fall, and winter are necessary. During these periods, there is the potential to lose the C gained during the growing season but further study will be necessary to determine if this is the case at the Daring Lake fen.

2) *Temporal and spatial variability in CO₂ flux is influenced most by factors that influence photosynthesis such as leaf area, light, and temperature.*

Lawn and tussock microtopography within the fen resulted in no significant differences in NEE. Instead, % vascular cover and LAI drove variations in NEE among collars regardless of microtopographic position.

Temporal variations in NEE were controlled by changes in air temperature and PAR, resulting in significant variation over the study period at the plot and ecosystem scales. At the plot scale, warmer, sunnier conditions enhanced uptake and release of CO₂; however, uptake (GEP) was enhanced to a greater extent than release (ER), resulting in greater overall C uptake (NEE) on warmer, sunny days. Both plot and ecosystem scale peaked at the same time during the mid-summer when biomass was greatest, light was not limiting, and temperatures were high.

3) *Temporal and spatial variability in CH₄ flux is influenced most by factors that affect anaerobic decomposition such as soil moisture conditions and soil temperatures.*

Emissions of CH₄ were significantly greater in wetter lawns than drier tussocks. There was little temporal variation in CH₄ fluxes at the plot scale likely as a result of

relatively constant moisture conditions (VWC). However, at the ecosystem scale, CH₄ emissions peaked with NEE and were related to variations in temperature and friction velocity. The persistent reduction in CH₄ emissions with high sustained turbulence has not been reported and more investigation is necessary to determine the reasons for this observation.

7.0 REFERENCES

- ACIA, Impacts of a Warming Arctic: Arctic Climatic Impact Assessment. Cambridge University Press, 2004.
- Aurela M, Riutta T, Laurila T, Tuovinen JP, Vesla T, Tuittila ES, Rinne J, Haapanala S, Laine J (2007) CO₂ exchange of a sedge fen in southern Finland – the impact of a drought period. *Tellus*, **59B**, 826-837.
- Alexandrova, VD (1980) The Arctic and Antarctic: Their Division into Geobotanical Areas. Cambridge University Press, Cambridge, UK.
- Baldocchi D (2003) Assessing the eddy covariance technique for evaluating carbon dioxide exchange rates of ecosystems: past, present and future. *Global Change Biology*, **9**, 479-492.
- Bartlett KB, Harriss RC. (1993) Review and Assessment of Methane emissions from Wetlands. *Chemosphere*, **26**, 311-320.
- Barber KE (1981) Peat Stratigraphy and Climatic Change: a Palaeological Test of Cyclic Peat Bog Regeneration. AA Balkema, Rotterdam.
- Basilika N, Moore TR, Jeannotte R, Bubier JL (2006) Nutrient input and Carbon and Microbial Dynamics in an Ombrotrophic Bog. *Geomicrobiology Journal*, **23**, 531-543.
- Bear J (1972) Dynamics of Fluids in Porous Media. Dover Publications, Mineola, New York, USA.
- Bellisario LM, Bubier JL, Moore TR (1999) Controls on CH₄ emissions from a northern peatland. *Global Biogeochemical Cycles*, **13:1**, 81-91.
- Bliss LC (1997) Arctic ecosystems of North America. Polar and alpine tundra. Elsevier, Amsterdam, NL, 509 – 539.
- Bockheim JG, Everett LR, Hinkel KM, Nelson FE, Brown J (1999) Soil organic carbon storage and distribution in arctic tundra, Borrow, Alaska. *Soil Science Society of America Journal*, **63**, 934-940.
- Bubier JL, Moore TR (1994) An Ecological Perspective on Methane Emissions from Northern Wetlands. *Trends in Ecology and Evolution*, **9:12**, 460-464.
- Bunnell FL, Tait DEN, Flanagan PW (1977) Microbial Respiration and Substrate Weight Loss – II. A Model of the Influences of Chemical Composition. *Soil Biol. Biochem.*, **9**, 41-47.

- Burn CR, Nelson FE. (2006). Comment on “A projection of severe near-surface permafrost degradation during the 21st century” by David M. Lawrence and Andrew G. Slater. *Geophysical Research Letters*, **33**: L21503.
- Bushaw KL, Zepp RG, Tarr MA, Schulz-Janders D, Bourbonniere RA, Hodson RE, Miller WL, Bronk DA, Moran MA (1996) Photochemical release of biologically available nitrogen from aquatic dissolved organic matter. *Nature*, **381**, 404-407.
- Callaghan TV, Björn LO, Chernov Y, Chapin T, Christensen TR, Huntley B, Ims RA, Johansson M, Jolly D, Jonasson S, Matveyeva N, Panikov N, Oechel W, Shaver G (2005) Effects on the Function of Arctic Ecosystems in the Short- and Long-term Perspectives. *Arctic Climate Impacts Assessment (ACIA)*, C. Symon, L. Arris and B. Heal, Eds., Cambridge University Press, Cambridge, 21-60.
- Carey, S (2003) Dissolved Organic Carbon Fluxes in a Discontinuous Permafrost Subarctic Alpine Catchment. *Permafrost and Periglacial Processes*, **14**, 161-171.
- Chanton JP, Whiting GJ (1995) Trace gas exchange in freshwater and coastal marine environments: Ebullition and transport by plants. In Matson, P. A. and Harriss, R. C. (eds.) *Biogenic Trace Gases: Measuring Emissions from Soil and Water*. Blackwell, Oxford. pp. 98–125.
- Chapin FS, Kittel TGF, Steffen WL (2000) Global and regional modeling of Arctic-boreal vegetation distribution and its sensitivity to altered forcing. *Global Change Biology*, **6**, 1-18.
- Christensen TR (1993) Methane emission from Arctic tundra. *Biogeochemistry*, **21**, 117-139.
- Christensen TR, Jonasson S, Callaghan TV, Havstrom M (1995). Spatial variation in high-latitude methane flux along a transect across Siberian and European tundra environments. *Journal of Geophysical Research*, **100**, 21035-21045.
- Christensen TR, Prentice IC, Kaplan J, Haxeltine AM, Sitch S (1996) Methane flux from northern wetlands and tundra: an ecosystem source modelling approach. *Tellus*, **48**, 652–661.
- Christensen TR, Friborg T, Sommerkorn M, Kaplan J, Illeris L, Soegaard H, Nordstroem C, Jonasson S (2000) Trace gas exchange in a high-arctic valley 1. Variations in CO₂ and CH₄ flux between tundra vegetation types. *Global Biogeochemical Cycles*, **14**, 701-713
- Clark JM, Lane SN, Chapman PJ, Adamson JK (2007) Export of dissolved organic carbon from and upland peatland during storm events: Implications for flux estimates. *Journal of Hydrology*, **347**, 438-447.

- Climatic Atlas of Canada (1984) *Map Series 1 & 2*. Government of Canada, Ottawa, ON.
- Corradi C, Kolle O, Walter K, Zimov SA, Schulze ED (2005) Carbon dioxide and methane exchange of a north-east Siberian tussock tundra. *Global Change Biology*, **11**, 1910-1925.
- Davidson EA, Janssens IA. (2006). Temperature sensitivity of soil carbon decomposition and feedbacks to climate change. *Nature*, **440**: 165–173.
- Dedysh SN, Khmelenia VN, Suzina NE, Trotsenko YA, Semrau JD, Liesack W, Tiedje JM (2002) *Methylocapsacidiphilagen*. nov., sp. nov., a novel methane-oxidizing and dinitrogen-fixing acidophilic bacterium from *Sphagnum* bog. *International Journal of Systematic and Evolutionary Microbiology*, **52**, 251-261.
- Dredge LA, Kerr DE, Wolfe SA (1999). Surficial materials and related ground ice conditions, Slave Province, N.W.T., Canada. *Canadian Journal of Earth Science*, **36**, 1227-1238.
- Elberling B (2007) Annual soil CO₂ effluxes in the High Arctic: The role of snow thickness and vegetation type. *Soil Biology & Biochemistry*, **39**, 646-654.
- Elberling B, Nordstrom C, Grondahl L, Sogaard H, Friborg T, Christensen TR, Strom L, Marchand F, Nijs I (2008) High-arctic soil CO₂ and CH₄ production controlled by temperature, water, freezing and snow. *Advances in Ecological Research*, **40**: 441-472.
- Fan SM, Wolfsy, SC, Bakwin PS, Jacob DJ (1992) Micrometeorological measurements of CH₄ and CO₂ exchange between the atmosphere and subarctic tundra. *Journal of Geophysical Research*, **97**, 16627-16643.
- Fox AM, Huntley B, Lloyd CR, Williams M, Baxter R (2008) Net ecosystem exchange over heterogeneous Arctic Tundra: Scaling between chamber and eddy covariance measurements. *Global Biogeochemical Cycles*, **22**, GB2027.
- Fraser CJD, Roulet NT, Moore TR (2001) Hydrology and dissolved organic carbon biogeochemistry in an ombrotrophic bog. *Hydrological processes*, **15**, 3151-3166.
- Friborg T, Christensen TR, Hansen BU, Nordstroem C, Soegaard H (2000) Trace gas exchange in a high-arctic valley 2. Landscape CH₄ fluxes measured and modeled using eddy correlation data. *Global Biogeochemical Cycles*, **14** (3), 715-723.
- Friborg T, Soegaard H, Christensen TR, Lloyd CR, Panikov NS (2003) Siberian wetlands: Where a sink is a source. *Geophysical Research Letters*, **30**:21, 2129-2132.

- Frolking S, Roulet N, Fuglestedt J (2006) How northern peatlands influence the Earth's radiative budget: Sustained methane emission versus sustained carbon sequestration. *Journal of Geophysical Research*, **111**, G01008.
- Gazovic M, Kutzbach L, Schreiber P, Wille C, Wilmking M (2010) Diurnal dynamics of CH₄ from a boreal peatland during snowmelt. *Tellus*, **62B**, 133-139.
- Gergel SE, Turner MG, Kratz TK (1999) Dissolved organic carbon as an indicator of the scale of watershed influence on lakes and rivers. *Ecological Applications*, **9**, 1377-1390.
- Gorham E (1991) Northern Peatlands: Role in the Carbon Cycle and Probable Responses to Climate Warming. *Ecological Applications*, **1 (2)**, 182-195.
- Granberg G, Mikkela C, Sundh I, Svensson BH, Nilsson M (1997) Sources of spatial variation in methane emission from mires in northern Sweden: A mechanistic approach in statistical modelling. *Global Biogeochemical Cycles*, **11**, 135-150.
- Griffis TJ, Rouse WR, Waddington JM (2000) Interannual variability of net ecosystem CO₂ exchange at a subarctic fen. *Global Change Biology*, **7**, 511-530.
- Griffis TJ, Rouse WR, Waddington JM (2000) Scaling net ecosystem CO₂ exchange from the community to landscape-level at a subarctic fen. *Global Change Biology*, **6**, 459-473.
- Grondahl L, Friberg T, Christensen TR, Ekberg A, Elberling B, Illeris L, Nordstrom C, Rennermalm A, Sigsgaard C, Sogaard H (2008) Spatial and Inter-Annual Variability of Trace Gas Fluxes in a Heterogeneous High-Arctic Landscape. *Advances in Ecological Research*, **40**, 473-498.
- Hayne S (2009) Controls on Atmospheric Exchanges of Carbon Dioxide and Methane for a Variety of Arctic Tundra Types. M.Sc. Thesis, Carleton University.
- Heikkinen JEP, Elsakov V, Martikainen PJ (2002) Carbon dioxide and methane dynamics and annual carbon balance in tundra wetland in NE Europe, Russia. *Global Biogeochemical Cycles*, **16(4)**, 1115.
- Heikkinen JEP, Maljanen M, Aurela M, Hargreaves KJ, Martikainen PJ (2002) Carbon dioxide and methane dynamics in a sub-Arctic peatland in northern Finland. *Polar Research*, **21(1)**, 49-62.
- Hornibrook ERC, Longstaffe FJ, Fyfe WS (1997) Spatial distribution of microbial methane production pathways in temperate zone wetland soils: Stable carbon and hydrogen isotope evidence. *Geochimica et Cosmochimica Acta*, **61 (4)**, 745-753.

- Intergovernmental Panel on Climate Change, IPCC (2007) *Climate Change 2007, Synthesis Report, Contribution of Working Groups I, II and III to the Fourth Assessment Report of the Intergovernmental Panel on Climate Change* (Core Writing Team; Pachauri RK, Reisinger A(eds)). IPCC, Geneva, Switzerland.
- IPCC, 2001: *Climate Change 2001: The Scientific Basis. Contribution of Working Group I to the Third Assessment Report of the Intergovernmental Panel on Climate Change* [Houghton, J.T., Y. Ding, D.J. Griggs, M. Noguer, P.J. van der Linden, X. Dai, K.Maskell, and C.A. Johnson (eds.)]. Cambridge University Press, Cambridge, United Kingdom and New York, NY, USA, 881pp.
- Johnson LC, Damman AWH (1991) Species-controlled Sphagnum decay on a South Swedish raised bog. *Oikos*, **61**, 234-242.
- Kalbitz K, Solinger S, Park J-H, Michalzik B, Matzner E (2000) Controls on the dynamics of dissolved organic matter in soils: a review. *Soil Science* **165**: 277–304.
- Kellner E, Waddington JM, Price JS (2005) Dynamics of biogenic gas bubbles in peat: Potential effects on water storage and peat deformation. *Water Resources Research*, **41**, W08417.
- King JY, Reeburgh WS, Regli SK (1998) Methane emission and transport by arctic sedges in Alaska: Results of a vegetation removal experiment. *Journal of Geophysical Research*, **103 (D22)**, 29083-29092.
- Kuhry P, Dorrepaal E, Hugelius G, Schuur EAG, Tarnocai C (2010) Potential Remobilization of Belowground Permafrost Carbon under Future Global Warming. *Permafrost and Periglacial Processes*, **21**, 208-214.
- Kutzbach L, Wagner D, Pfeiffer E-M (2004) Effect of microrelief and vegetation on methane emissions from wet polygonal tundra, Lena Delta, Northern Siberia. *Biogeochemistry*, **69**, 341-362.
- Kutzbach L, Schneider J, Sachs T, Giebels M, Nykanen H, Shurpali NJ, Martikainen PJ, Alm J, Wilkening M (2007) CO₂ flux determination by closed-chamber methods can be seriously biased by inappropriate application of linear regression. *Biogeosciences*, **4**, 1005-1025.
- Kwon HJ, Oechel WC, Zulueta RC, Hastings SJ (2006) Effects of climate variability on carbon sequestration among adjacent wet sedge tundra and moist tussock tundra ecosystems. *Journal of Geophysical Research*, **111**, G03014.
- Laflour PM, Griffis TJ, Rouse WR (2001) Interannual variability in net ecosystem CO₂ exchange at the arctic treeline. *Arctic, Antarctic, and Alpine Research*, **33**, 149-157.

- Lafleur PM, Humphreys ER (2008) Spring warming and carbon dioxide exchange over low Arctic tundra in central Canada. *Global Change Biology*, **14**, 740-756.
- Lai DYF (2009) Methane dynamics in northern peatlands: A review. *Pedosphere*, **19**, 409-421.
- Liblik LK, Moore TR, Bubier JL, Robinson SD (1997) Methane emissions from wetlands in the zone of discontinuous permafrost: Fort Simpson, Northwest Territories, Canada. *Global Biogeochemical Cycles*, **11** (4), 485-494.
- Llyod J, Taylor JA (1994) On the temperature dependence of soil respiration. *Functional Ecology*, **8**, 315-323.
- Long KD, Flanagan LB, Cai T (2010) Diurnal and seasonal variation in methane emissions in a northern Canadian peatland measured by eddy covariance. *Global Change Biology*, **16**(9), 2420-2435.
- Luo Y, Zhuo X (2006) Soil Respiration and the Environment. Burlington, MA, and San Diego, CA, USA: Academic Press pp. 320.
- Merbold L, Kutsch WL, Corradi C, Kolle O, Rebmann C, Stoy PC, Zimov SA, Schulze ED (2009) Artificial drainage and associated carbon fluxes (CO₂/CH₄) in a tundra ecosystem. *Global Change Biology*, **15**, 2599-2614.
- Moore TR, Basiliko N (2006). Decomposition. *Boreal Peatland Ecosystems*, **188**, 126-143.
- Moore TR, Roulet NT, Waddington JM (1998) Uncertainty in predicting the effect of climatic change on the carbon cycling of Canadian peatlands. *Climatic Change*, **40**: 229-245.
- Nilsson M, Sagerfors J, Buffam I, Laudon H, Eriksson T, Grelle A, Klemetssons L, Wesliens P, Lindroth A (2008) Contemporary carbon accumulation in a boreal oligotrophic minerogenic mire – a significant sink after accounting for all C-fluxes. *Global Change Biology*, **14**, 2317-2332.
- Nobrega S, Grogan P (2008) Landscape and Ecosystem-Level Controls on Net Carbon Dioxide Exchange along a Natural Moisture Gradient in Canadian Low Arctic Tundra. *Ecosystems*, **11**, 377-396.
- Nungesser MK (2003) Modelling microtopography in boreal peatlands: hummocks and hollows. *Ecological Modelling*, **165**, 175-207.

- Nykanen H, Heikkinen JEP, Pirinen L, Tiilikaninen K, Martikainen PJ (2003) Annual CO₂ and CH₄ fluxes on a subarctic peat mire during climatically different years. *Global Biogeochemical Cycles*, **17**, 1801-1818.
- Oberbauer SF, Tweedie CE, Welker JM, Fahnestock JT, Henry GHR, Webber PJ, Hollister RD, Walker MD, Kuchy A, Elmore E, Starr G (2007) Tundra CO₂ fluxes in response to experimental warming across latitudinal and moisture gradients. *Ecological Monographs*, **77** (2), 221-238.
- Obst J (2008) *Classification of Landcover, Vegetation Communities, Ecosystems and Habitats in the East Daring Lake Basin, Northwest Territories*. Department of Environment and Natural Resources, Wildlife Division, Government of the Northwest Territories and Environment and Conservation Division, Indian and Northern Affairs Canada, Yellowknife, Northwest Territories.
- Oechel WC, Hastings SJ, Vourlitis G, Jenkins M, Riechers G, Grulke N (1993) Recent change of Arctic tundra ecosystems from a carbon sink to a source. *Nature*, **361**, 520-523.
- Oechel WC and Vourlitis GL (1994) The effects of climate-change on land atmosphere feedbacks in Arctic tundra regions. *Trends in Ecology & Evolution*, **9** (9), 324-329.
- Oechel WC, Vourlitis GL, Hastings SJ, Ault R, Bryant P (1998) The effects of water table manipulation and elevated temperature on the net CO₂ flux of a wet-sedge tundra ecosystem. *Global Change Biology*, **4**, 77-90.
- Oechel WC, Vourlitis GL, Hastings SJ, Zulueta RC, Hinzman L, Kane D (2000) Acclimation of ecosystem CO₂ exchange in the Alaskan Arctic in response to decadal climate warming. *Nature*, **406**, 978-981.
- Ohlson M, Dahlberg B (1991) Rate of peat increment in hummock and lawn communities on Swedish mires during the last 150 years. *Oikos*, **61**, 369-378.
- Okolo I (2008) Analysis of Long Term Carbon Accumulation in an Arctic Fen. B.Sc Thesis, Institute for Environmental Science, Carleton University, Ottawa, ON.
- Panikov N. S (1999) Fluxes of CO₂ and CH₄ in high latitude wetlands: measuring, modeling, and predicting response to climate change. *Polar Research*, **18**, 237-244.
- Pastor J, Solin J, Bridgman SD, Updegraff K, Harth C, Weishampel P, Dewey B (2003) Global warming and the export of dissolved organic carbon from boreal peatlands. *Oikos*, **100**, 380-386.

- Pawson RR, Lord DR, Evans MG, Allott THE (2008) Fluvial organic carbon flux from an eroding peatland catchment, southern pennines, UK. *Hydrol. Earth Syst. Sci.*, **12**, 625-634.
- Post WM, Emanuel WR, Zinke PJ, Strangenberg, AG (1982) Soil carbon pools and world life zones. *Nature* **298**, 156–159.
- Piquette S (2010) Quantification of Greenhouse Gas Flux and Net Ecosystem Exchange in Variable Ecosystems in the Daring Lake, NWT Area. Undergraduate Thesis in Physical Geography and Earth Science, Carleton University, Ottawa, Ontario, Canada.
- Reth S, Reichstein M, Falge E (2005) The effect of soil water content, soil temperature, soil pH-value and the root mass on soil CO₂ efflux – A modified model. *Plant and Soil*, **268**, 21-33.
- Rinne J, Riutta T, Pihlatie M, Aurela M, Haapanala S (2007) Annual cycle of methane emission from a boreal fen measured by the eddy covariance technique. *Tellus*, **59B**, 449-457.
- Riutta T, Laine J, Aurela M, Rinne J, Vesala T, Laurila T, Haapanala S, Pihlatie M, Tuittila E-S (2007) Spatial variation in plant community functions regulates carbon gas dynamics in a boreal fen ecosystem. *Tellus*, **59B**, 838-852.
- Roulet N, Lafleur PM, Richard PJ, Moore TR, Humphreys ER, Bubier J (2007) Contemporary carbon balance and late Holocene carbon accumulation in a northern peatland. *Global Change Biology*, **13**, 397-411.
- Sachs T, Wille C, Boike J, Kutzbach L (2008) Environmental controls on ecosystem-scale CH₄ emission from polygonal tundra in the Lena River Delta, Siberia. *Journal of Geophysical Research-Biogeosciences*, **113**, G00A03.
- Schindler DW, Curtis PJ (1997) The role of DOC in protecting freshwaters subjected to climatic warming and acidification from UV exposure. *Biogeochemistry*, **36**, 1-8.
- Schmid HP (1994) Source areas for scalars and scalar fluxes. *Boundary-Layer Meteorology*, **67** (3), 293-318.
- Schrier-Uijl AP, Kroon PS, Hensen A, Leffelaar PA, Berendse F, Veenendaal EM (2010) Comparison of chamber and eddy covariance-based CO₂ and CH₄ emission estimates in a heterogeneous grass ecosystem on peat. *Agricultural and Forest Meteorology*, **150**, 825-831.
- Schuepp PH, Leclerc MY, Macpherson JI, Desjardins RL (1990) Footprint Prediction of Scalar Fluxes from Analytical Solutions of the Diffusion Equation. *Boundary-Layer Meteorology*, **50** (1-4), 355-373.

- Schuur EAG, Bockheim J, Canadell JG, Euskirchen E, Field CB, Goryachkin SV, Hagemann S, Kuhry P, Lafleur PM, Lee H, Mazhitova G, Nelson FE, Rinke A, Romanovsky VE, Shiklomanov N, Tarnocai C, Venevsky S, Vogle JG, Zimov SA (2008) Vulnerability of Permafrost Carbon to Climate Change: Implications for the Global Carbon Cycle. *BioScience*, **58** (8), 701-714.
- Segers S (1998) Methane production and methane consumption: a review of processes underlying wetland methane fluxes. *Biogeochemistry*, **41**, 23-51.
- Shumacher, BA (2002) Methods for the Determination of Total Organic Carbon (TOC) in Soils and Sediments. United States Environmental Protection Agency. Las Vegas, USA.
- Soegaard H, Nordstroem C (1999) Carbon dioxide exchange in a high-arctic fen estimated by eddy covariance measurements and modeling. *Global Change Biology*, **5**, 547-562.
- Strack M, Waddington JM, Tuittila ES (2004) Effect of water table drawdown on northern peatland methane dynamics: Implications for climate change. *Global Biogeochemical Cycles*, **18**, GB4003.
- Strack M, Kellner E, Waddington JM (2005) Dynamics of biogenic gas bubbles in peat and their effects on peatland biogeochemistry. *Global Biogeochemical Cycles*, **19**, GB1003.
- Strack M, Waddington JM, Rochefort L, Tuittila ES (2006) Response of vegetation and net ecosystem carbon dioxide exchange at different peatland microforms to water table drawdown. *Journal of Geophysical Research-Biogeosciences*, **111**(G2), G02006.
- Strack M, Waddington JM, Bourbonniere RA, Buckton EL, Shaw K, Whittington P, Price JS (2008) Effect of water table drawdown on peatland dissolved organic carbon export and dynamics. *Hydrological Processes*, **22**, 3373–3385.
- Strack M, Price JS (2009) Moisture controls on carbon dioxide dynamics of peat-Sphagnum monoliths. *Ecohydrology*, **2**, 34-41.
- Strom L, Ekberg A, Mastepanov M, Christensen TR (2003) The effect of vascular plants on carbon turnover and methane emissions from a tundra wetland. *Global Change Biology*, **9**, 1185-1192.
- Sullivan FS, Arens SJT, Chimner RA, Welker JM (2008) Temperature and Microtopography Interact to Control Carbon Cycling in a High Arctic Fen. *Ecosystems*, **11**, 61-76.

- Tarnocai C (2000) Carbon pools in soils of the Arctic, subarctic, and boreal regions of Canada. In: *Global Climate Change and Cold region Ecosystems. Advances in Soil Science* (eds Lal R, Kimble JM, Stewart BA), pp. 91-103. CRC Press LLC, New York.
- Tarnocai C, Canadell JG, Schuur EAG, Kuhry P, Mazhitova G, Zimov S (2009) Soil organic carbon pools in the northern circumpolar permafrost region. *Global Biogeochemical Cycles*, **23**, GB2023.
- Tokida T, Miyazaki T, Mizoguchi M, Nagata, Takakai F, Kagemota A, Hatano R (2007) Falling atmospheric pressure as a trigger for methane ebullition from peatland. *Global Biogeochemical Cycles*, **21**, GB2003.
- Torn MS, Chapin FS (1993) Environmental and biotic controls over methane flux from arctic tundra. *Chemosphere*, **26 (1-4)**, 357-368.
- Treat CC, Bubier JL, Varner RK, Crill PM (2007) Timescale dependence of environmental and plant-mediated controls on CH₄ flux in a temperate fen. *Journal of Geophysical Research-Biogeosciences*, **112(G1)**, G01014.
- Twine TE, Kustas WP, Norman JM, Cook DR, Houser PR, Meyers TP, Prueger JH, Starks PJ, Wesely ML (2000) Correcting eddy-covariance flux underestimates over a grassland. *Agricultural and Forest Meteorology*, **103**, 279–300.
- Vourlitis GL, Oechel WC (1999) Eddy covariance measurements of CO₂ and energy fluxes of an Alaskan tussock tundra ecosystem. *Ecology*, **80**, 686–701.
- Vourlitis GL, Harazono Y, Oechel WC, Yoshimoto M, Mano M (2000) Spatial and temporal variations in hectare-scale net CO₂ flux, respiration and gross primary production of Arctic tundra ecosystems. *Functional Ecology*, **14**, 203-214.
- Waddington JM, Roulet NT (1996) Atmosphere-wetland carbon exchanges: scale dependency of CO₂ and CH₄ exchange on the developmental topography of a peatland. *Global biogeochemical Cycles*, **10**, 233-245.
- Waddington JM, Roulet NT (1997) Groundwater flow and dissolved carbon movement in a boreal peatland. *Journal of Hydrology*, **191**, 122-138.
- Waldron S, Flowers H, Arlaud C, McFarlane S (2008) The significance of organic carbon and nutrient export from peatland-dominated landscapes subject to disturbance. *Biogeosciences Discussion*, **5**, 1139-1174.
- Walker DA, Reynolds MK, Daniels FJA, Einarsson E, Elvebakk A, Gould WA, Katenin AE, Kholod SS, Markon CJ, Melnikov ES, Moskalenko NG, Talbot SS, Yurtsev BA (2005) The Circumpolar Arctic vegetation map. *Journal of Vegetation Science*, **16**, 267-282.

- Wangersky PJ (1993) Dissolved organic carbon methods: a critical review. *Marine Chemistry*, **41**, 61-74.
- Warner BG, Rubec CDA (1997) The Canadian Wetland Classification System, Second Edition. Waterloo Canada: Wetland Research Centre, University of Waterloo.
- Webb EK, Pearman GI, Leuning R (1980) Correction of flux measurements for density effects due to heat and water-vapour transfer. *Quarterly Journal of the Royal Meteorological Society*, **106(447)**, 85-100.
- Welker JM, Fahnestock JT, Henry GHR, O’Dea KW, Chimner RA (2004) CO₂ exchange in three Canadian High Arctic ecosystems: response to long-term experimental warming. *Global Change Biology*, **10**, 1981–1995.
- Whalen SC (2005) Biogeochemistry of Methane Exchange between Natural Wetlands and the Atmosphere. *Environmental Engineering Science*, **22 (1)**, 73-94.
- Whalen SC, Reeburgh WS (1990) Consumption of atmospheric methane by tundra soils. *Nature*, **346**, 160-163.
- Whalen SC, Reeburgh WS, Barber VA (1992) Oxidation of methane in Boreal forest soils – A comparison of 7 measures. *Biogeochemistry*, **16**, 181-211.
- Wille C, Kutzbach L, Sachs T, Wagner D, Pfeiffer E-M (2008) Methane emission from Siberian arctic polygonal tundra: eddy covariance measurements and modeling. *Global Change Biology*, **14**, 1395–1408.
- Wilson KS, Humphreys ER (2010) Carbon Dioxide and methane fluxes from Arctic mudboils. *Canadian Journal of Soil Science*, **90 (3)**, 441-449.
- Worrall F, Reed M, Warburton J, Burt T (2003) Carbon budget for a British upland peat catchment. *The Science of the Total Environment*, **312**, 133–146.
- Wuebbles DJ, Hayhoe K (2002) Atmospheric methane and global change. *Earth-Science Reviews*, **57**, 177-210.
- Zhang T, Barry RG, Knowles K, Heginbottom JA, Brown J. (1999) Statistics and characteristics of permafrost and ground-ice distribution in the Northern Hemisphere. *Polar Geography*, **23**: 132–154.
- Zhuang QL, Melillo JM, Sarofirn MC, Kicklighter DW, McGuire AD, Felzer BS, Sokolov A, Prinn RG, Steudler PA, Hu SM (2006) CO₂ and CH₄ exchanges between land ecosystems and the atmosphere in northern high latitudes over the 21st century. *Geophysical Research Letters*. **33 (17)**, L17403.

Zimov SA, Walter KM, Chanton JP (2006) Methane bubbling from Siberian thaw lakes as a positive feedback to climate warming. *Nature*, **443**, 71-75.

Zimov SA, Schuur EAG, Chapin FS (2006b) Permafrost and the global carbon budget. *Science*, **312**, 1612 – 1613.